CHAPTER V

RESULTS & DISCUSSIONS

5.1 Theoretical Data Analysis

5.1.1 Cahn-Hilliard's Theory

Intensities were calculated from Cahn-Hilliard's theory by using equation (3.2.27). The $R(q)$ values were obtained from the slope of natural logarithm of intensity over time. The $S(q,o)-S_x(q)$ values were obtained from the intercept of natural logarithm of intensity and time curve. The error value is difference value between calculated value and experiment value.

5.1.2 Langer, Bar-on and Miller's Theory

Experimental data at one angle were fitted with equation (4.2.6) using MATHEMATICA program. From fit data, we obtain the coefficients parameter; A, B, C and D and intensity factor E. Inserting coefficients and intensity factor in the right hand side equation (4.2.6) can provide natural logarithm of intensity. The predicted intensities were obtained by take exponential of natural logarithm of intensity over time at constant angle. The error value is difference between calculated value and experiment value.

5.1.3 Akcasu's Theory

Inserting $R(q)$, time step (Δt) and intensity values $(I(q,t+\Delta t), I(q,t))$ from experiment into equation (4.3.5) can provide coefficient parameters: A', B', C'

and D' using MATHEMATICA program. These parameters were used to predict intensity at another time step using equation (4.3.6). The error is difference value between calculated value and experiment value.

5.1.4 Nauman's Theory

Inserting time step (Δt) and intensity values $(I(q+\Delta q,t), I(q,t))$ from experiment into equation (4.4.6) can provide coefficient parameters; A'', B'' using MATHEMATICA program. After these coefficient parameters were expanded using power law. These coefficient parameters were fitted with equation (4.2.9) and (4.2.10) can provide new coefficient parameters; f, h, j, l, f', h', j' and l'. The new parameters were used to predict intensity at another time step using equation (4.3.11). The error is difference value between calculated value and experiment value.

5.2 Results of Intensity Calculated from each Theory

The angle for scattered light intensity at 35° was the angle at which the spinodal peaks were observed for the 30%w and 70%w TMPC/PS blends. So, we consider intensities at this angle. The summarized data at the angle of 35° for five temperatures are shown in Fig. (5.1-5.4).

In Fig. (5.1), the 50%w TMPC/PS blends was prepared by solvent casting, it showed typical spinodal behaviour. The intensity grows up exponentially at the beginning and decreases when the peaks shift to low q. From the curve, the spinodal decomposition process occurs much quicker when the experimental temperature increases as expected.

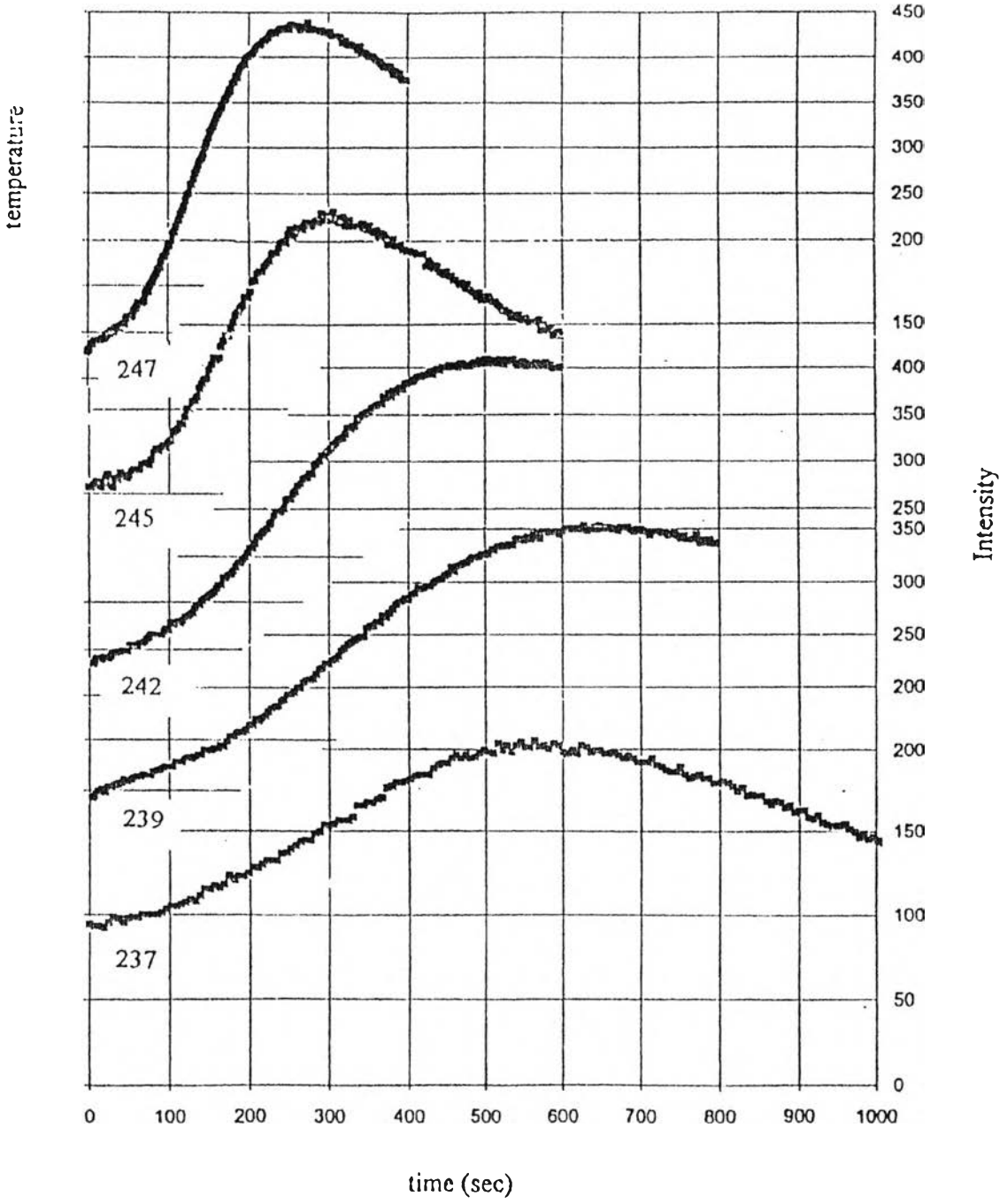

Fig. 5.1 Spinodal Characteristic of 50%w TMPC/PS blends at 35° [Thongyai, 1994]

The spinodal characteristics of melt mixed samples of 50%w TMPC/PS blends at 35° are shown in Fig.(5.2). From this figure, linearization limits were within 100 seconds. The intensity increased abruptly within 100 seconds and then decreased all through the experiments. These steep curves can not be compared with the smooth curves obtained in the case of solvent cast samples (Fig.5.1).

From Fig.(5.3), the 30%w TMPC/PS blends also shows typical Cahn-Hillard spinodal behaviour. The intensity increases exponentially for a long time and did not decrease even after the experiment finished. This may be because the 30%w TMPC needs more time to develop its final concentration than the 50%w TMPC.

In Fig.(5.4), the 70%w TMPC/PS blends shows quite different characteristics. The intensity starts to grow exponential only after 800 seconds.

5.2.1 Intensity of 30%w TMPC/PS Blends

Fig. 5.5 shows the intensity data calculated from various theories of 30%w TMPC/PS blends at 271 °C and at the angle of 35 ° ,it appeared that the intensity of Cahn-Hilliard smoothly increases with increasing time. The intensities of Akcasu and Langer, Bar-on and Miller are quite the same as the intensity from experiment. The results of Nauman and Cahn-Hilliard highly differ from experimental results. It shows the Akcasu's and Langer, Bar-on, Miller's theories can be used to fit the data better than the other two theories.

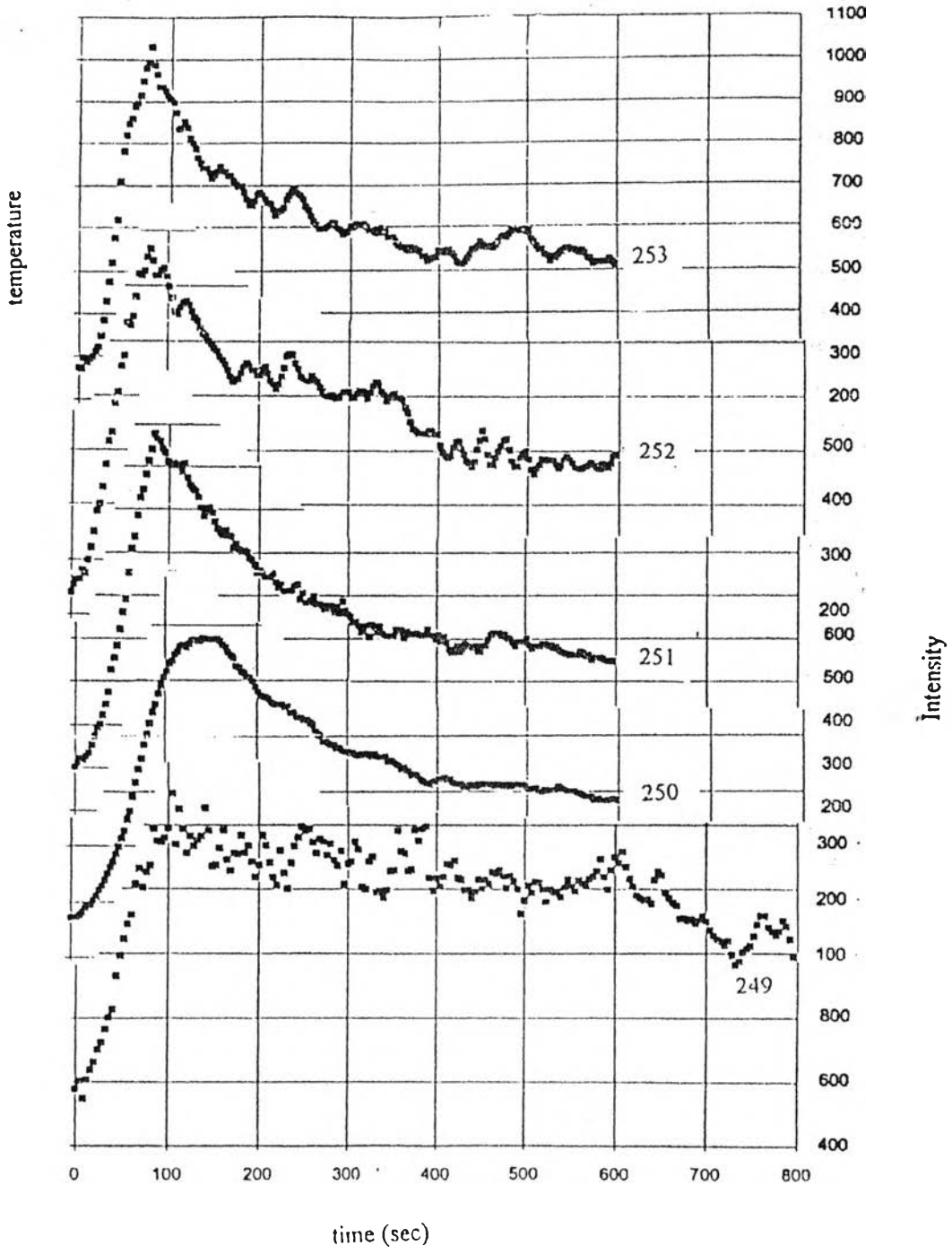

Fig. 5.2 Spinodal Characteristic of 50%w TMPC/PS blends melt mixed at 35°

[Thongyai, 1994]

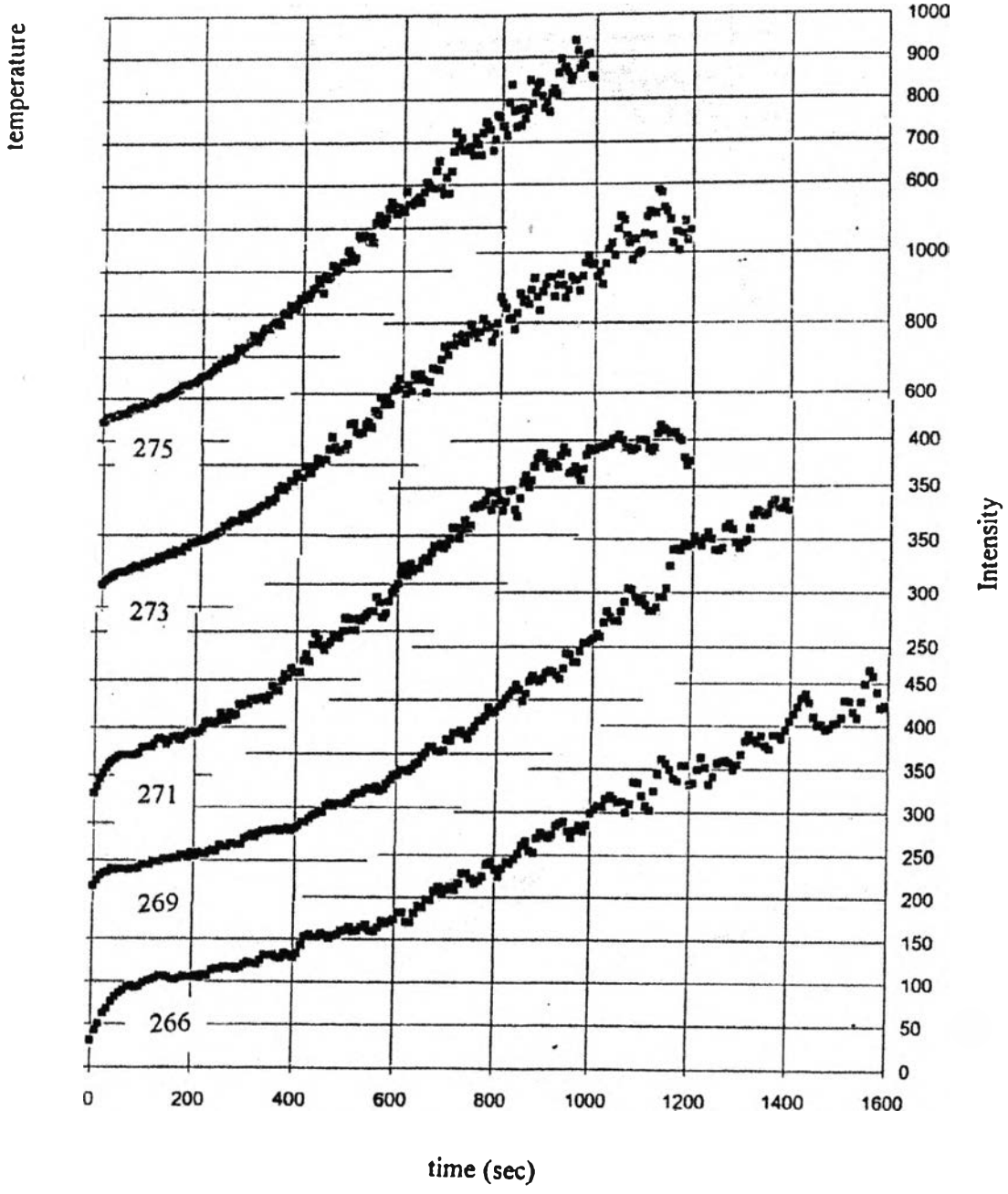

Fig. 5.3 Spinodal Characteristic of 30%w TMPC/PS blends at 35° [Thongyai, 1994]

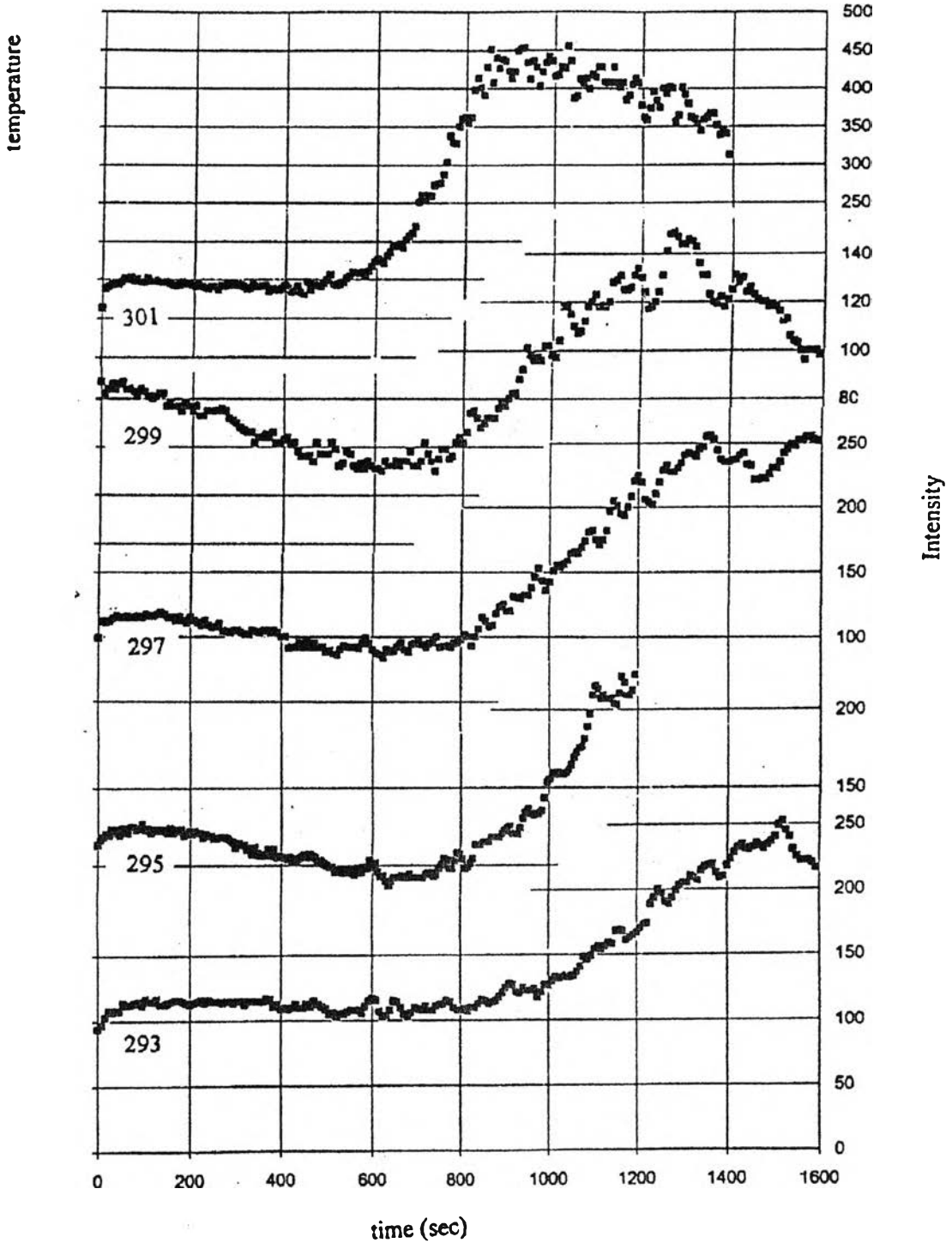

Fig. 5.4 Spinodal Characteristic of 70%w TMPC/PS blends at 35° [Thongyai, 1994]

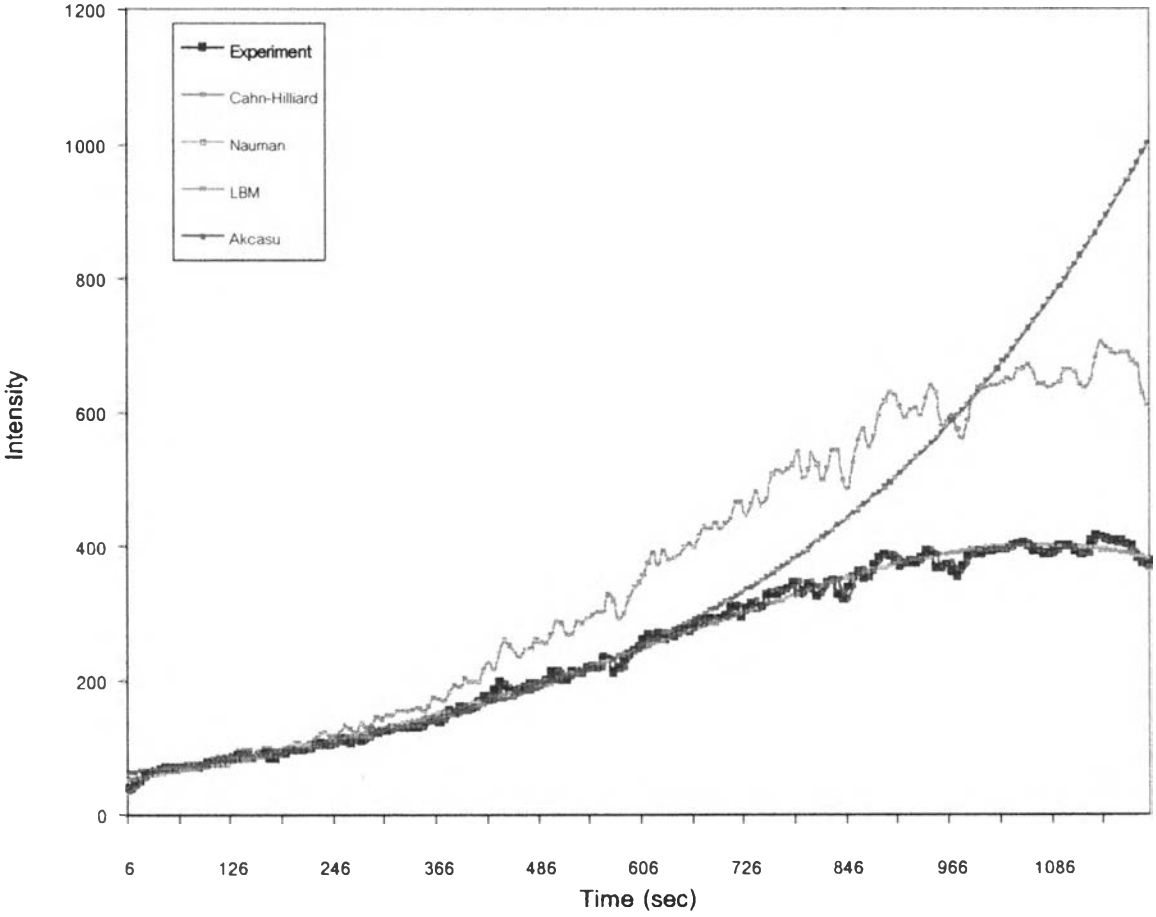

Fig.5.5 The intensity data of 30%w TMPC/PS blends at 271°C and the angle of 35°, obtained from the experiment and calculated from various theories.

5.2.2 Intensity of 50%w TMPC/PS Blends (Prepared by Solvent Casting)

Fig.5.6 shows the intensity calculated from various theories of 50%w TMPC/PS blends, that were prepared by solvent casting method at 239 °C and at the angle of 35 °, it appeared that the intensity of Cahn-Hilliard smoothly increases with increasing time. The intensities of Akcasu and Langer, Bar-on and Miller are quite the same as the experimental ones. At the beginning of the spinodal decomposition process, the results of Cahn-Hilliard do not differ from experimental results, but at longer time they are very different. It shows that Cahn-Hilliard theory can be explained only at the beginning of phase decomposition. The intensities of Akcasu and Langer-Baron-Miller theories can be used to fit the data better than the other two theories. So these two theories can be used to explain this system at all range of testing. In Fig.5.6, the intensities predicted by Nauman have small error.

5.2.3 Intensity of 50%w TMPC/PS blends (Prepared by Melt Mixed)

Fig.5.7 shows the intensity calculated from various theories of 50%w TMPC/PS blends, that were prepared by melt mixed method at 251 °C and at the angle of 35 °, it appeared that the intensity of Cahn-Hilliard smootly increases with increasing time. It shows that Cahn-Hilliard's theory can be used to explained only at the early stage. The intensities of Akcasu and Langer, Bar-on and Miller, and Nuaman are slightly different from the intensity of experiment. These three theories can be used to explain the spinodal decomposition in this system.

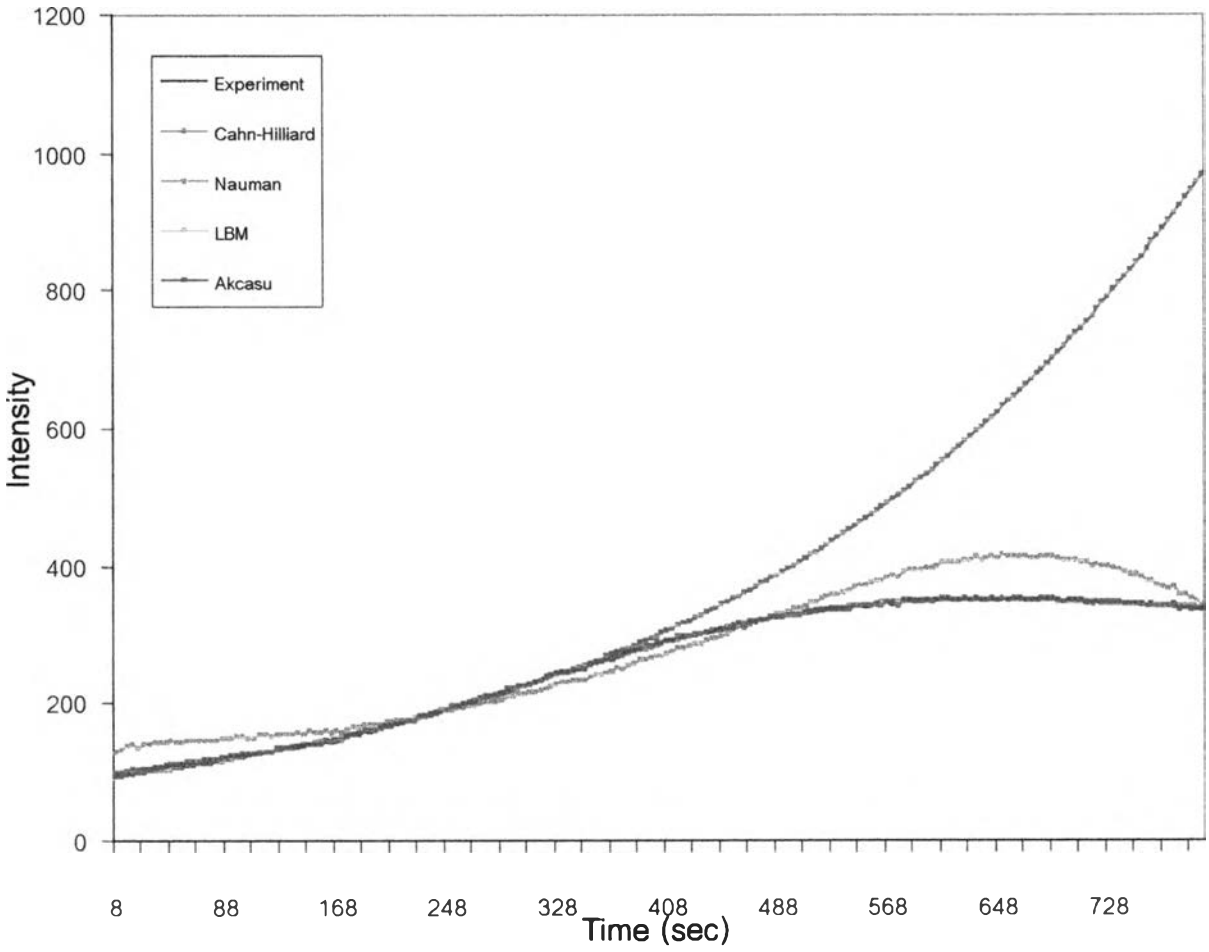

Fig.5.6 The intensity data of 50%w TMPC/PS blends (Prepared by solvent casting) at 239^{o}C and the angle of 35^{o}, obtained from the experiment and calculated from various theories.

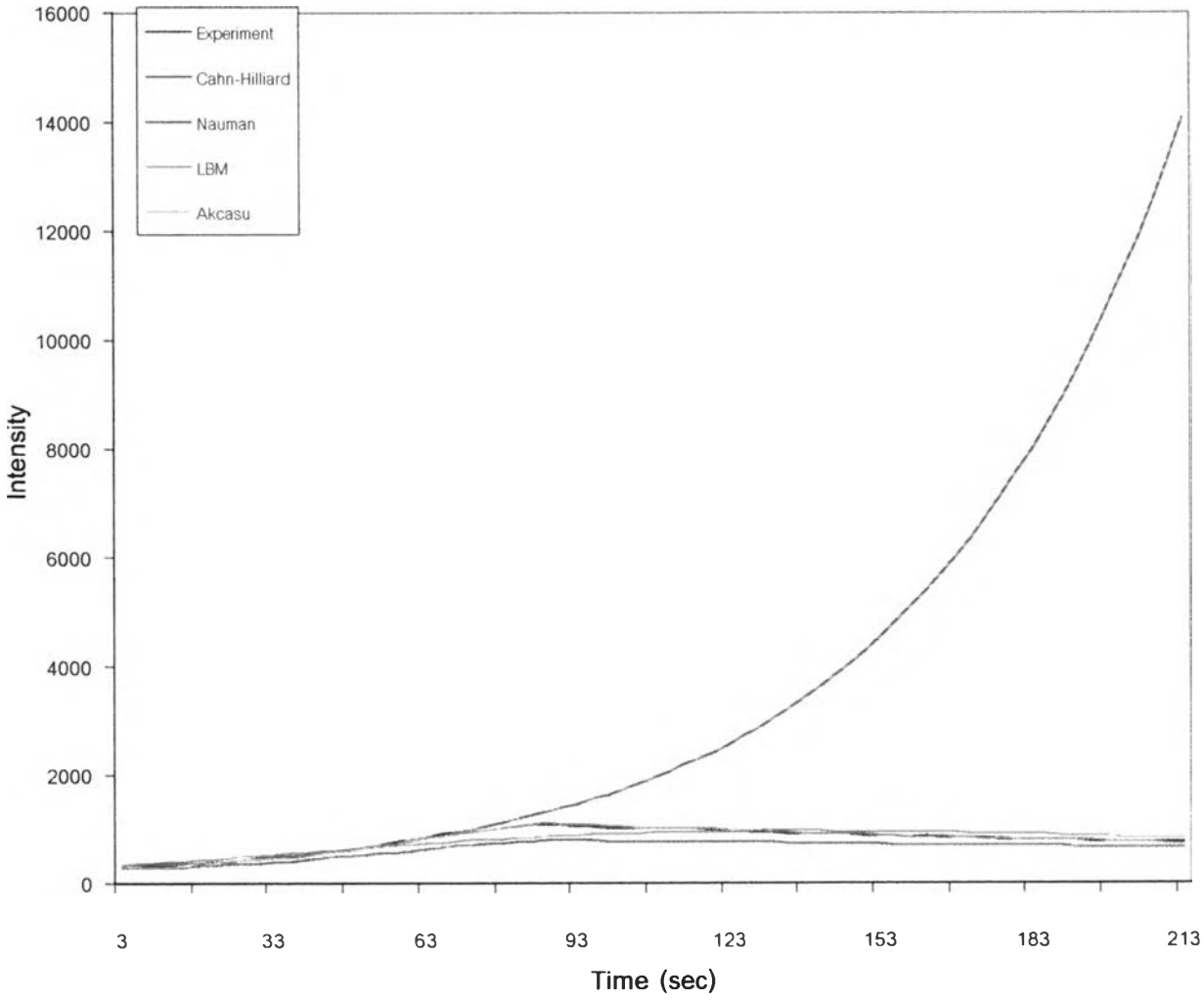

Fig.5.7 The intensity data of 50%w TMPC/PS blends (Prepared by melt mixed) at 251^{o}C and the angle of 35^{o}, obtained from the experiment and calculated from various theories.

5.2.4 Intensity of 70%w TMPC/PS blends

Fig. 5.8 shows the intensity calculated from various theory of 70%w TMPC/PS blends at 297 °C and at the angle of 35 °. It appears that the intensity of Cahn-Hilliard smootly increases with increasing time. For this system, the intensity from Akcasu's theory seems to give the best fit to the experimental data compared with other theories.

5.3 Part I : The Percent Relative Average Error Results of TMPC/PS Blends

The percent relative average error value is calculated by

$$\% \text{ Relative Average Error} = \frac{\sum_{t=1}^{n} \left| \frac{I_{Exp,t} - I_{Th,t}}{I_{Exp,t}} \right| (100)}{n}$$

Where I_{Exp} = Experimental data

I_{Th} = Calculated data of each theory

n = Number of data

t = time

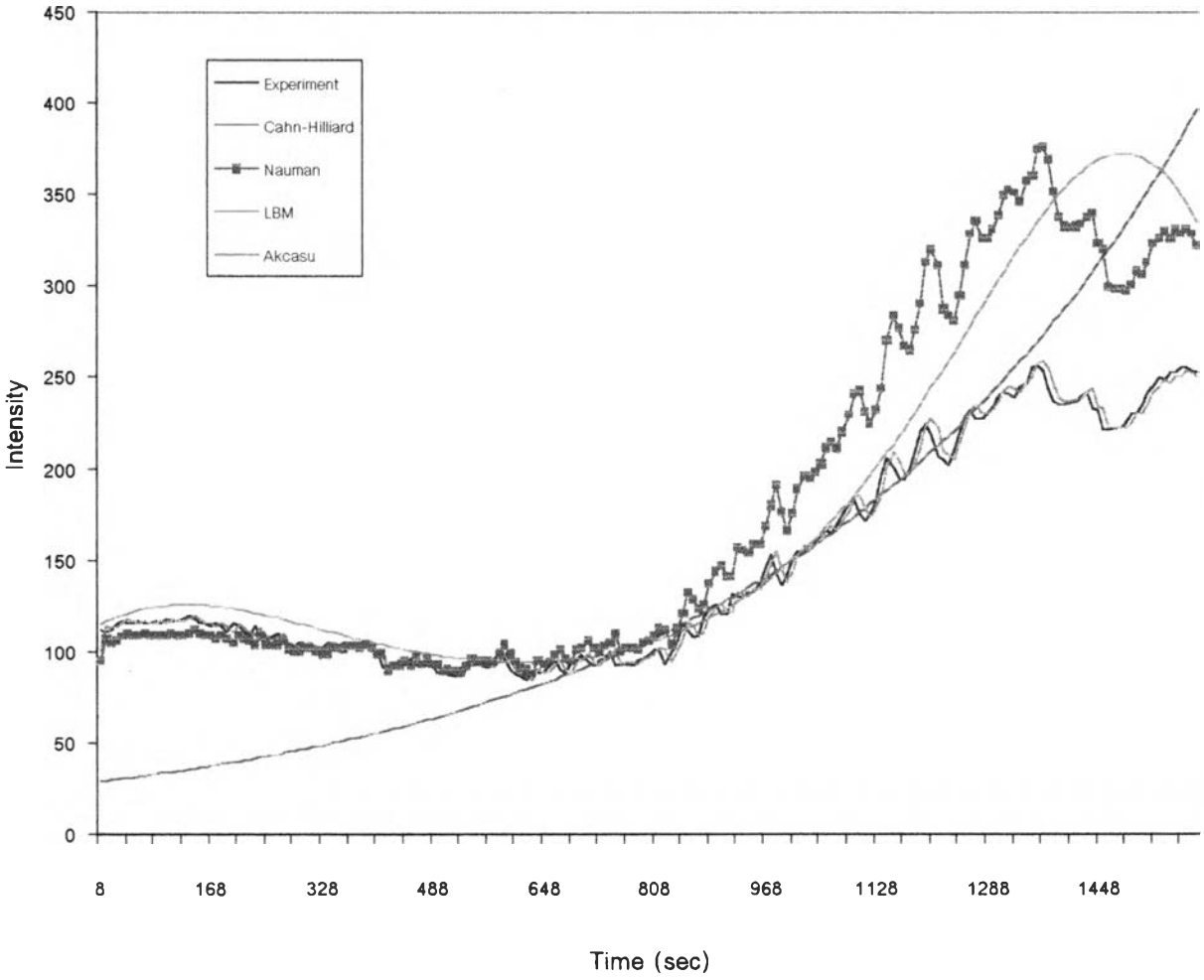

Fig.5.8 The intensity data of 70%w TMPC/PS blends at 297^{o}C and the angle of 35^{o}, obtained from the experiment and calculated from various theories.

5.3.1 The Percent Relative Average Error Results of 30%w TMPC/PS Blends

5.3.1.1 Test of Cahn-Hilliard's Theory

In Fig.5.9, it shows the percent relative average error between experimental and calculated results at any angle. When the angle scattering increased, The percent relative average error increase in all five temperatures from 30% TMPC data. From graph patterns, they show that the different temperatures, the different intensities that predicted from the theories and minus by the real data difference from each other too. At low temperatures have less the percent relative average error values than the higher temperatures. This results shows that the temperature influenced to intensity data of testing, and at low temperature can fit the experimental result better than higher temperatures.

5.3.1.2 Test of Langer, Bar-on and Miller's Theory

In Fig.5.10, it shows the percent relative average error between experiments and from calculated results. When the angle scattering increased, the most of the percent relative average error do not varied in five temperatures.

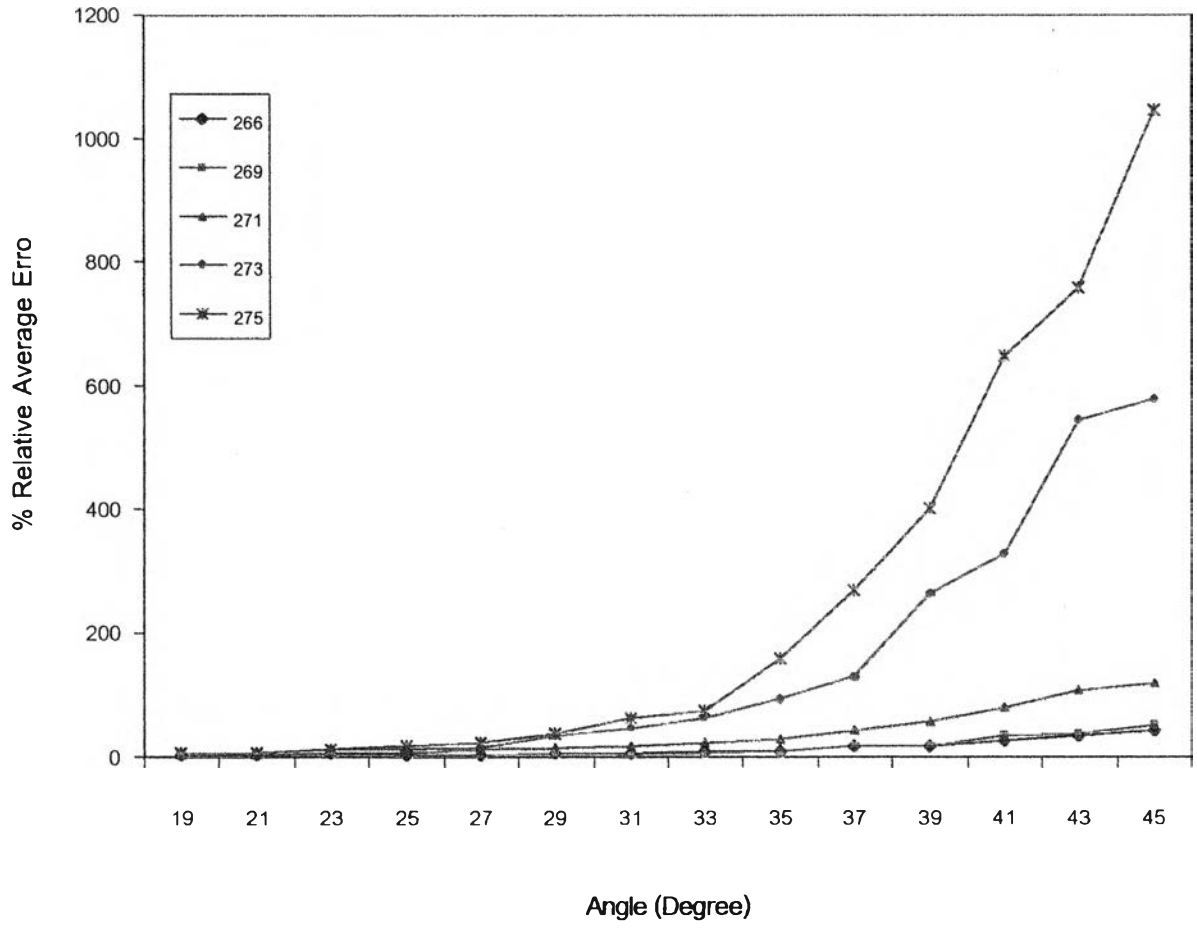

Fig.5.9 The percent relative average error of 30%w TMPC/PS blends at different temperatures, calculated from Cahn-Hilliard's theory.

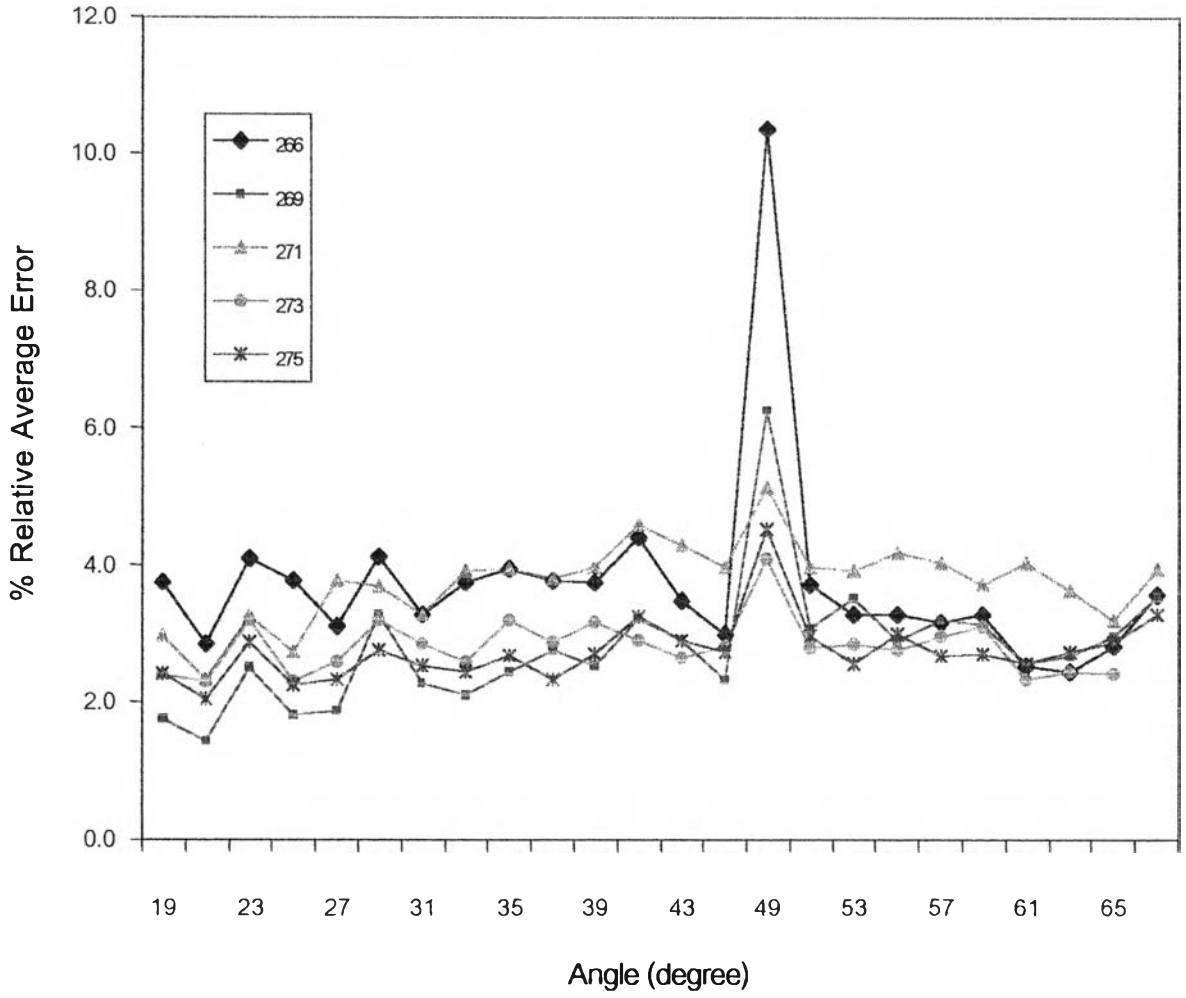

Fig.5.10 The percent relative average error of 30%w TMPC/PS blends at different temperatures, calculated from Langer, Bar-on and Miller's theory.

5.3.1.3 Test of Akcasu's Theory

In Fig.5.11, it shows the percent relative average error between experiment and calculated results. When the angle scattering increased, the most of the percent relative average error values do not varied in five temperatures, and the graph pattern like as Langer, Bar-on and Miller's (Fig 5.10). At 266, 269, 271°C have less the percent relative average error value than the higher temperatures (273, 275°C). This results show that the temperatures will incline to influence the fit data of testing and at low temperatures can fit experimental results better than higher temperatures.

5.3.1.4 Test of Nauman's Theory

From the fitted experimental data of Nauman's theory, show data that the high temperature data have less total difference value than the lower temperature data. The intensities differ from other theory. At 266°C have high difference from experimental result as show in Fig. 5.12. The percent relative average error increased at low angle, and decreased at high angle.

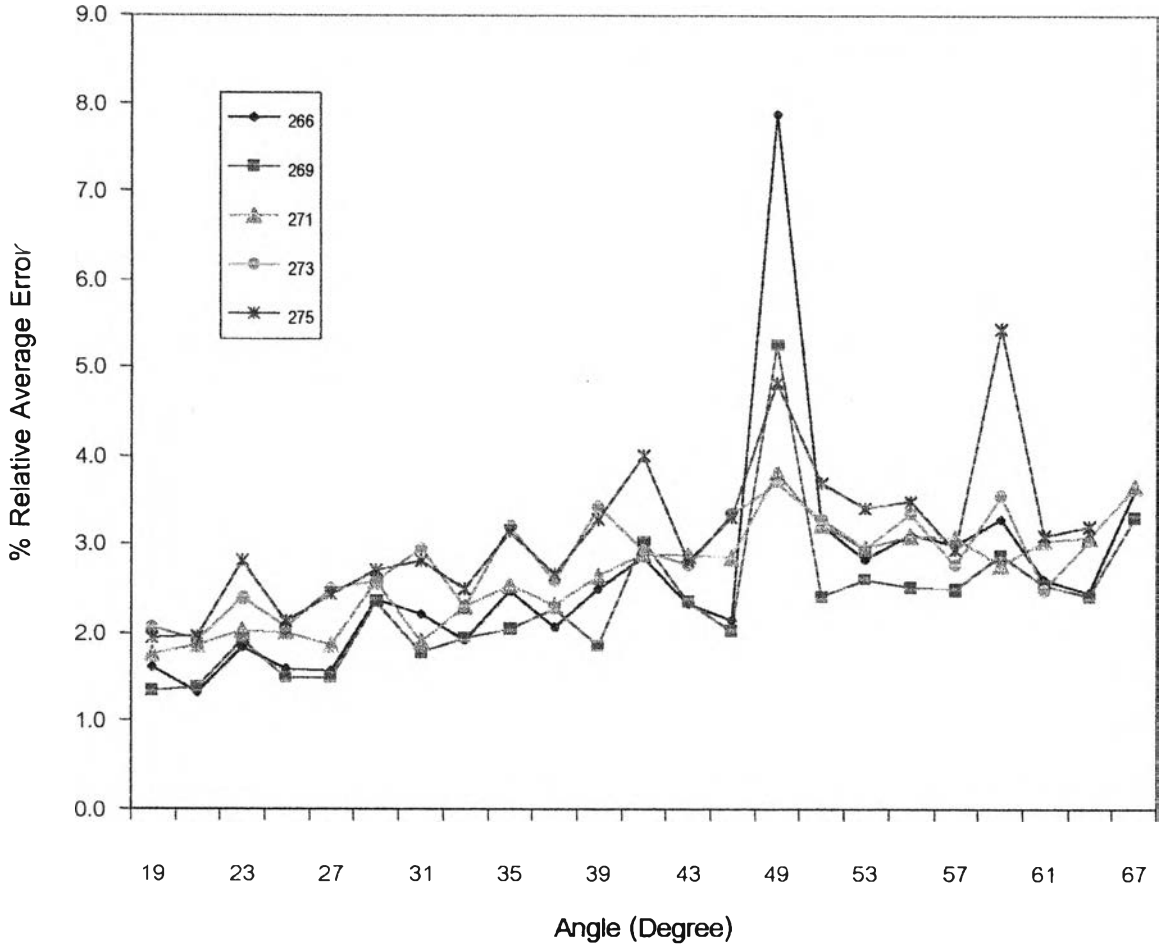

Fig.5.11 The percent relative average error of 30%w TMPC/PS blends at different temperatures, calculated from Akcasu's theory.

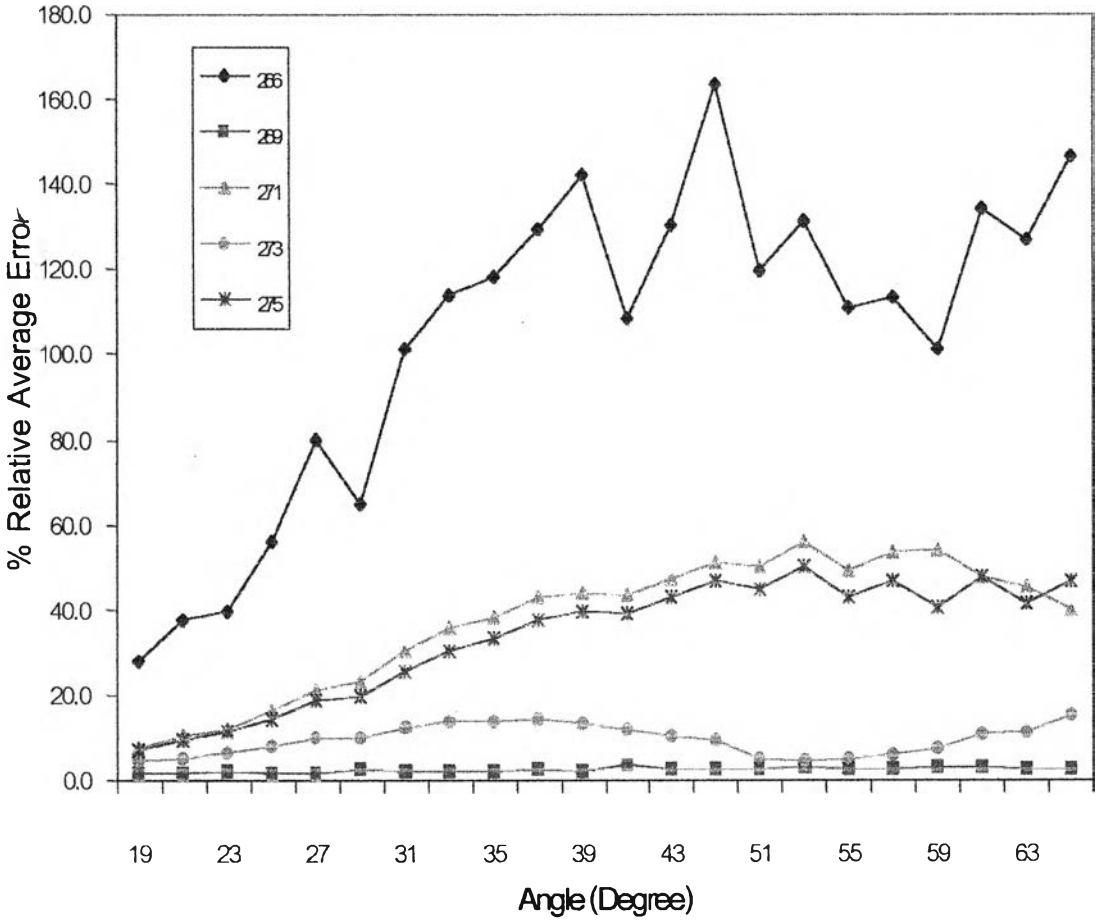

Fig.5.12 The percent relative average error of 30%w TMPC/PS blends at different temperatures, calculated from Nauman's theory.

5.3.2 The Percent Relative Average Error of 50% TMPC/PS Blends Results, Prepared by Solvent Casting

5.3.2.1 Test of Cahn-Hilliard's Theory

In Fig.5.13, it shows the percent relative average error between experimental data and calculated results. When the angle for scattered intensity increased, the percent relative average error values increased for every temperature. From graph patterns, they it seem to be that the higher temperatures induce an increase in the percent relative average error values. At low temperatures, the percent relative average error value is less than that of the higher temperatures data at every angle. It showed that at low temperature the Cahn-Hilliard theory can be used to fit experimental results better than at higher temperature data. At high temperature (247°C), biggest derivation from experimental results was observed for the case of Cahn-Hilliard theory.

5.3.2.2 Test of Langer, Bar-on and Miller's Theory

In Fig. 5.14, At the temperature of 237, 239, 242 °C, the percent relative average error do not vary much for all angles. But for the temperature of 245, 247 °C, it showed higher error values, especially at high angle range.

5.3.2.3 Test of Akcasu's Theory

In Fig.5.15, it shows that as the angle increased, the percent relative average error values increased for every temperature. Furthermore, the percent relative average error is indifferent as changing temperature. It shows that the intensity from Akcasu's theory can fit well with experimental results.

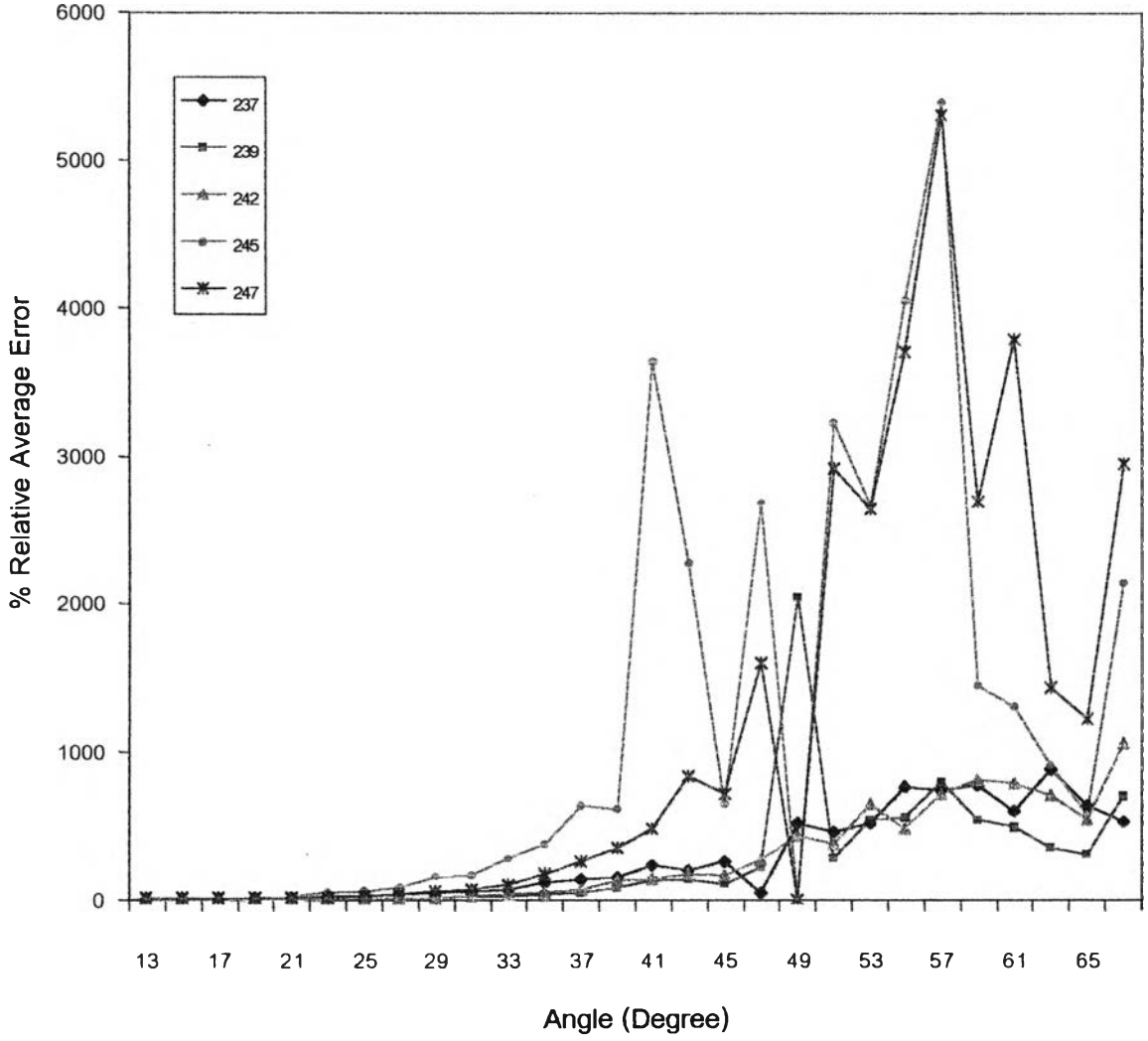

Fig.5.13 The percent relative average error of 50%w TMPC/PS blends (Prepared by solvent casting) at different temperatures, calculated from Cahn-Hilliard's theory.

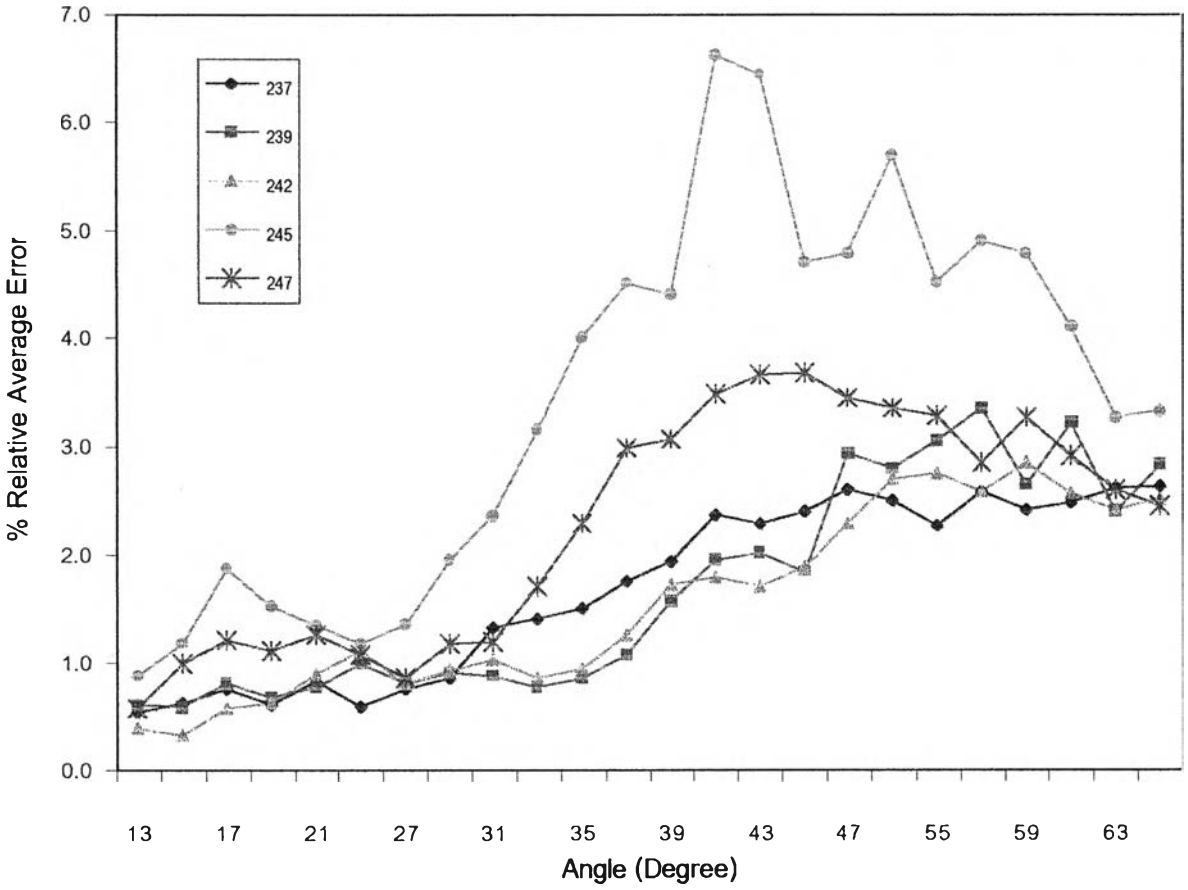

Fig.5.14 The percent relative average error of 50%w TMPC/PS blends (Prepared by solvent casting) from five temperatures, calculated from Langer, Bar-on and Miller's theory.

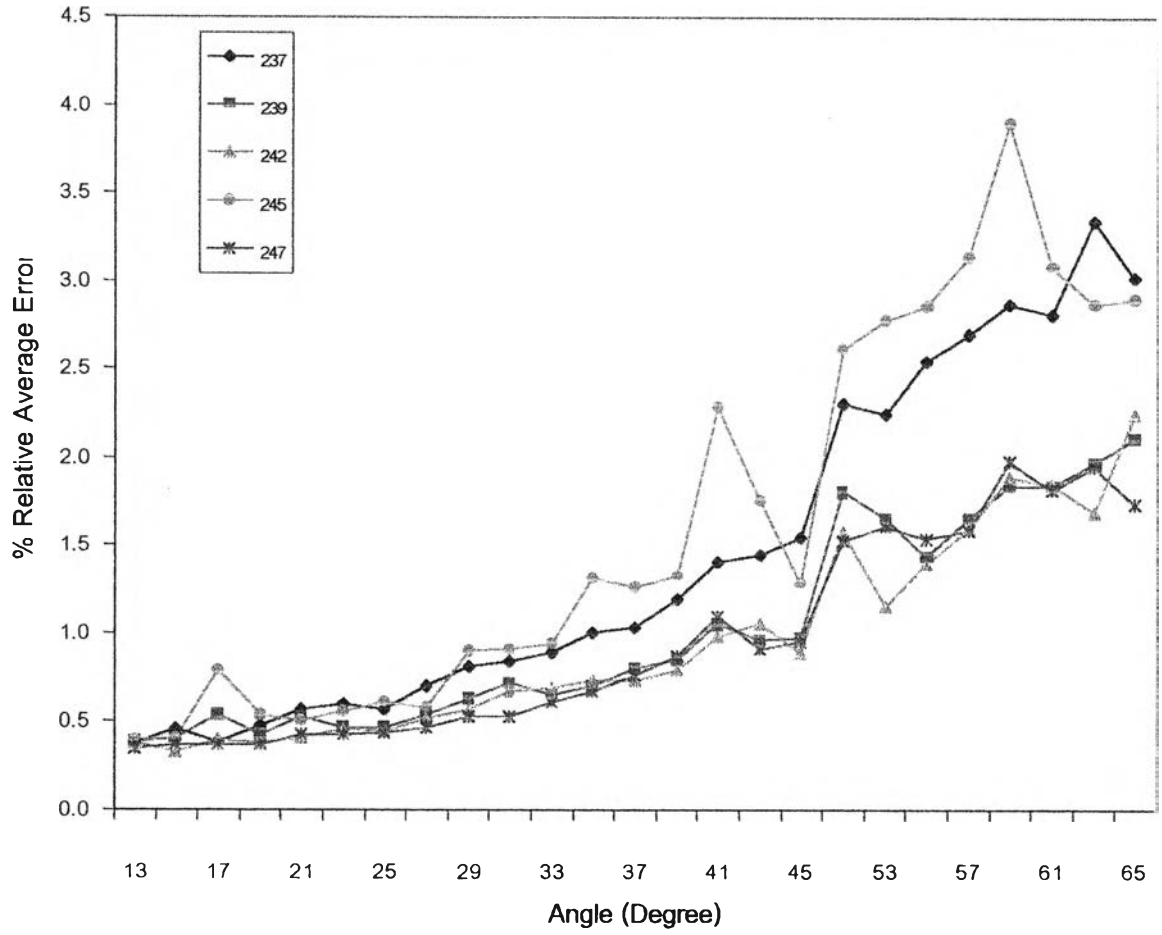

Fig.5.15 The percent relative average error of 50%w TMPC/PS blends (Prepared by solvent casting) from five temperatures, calculated from Akcasu's theory.

5.3.2.4 Test of Nauman's Theory

In Fig. 5.16, it shows that the percent relative average error at 239, 242, 245°C are smooth while the ones at 237, 247°C are considerably different. It shows that at 237, 247°C are the percent relative average error not in a good fit by this theory.

5.3.3 The Percent Relative Average Error Results of 50% TMPC/PS Blends, Prepared by Melt Mixed

5.3.3.1 Test of Cahn-Hilliard's Theory

Fig.5.17-1 shows the percent relative average error of 50%w TMPC/PS blends at 249, 250, 251 and 252°C. Fig.5.17-2 shows the percent relative average error of 50%w TMPC/PS blends at 253°C. They show that the percent relative average error at the highest temperature (253°C) are the biggest values as the angle increases, and they are different from other temperatures. This results show that at high temperature the Cahn-Hilliard theory is not in a good fit with the experimental data.

5.3.3.2 Test of Langer, Bar-on and Miller's Theory

In Fig. 5.18, it shows that when the angle increased, the percent relative average error do not vary at every temperature. These results show the intensity from Langer, Bar-on and Miller's theory can fit with the experimental results.

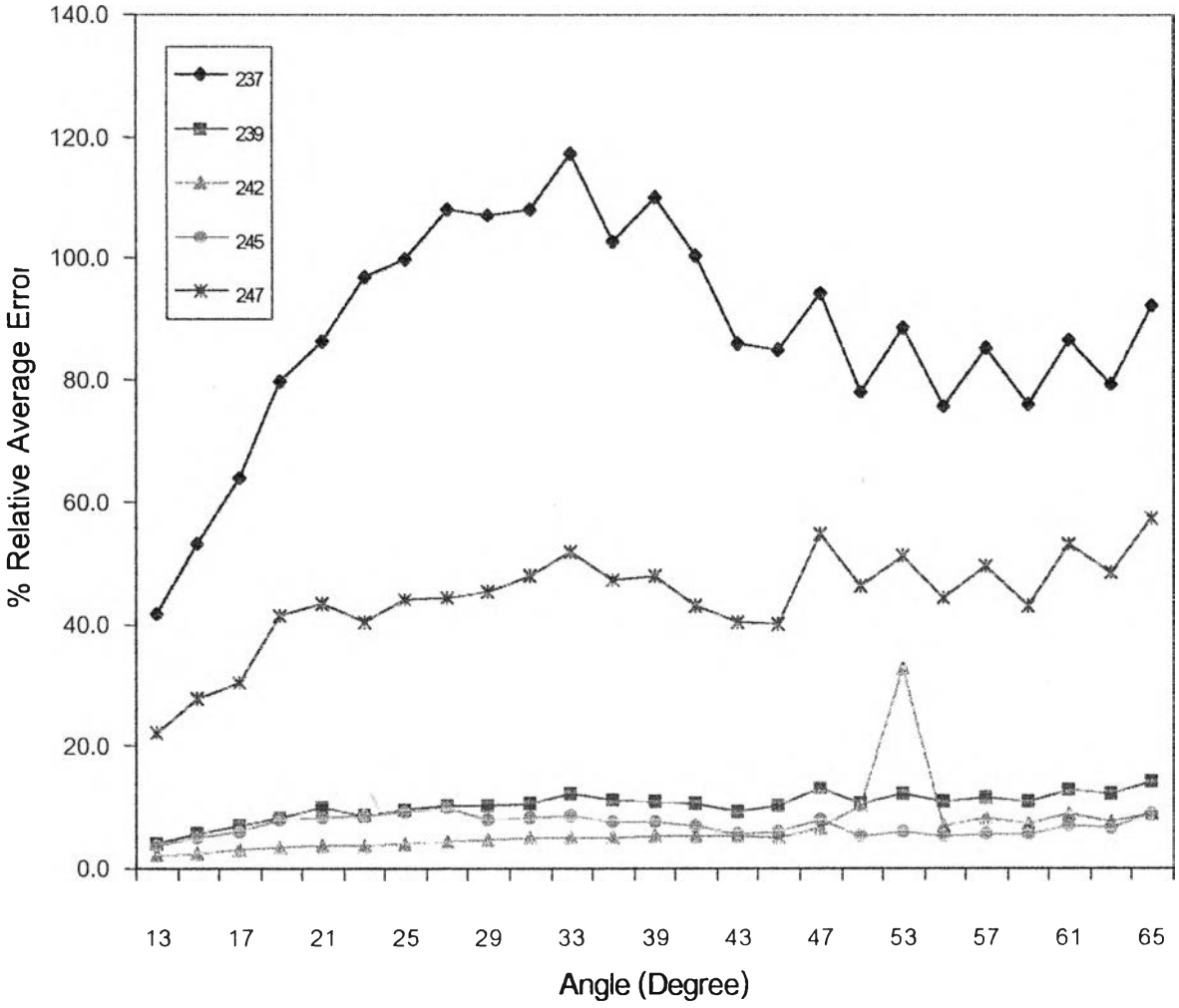

Fig.5.16 The percent relative average error of 50%w TMPC/PS blends (Prepared by solvent casting) from five temperatures, calculated from Nauman's theory.

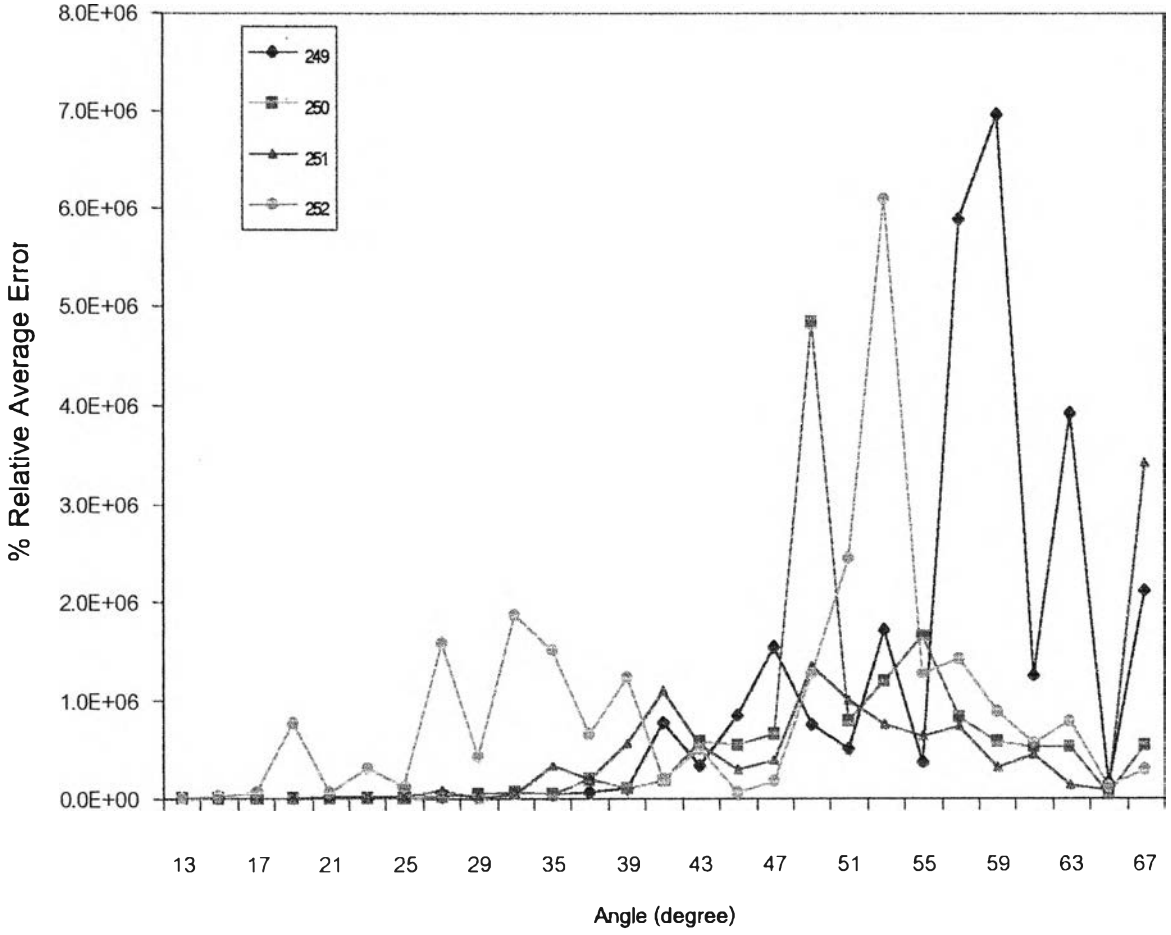

Fig.5.17-1 The percent relative average error of 50%w TMPC/PS blends (Prepared by melt mixed) at four temperatures, calculated from Cahn-Hilliard's theory.

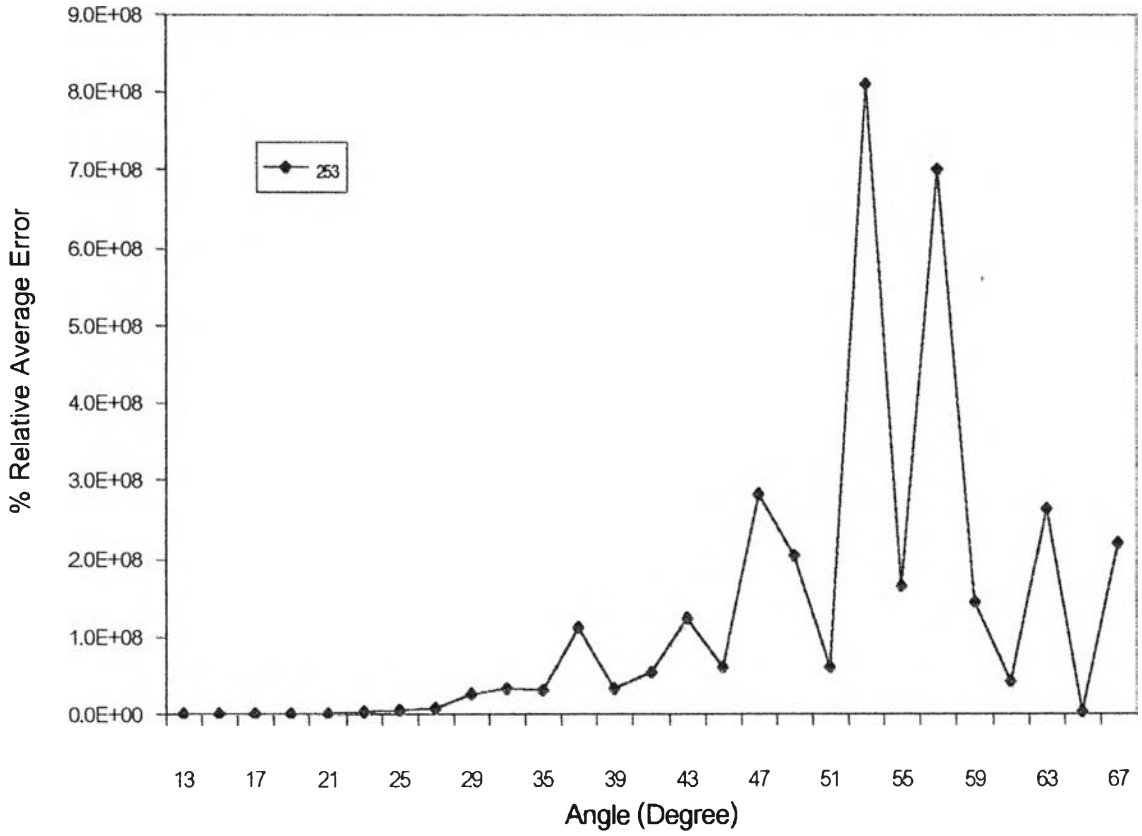

Fig.5.17-2 The percent relative average error of 50%w TMPC/PS blends (Prepared by melt mixed) at one temperature, calculated from Cahn-Hilliard's theory.

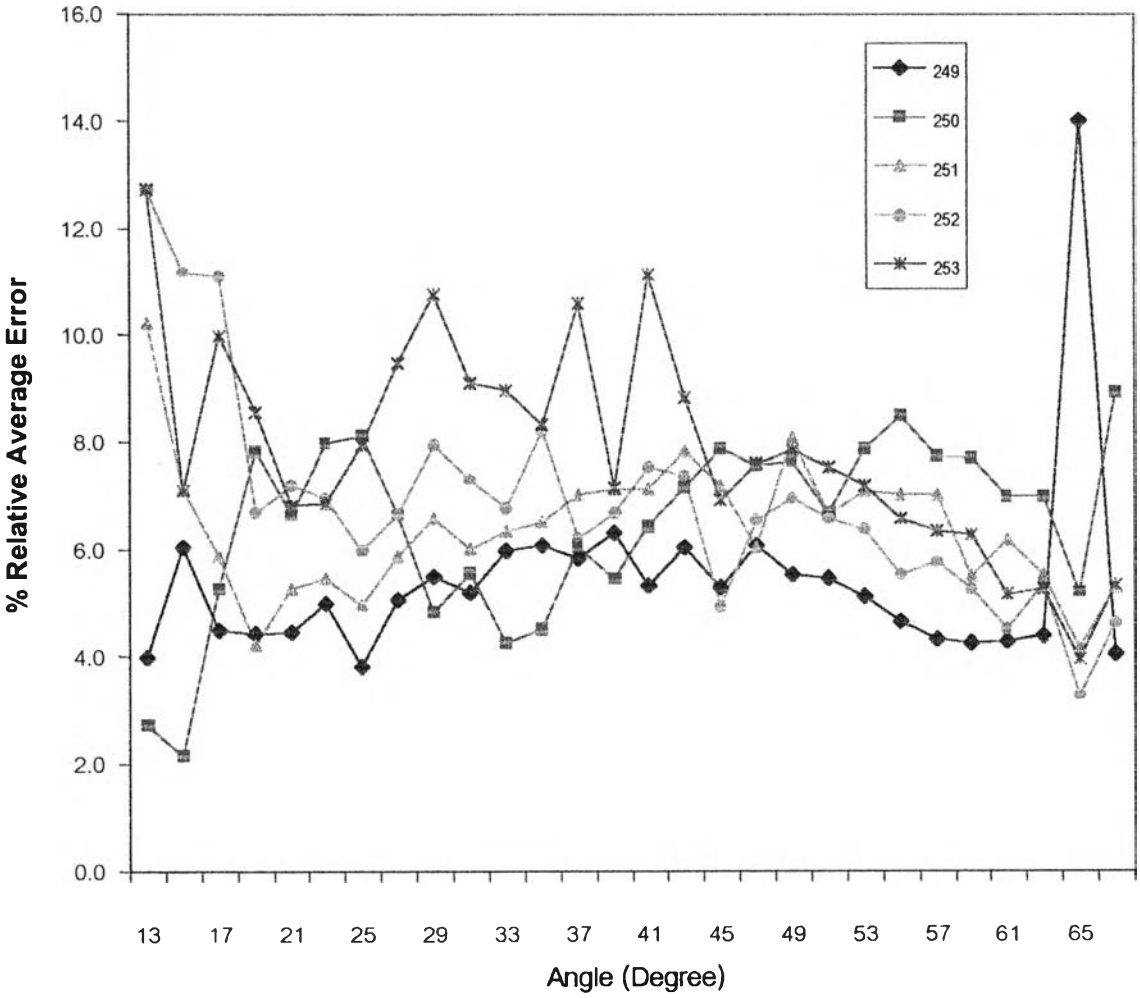

Fig.5.18 The percent relative average error of 50%w TMPC/PS blends (Prepared by melt mixed) from five temperatures, calculated from Langer, Bar-on and Miller's theory.

5.3.3.3 Test of Akcasu's Theory

In Fig 5.19, it shows that at 249 °C the system has the biggest percent relative average error and the error decreased with increasing angles. At other temperatures the error is similar and slightly decreases with increasing angles.

5.3.3.4 Test of Nauman's Theory

In Fig. 5.20, it shows that the percent relative average error slightly decrease with increasing angles at every temperature. It appeared that at high angle, the data can be better fitted by Nauman's theory than at the lower angle data.

5.3.4 The Percent Relative Average Error Results of 70% TMPC/PS Blends

5.3.4.1 Test of Cahn-Hilliard's Theory

In Fig. 5.21, it shows that for the percent relative average error of 70% TMPC/PS blends, the lower temperatures are, the smaller the percent relative average error values are. At 301 °C, the experimental data do not well fit by Cahn-Hilliard theory. It appeared that at higher temperatures the Cahn-Hilliard theory can not fit well with the experimental data for this system.

5.3.4.2 Test of Langer, Bar-on and Miller's Theory

In Fig 5.22, it shows that the percent relative average error slightly change at different temperatures, they appeared that these results of fitted data are not very different. But at 297°C and low angle values, the percent relative average error are quite high.

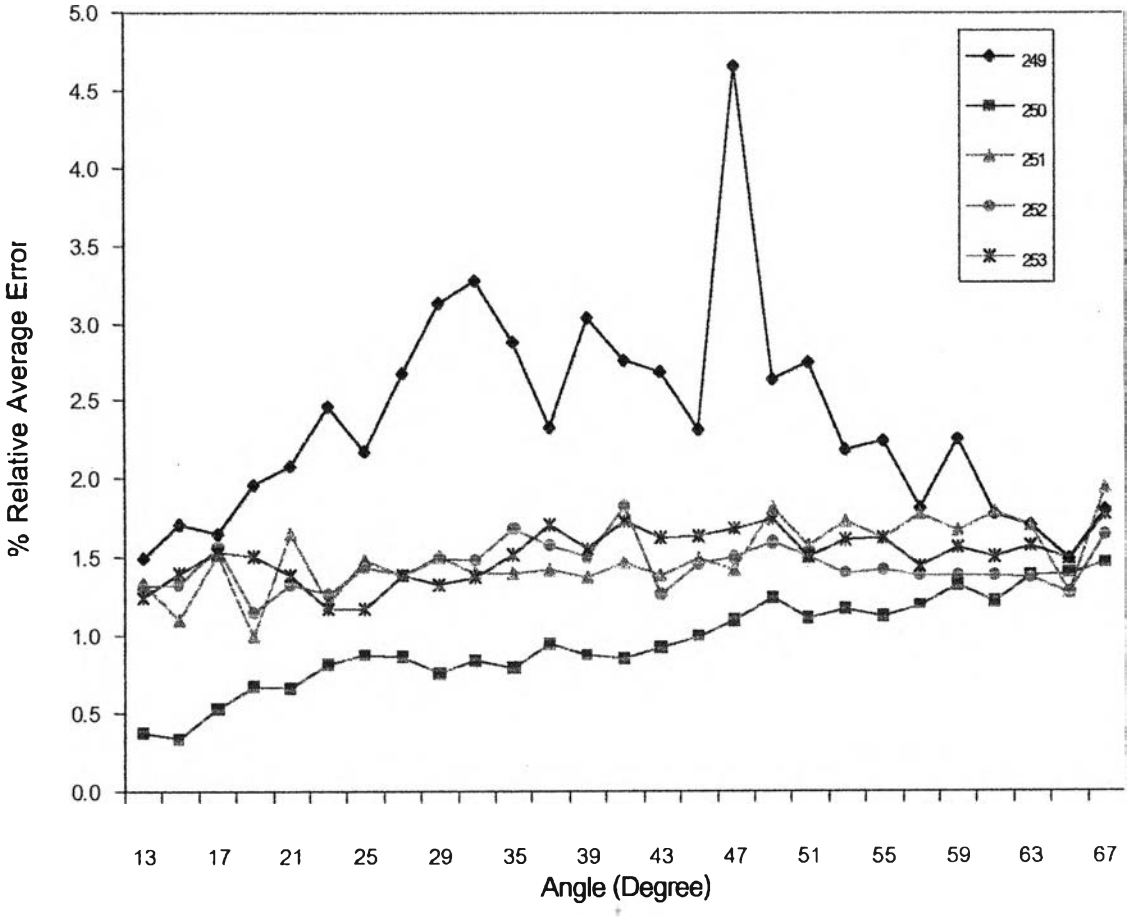

Fig.5.19 The percent relative average error of 50%w TMPC/PS blends (Prepared by melt mixed) from five temperatures, calculated from Akcasu's theory.

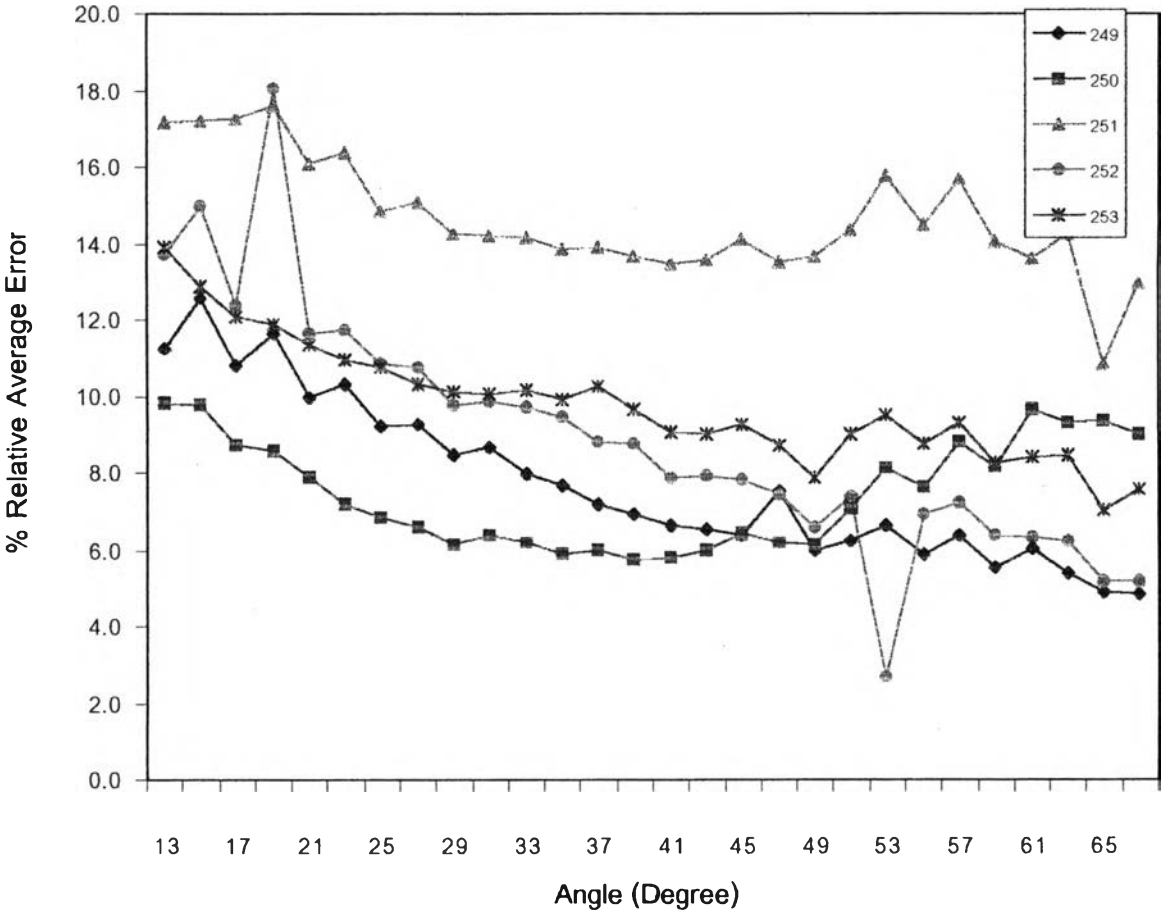

Fig.5.20 The percent relative average error of 50%w TMPC/PS blends (Prepared by melt mixed) from five temperatures, calculated from Nauman's theory.

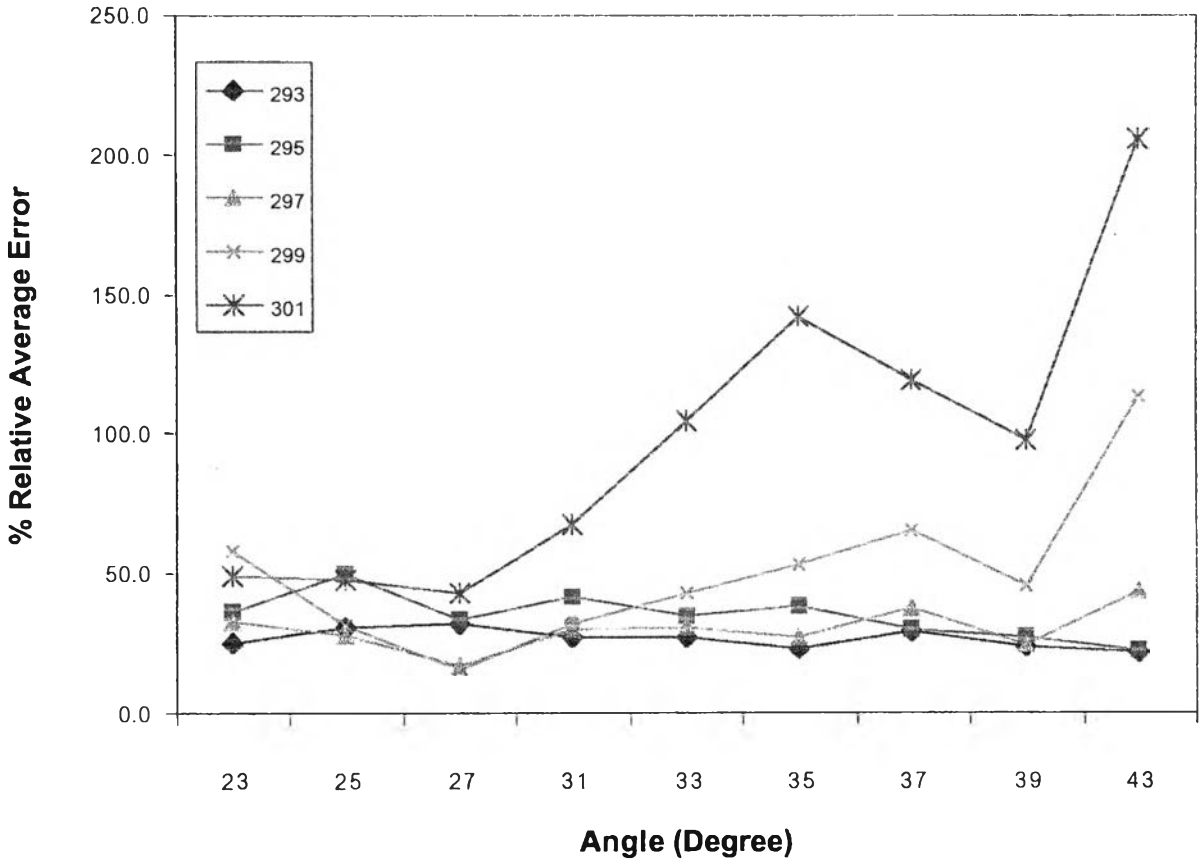

Fig.5.21 The percent relative average error of 70%w TMPC/PS blends from five temperatures, calculated from Cahn-Hilliard's theory.

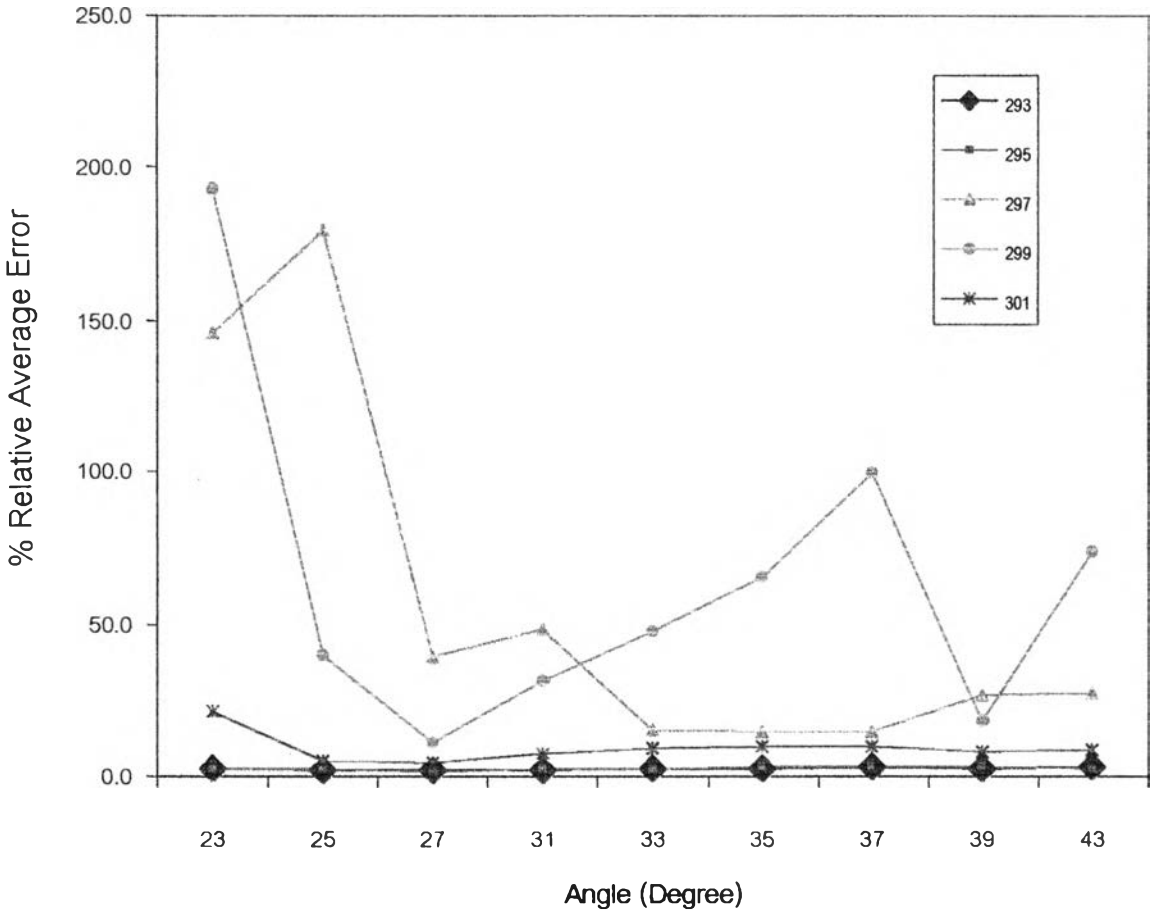

Fig.5.22 The percent relative average error of 70%w TMPC/PS blends from five temperatures, calculated from Langer, Bar-on and Miller's theory.

5.3.4.3 Test of Akcasu's Theory

In Fig. 5.23, it shows that for the percent relative average error of 70% TMPC/PS blends, the lower the temperatures are, the smaller the percent relative average error values are. At 301 °C, the experimental data do not well fit by Akcasu theory. It appeared that at higher temperatures the Akcasu theory can not fit well with the experimental data for this system.

5.3.4.4 Test of Nauman's Theory

In Fig 5.24, it shows that the percent relative average error slightly change at different temperatures, they appeared that these results of fitted data are not very different. But at 299°C and low angle values, the percent relative average error are quite high.

5.3.5 Comparison of 50%TMPC/PS Blends Prepared by Solvent Casting Method and Melt Mixed Method.

5.3.5.1 Comparison Results of Cahn-Hilliard's Theory

In Fig.5.25, it shows the percent relative average error of 50%TMPC/PS blends prepared by solvent cast and melt mixed methods. It appeared that the percent relative average error of solvent cast sample is mush less than the percent relative average error of melt mixed one at every angle. The percent relative average error of solvent cast sample seem to increase with increasing angles. These results from sample prepared by solvent cast method can be fit with the Cahn-Hilliard thery better than that from melt mixed method.

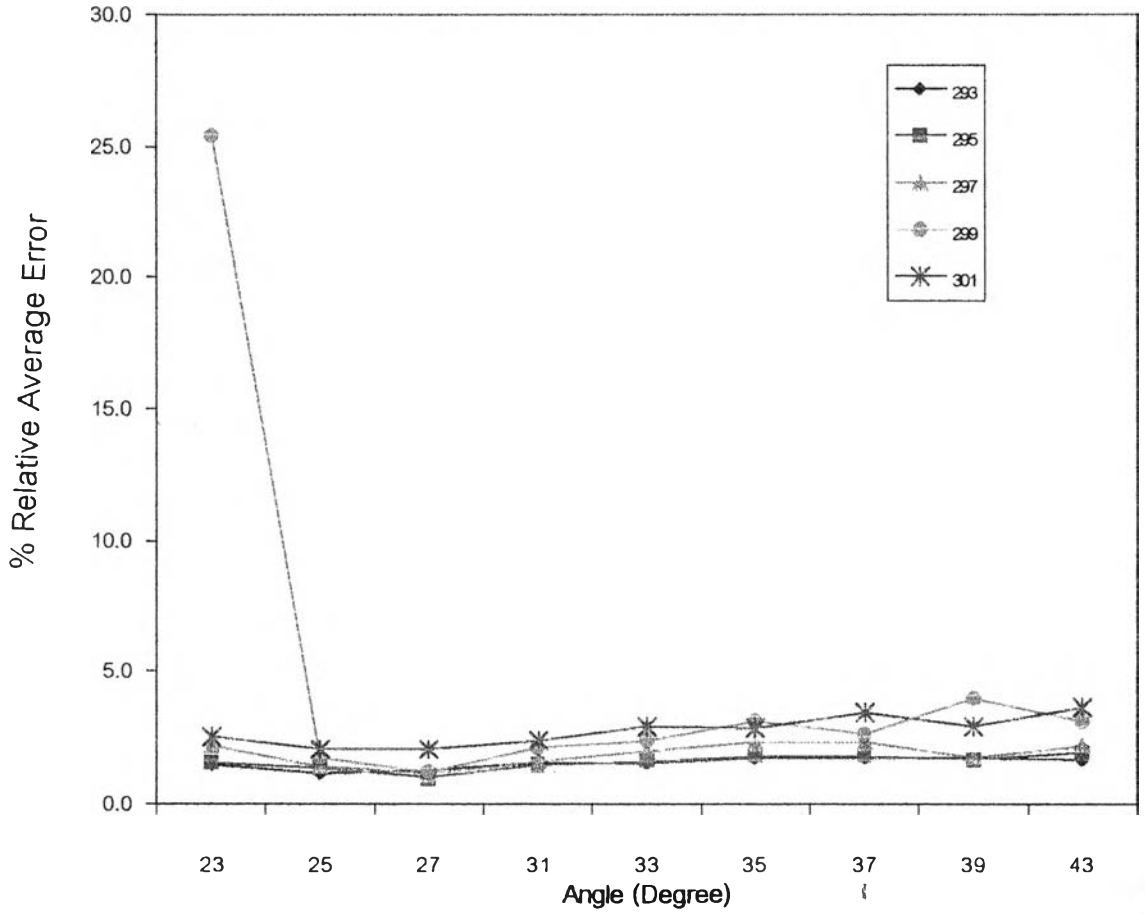

Fig.5.23 The percent relative average error of 70%w TMPC/PS blends from five temperatures, calculated from Akcasu's theory.

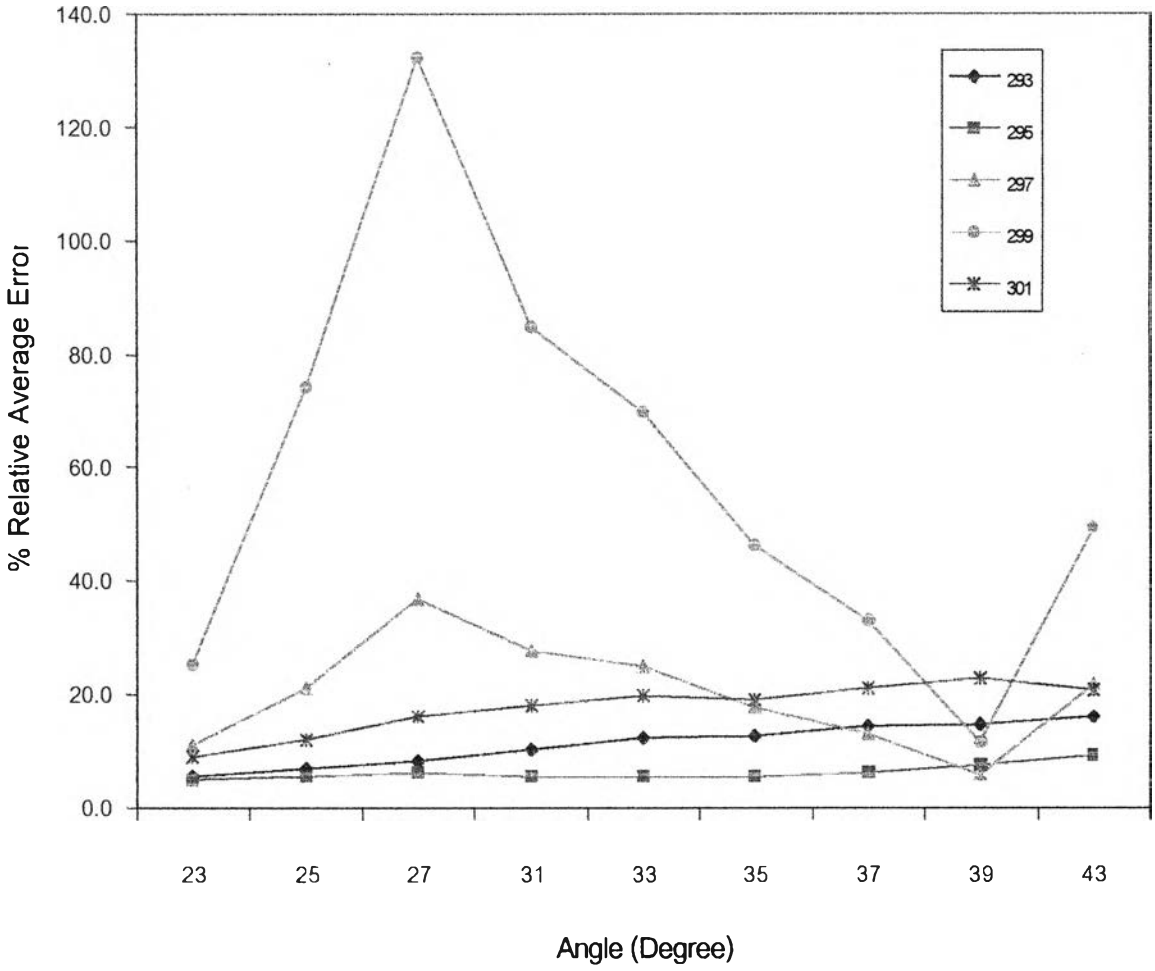

Fig.5.24 The percent relative average error of 70%w TMPC/PS blends from five temperatures, calculated from Nauman's theory.

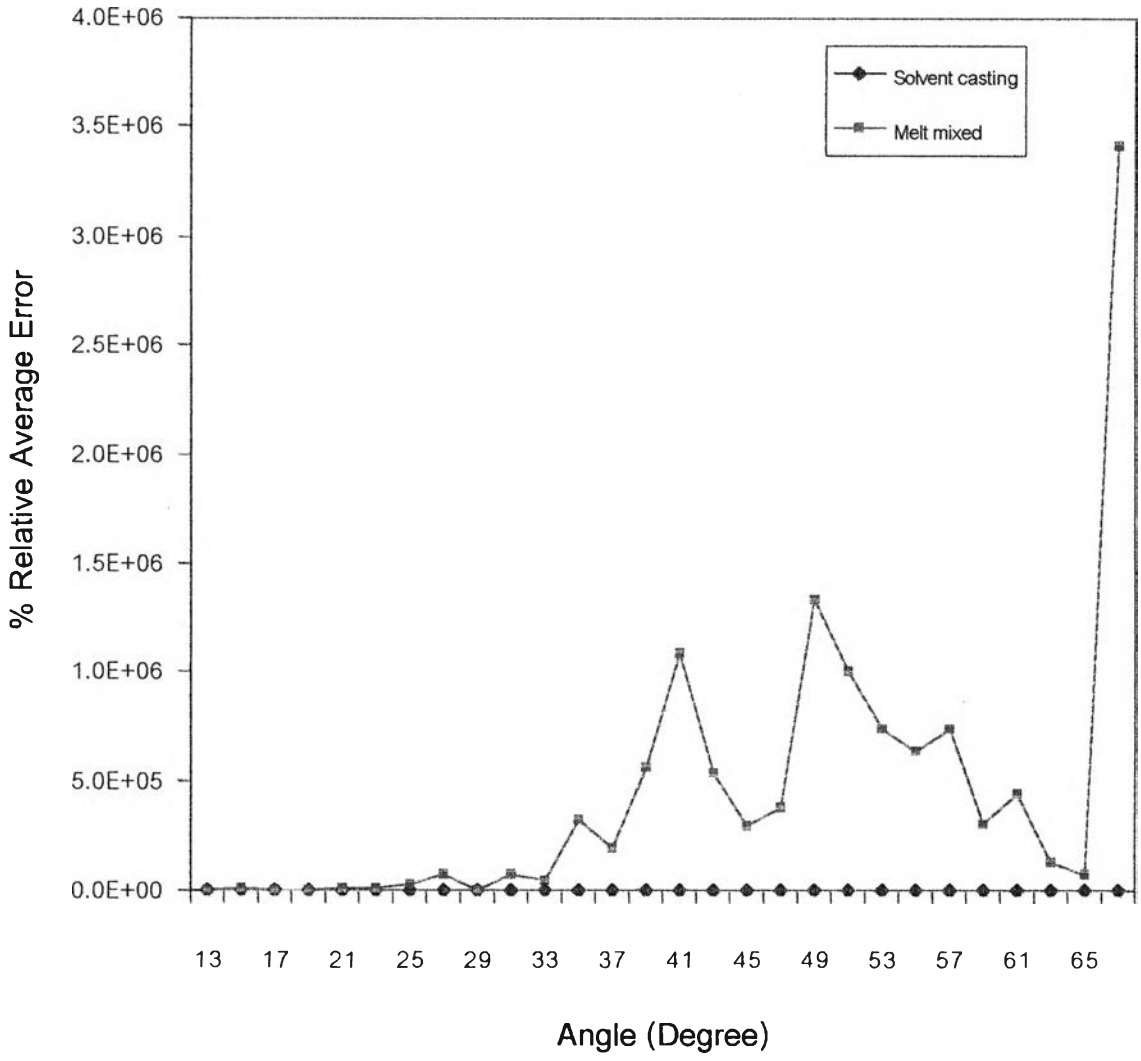

Fig.5.25 The percent relative average error of 50%w TMPC/PS blends calculated from Cahn-Hilliard's theory, prepared by solvent casting at 242 °C and prepared by melt mixed at 251 °C.

5.3.5.2 Comparison Results of Langer, Bar-on and Miller's Theory

In Fig.5.26, it shows the percent relative average error of 50%TMPC/PS blends prepared by solvent cast and melt mixed methods. It appeared that the percent relative average error of solvent cast sample is mush less than the percent relative average error of melt mixed one at every angle. These results from sample prepared by solvent cast method can be fit with the Langer, Bar-on and Miller theory better than that from melt mixed method.

5.3.5.3 Comparison Results of Akcasu's Theory

In Fig.5.27, it shows the percent relative average error of 50%TMPC/PS blends prepared by solvent cast and melt mixed methods. It appeared that the percent relative average error of solvent cast sample is mush less than the percent relative average error of melt mixed one at every angle. The percent relative average error of solvent cast sample increase with increasing angles. These results from sample prepared by solvent cast method can be fit with the Akcasu theory better than that from melt mixed method.

5.3.5.4 Comparison Results of Nauman's Theory

In Fig.5.28, it shows the percent relative average error of 50%TMPC/PS blends prepared by solvent cast and melt mixed methods. It appeared that the percent relative average error of solvent cast sample is mush less than the percent relative average error of melt mixed one at every angle. The percent relative average error of melt mixed sample decrease with increasing angles. These results from sample prepared by solvent cast method can be fit with the Nauman theory better than that from melt mixed method.

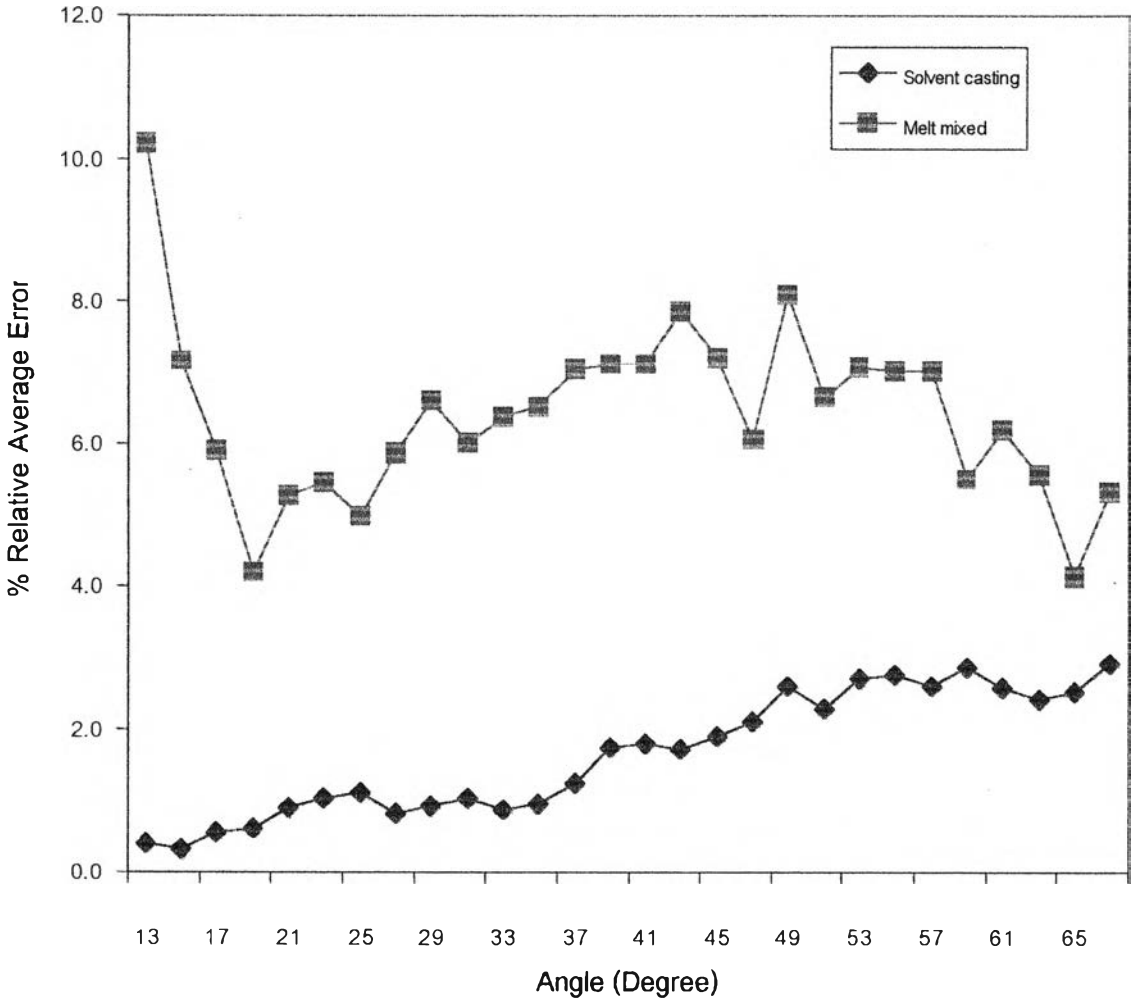

Fig.5.26 The percent relative average error of 50%w TMPC/PS blends calculated from Langer, Bar-on and Miller's theory, prepared by solvent casting at 242 °C and prepared by melt mixed at 251 °C.

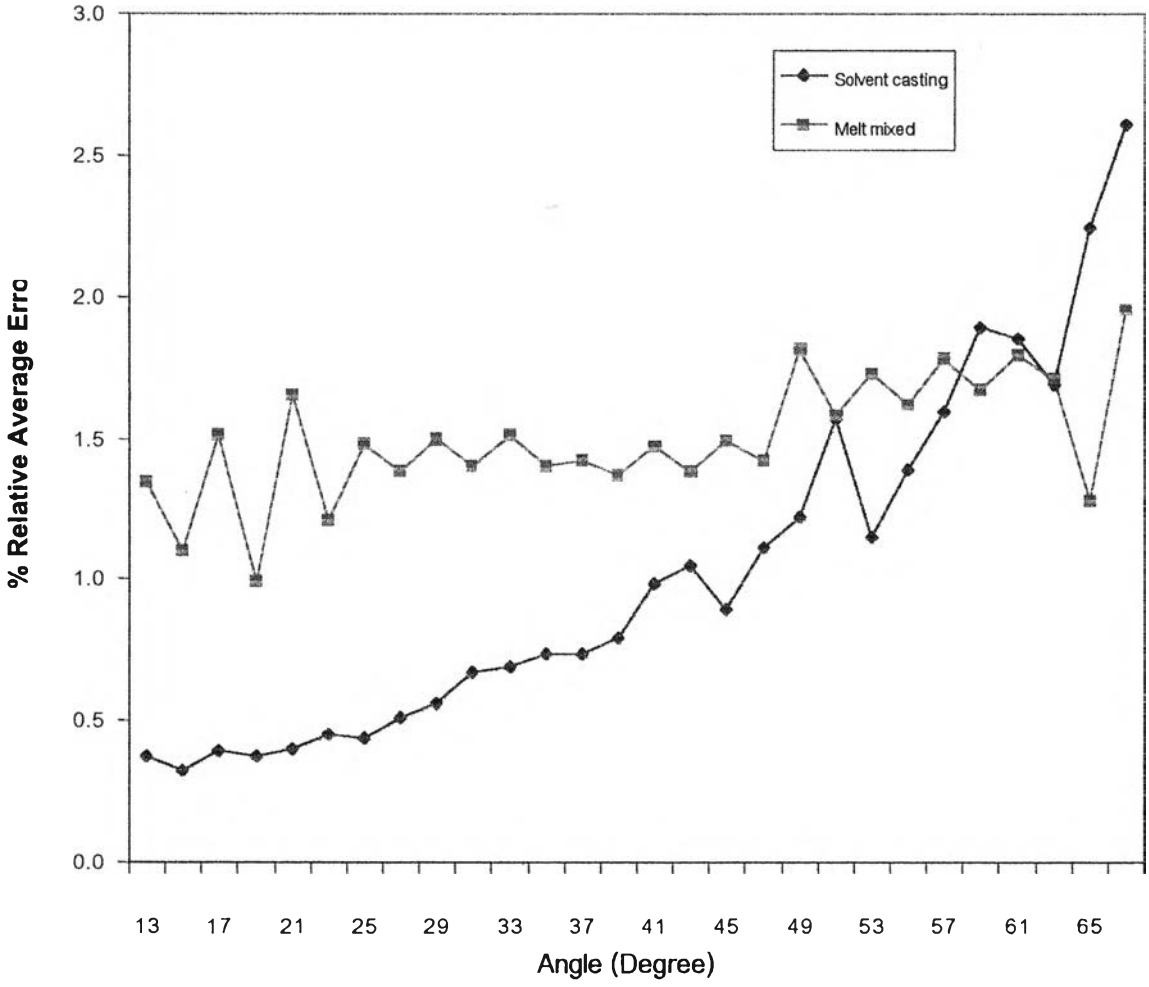

Fig.5.27 The percent relative average error of 50%w TMPC/PS blends calculated from Akcasu's theory, prepared by solvent casting at 242 °C and prepared by melt mixed at 251 °C.

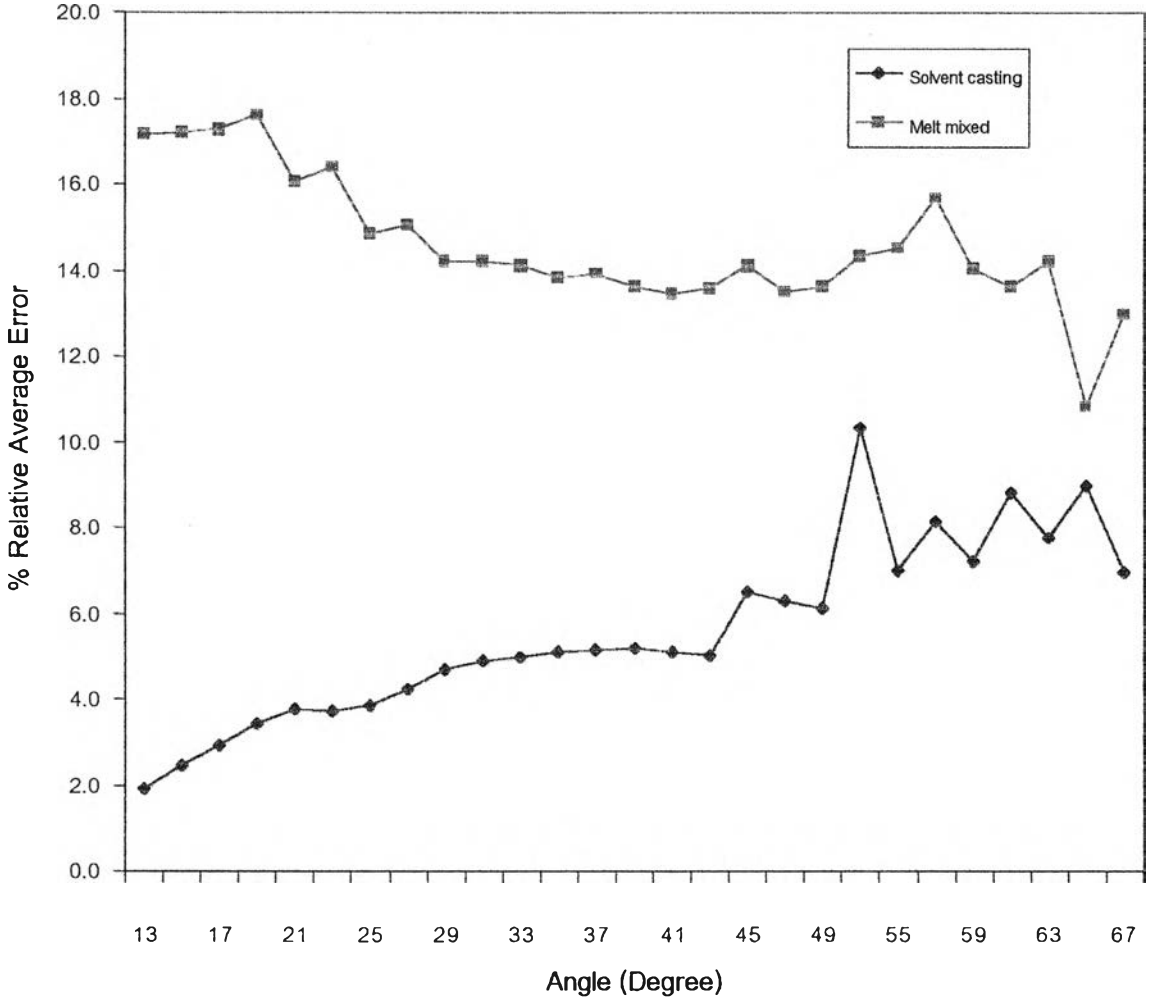

Fig.5.28 The percent relative average error of 50%w TMPC/PS blends calculated from Nauman's theory, prepared by solvent casting at 242 °C and prepared by melt mixed at 251 °C.

5.3.6 Comparison of each Theory

5.3.6.1 Comparison of each theory on 30%TMPC/PS Blends

In Fig. 5.29, it shows the percent relative average error of 30%w TMPC/PS blends at 266 °C. It appeared that Langer, Bar-on and Miller's, and Akcasu's theories give less difference than Canh-Hilliard and Nauman. It shows Akcasu's and Langer, Bar-on and Miller 's theories can fit experimental data better than other two theories.

In Fig. 5.30, it shows the percent relative average error of 30%w TMPC/PS blends at 269 °C. It appeared that at small angle, the percent relative average error of each theory is small, but at high angle the percent relative average error of Cahn-Hilliard increase. The percent relative average error from Langer, Bar-on and Miller's, and Akcasu's and Nauman's theories are not different among each other.

In Fig.5.31, it shows the percent relative average error of 30%w TMPC/PS blends at 271°C. The percent relative average error from Langer, Bar-on and Miller's, and Akcasu's theories are small. These two theories can fit with experimental data better than the Cahn-Hilliard's and Nauman's theories, and can be used to explain the phase separation data more widely.

In Fig.5.32, it shows the percent relative average error of 30%w TMPC/PS blends at 273 °C. The percent relative average error from Langer, Bar-on and Miller's, and Akcasu's theories are small. These two theories can fit with experimental data better than the Cahn-Hilliard's and Nauman's theories, and can be used to explain the phase separation data more widely.

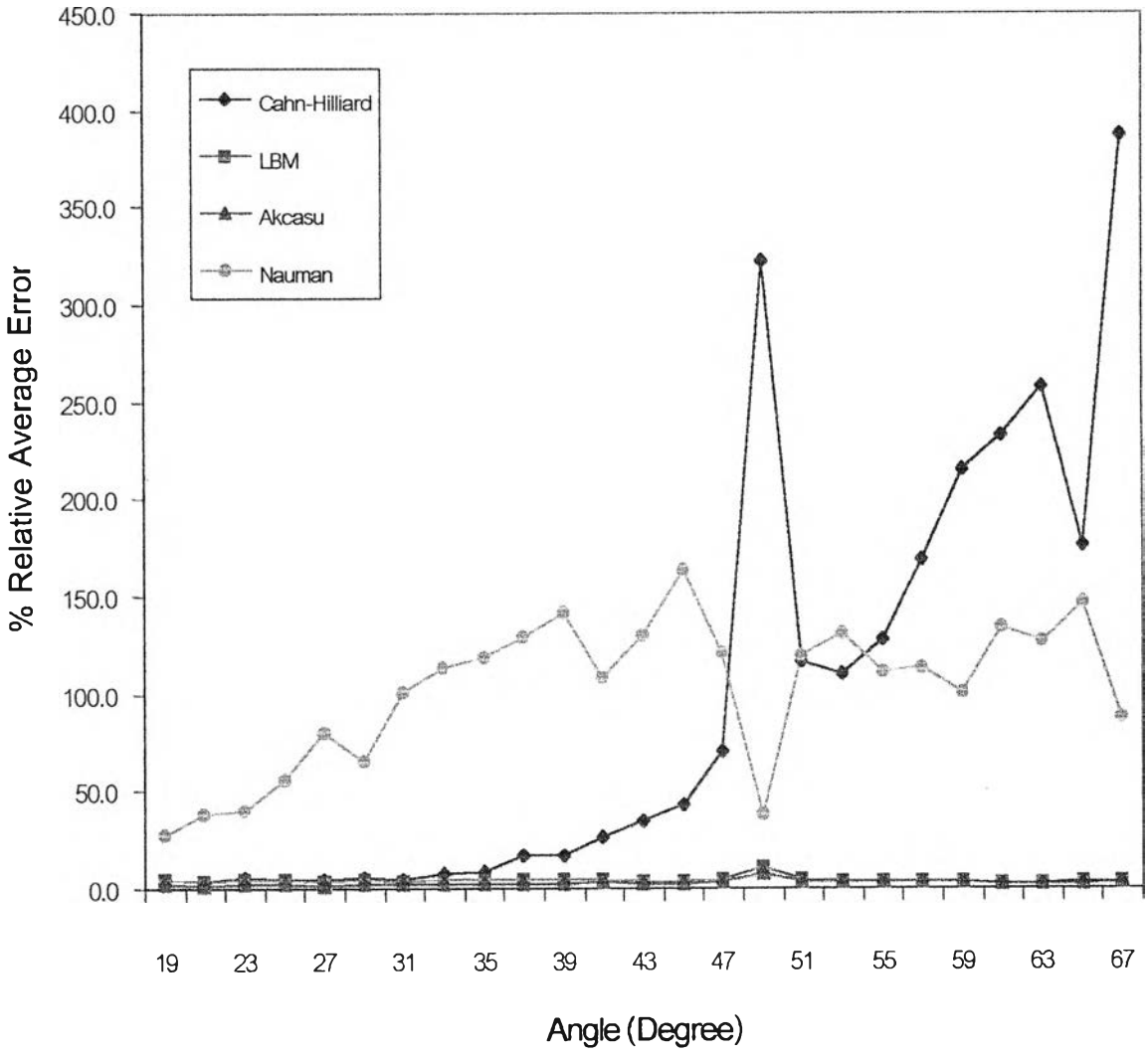

Fig.5.29 The percent relative average error of 30%w TMPC/PS blends at 266 °C of each theory.

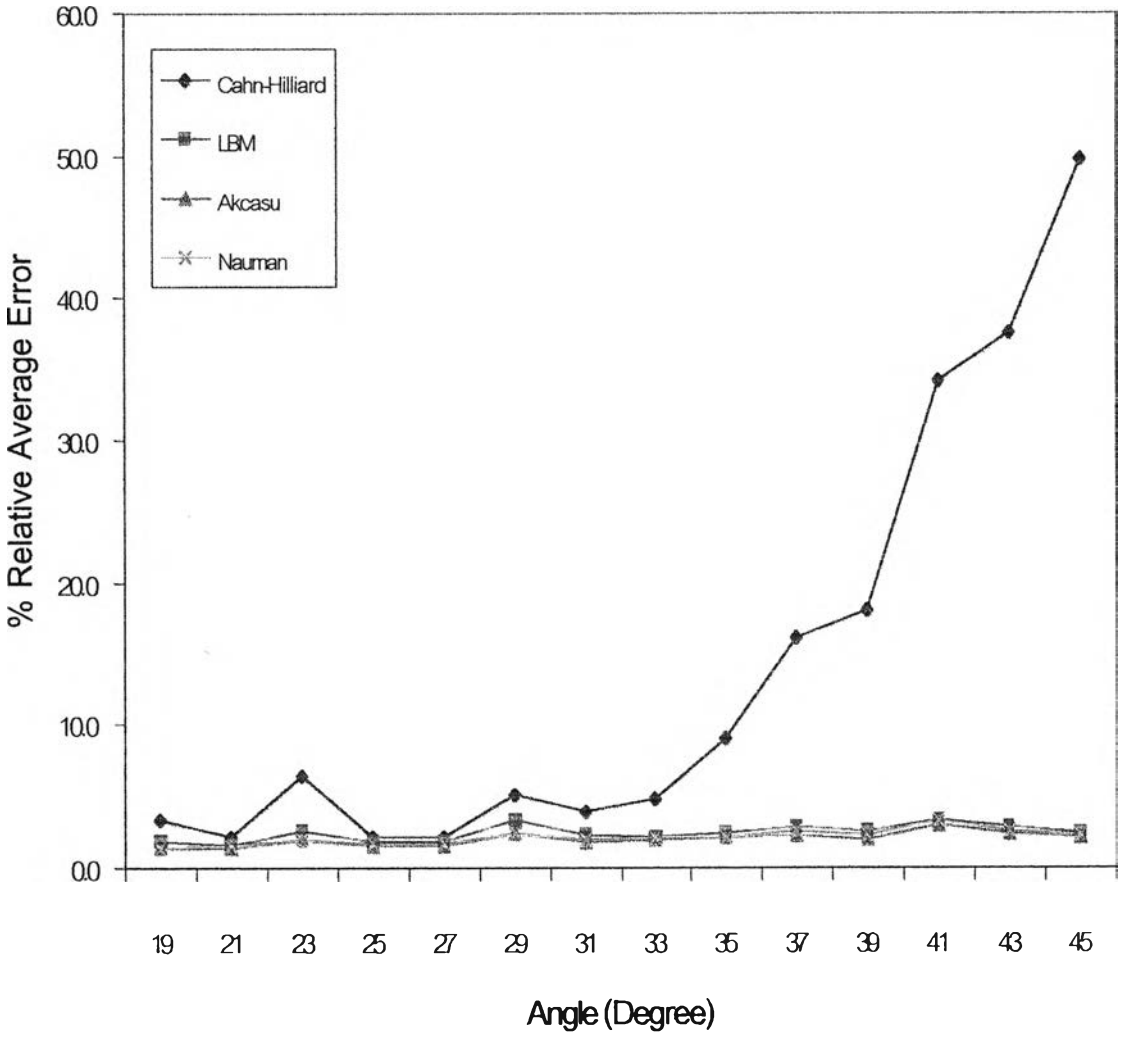

Fig.5.30 The percent relative average error of 30%w TMPC/PS blends at 269 °C of each theory.

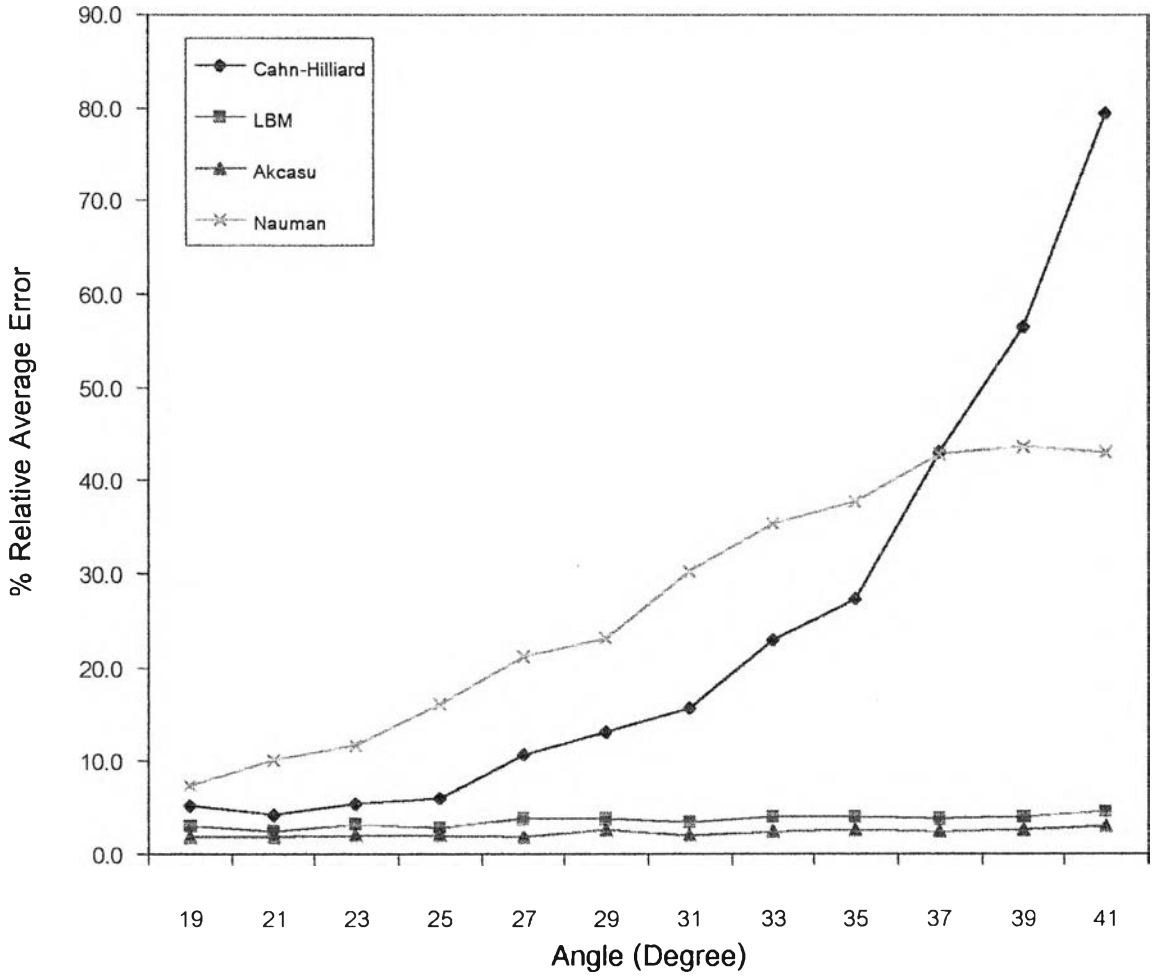

Fig.5.31 The percent relative average error of 30%w TMPC/PS blends at 271 °C of each theory.

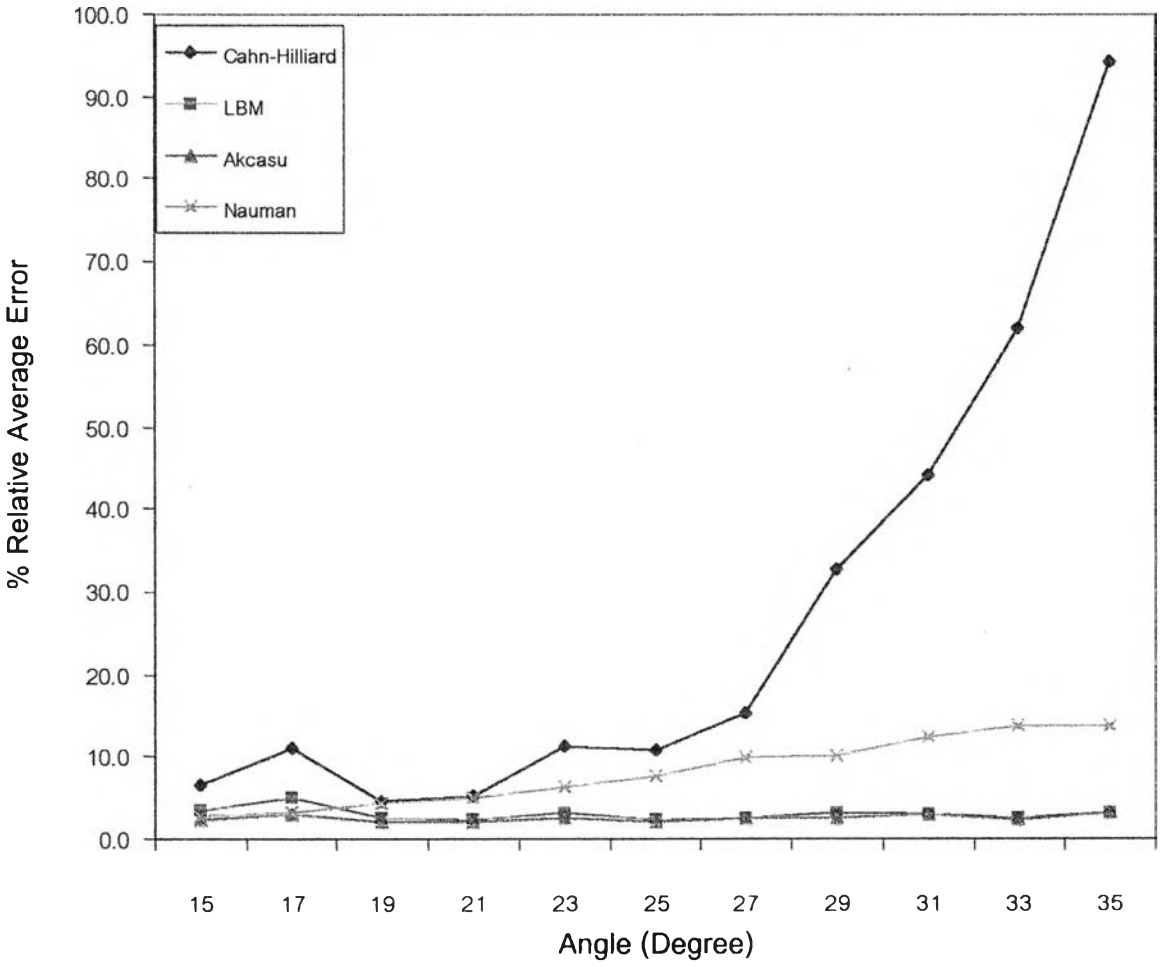

Fig.5.32 The percent relative average error of 30%w TMPC/PS blends at 273 °C of each theory.

In Fig.5.33, it shows the percent relative average error of 30%w TMPC/PS blends at 275 °C. The percent relative average error from Langer, Bar-on and Miller's, and Akcasu's theories are small. These two theories can fit with experimental data better than the Cahn-Hilliard's and Nauman's theories, and can be used to explain the phase separation data more widely.

5.3.6.2 Comparison of each theory on 50%TMPC/PS Blends (Prepared by Solvent Casting)

In Fig.5.34, it shows the percent relative average error of 50%w TMPC/PS blends at 237 °C. It appeared that the percent relative average error from Langer, Bar-on and Miller's, and Akcasu's theories are less than those from Canh-Hilliard's and Nauman's theories. The percent relative average error of Canh-Hilliard increase with increasing angles, while the percent relative average error of Nauman decrease with increasing angles of the scattered intensity.

In Fig.5.35, it shows the percent relative average error of 50%w TMPC/PS blends at 239 °C. It appeared that the percent relative average error from Langer, Bar-on and Miller's, and Akcasu's theories are less than those from Canh-Hilliard's and Nauman's theories. The percent relative average error of Canh-Hilliard increase with increasing angles, while the percent relative average error of Nauman decrease with increasing angles of the scattered intensity.

In Fig.5.36, it shows the percent relative average error of 50%w TMPC/PS blends at 242 °C. It appeared that the percent relative average error from Langer, Bar-on and Miller's, and Akcasu's theories are less than those from Canh-Hilliard's and Nauman's theories. The percent relative average error of Canh-Hilliard increase with increasing angles. The percent relative average error of Nauman's theory does not change much.

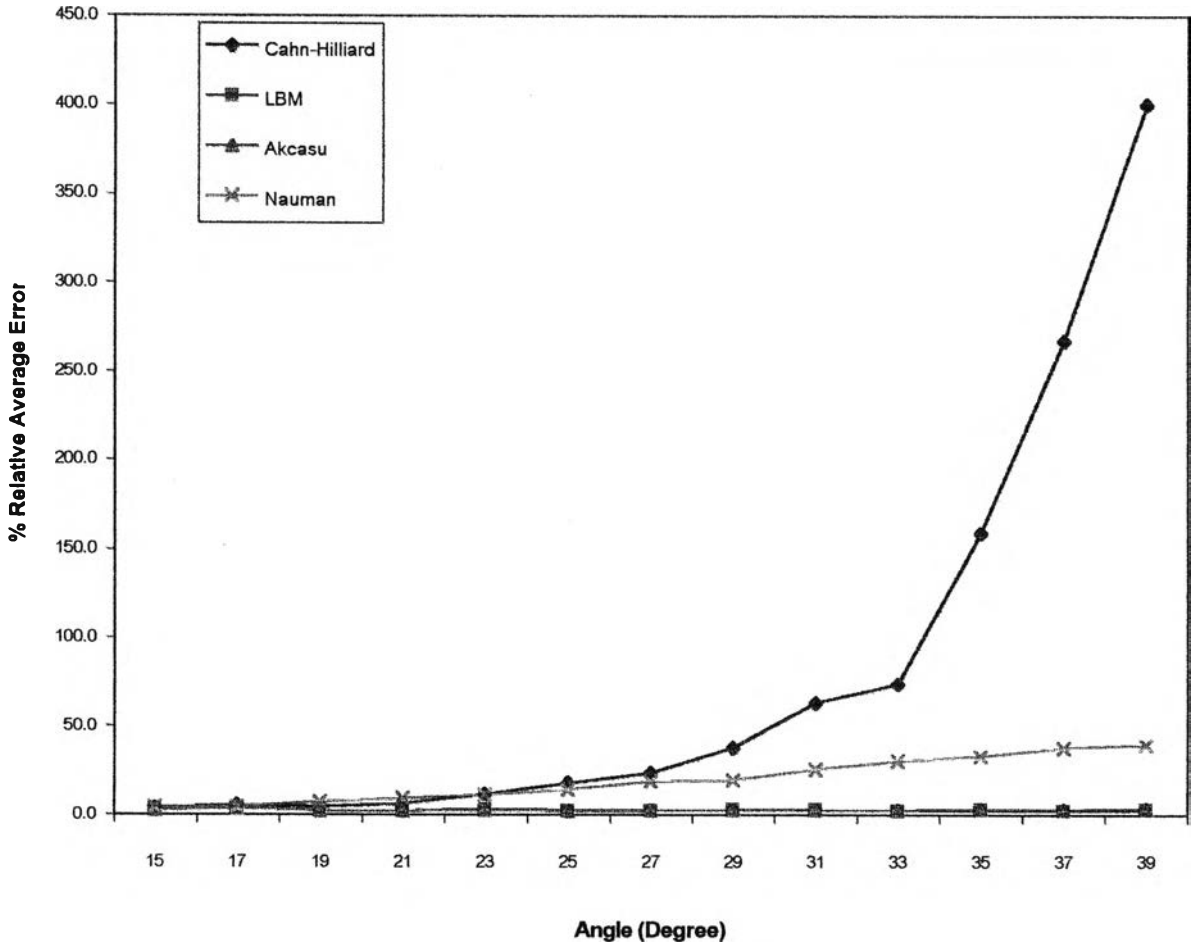

Fig.5.33 The percent relative average error of 30%w TMPC/PS blends at 275 °C of each theory.

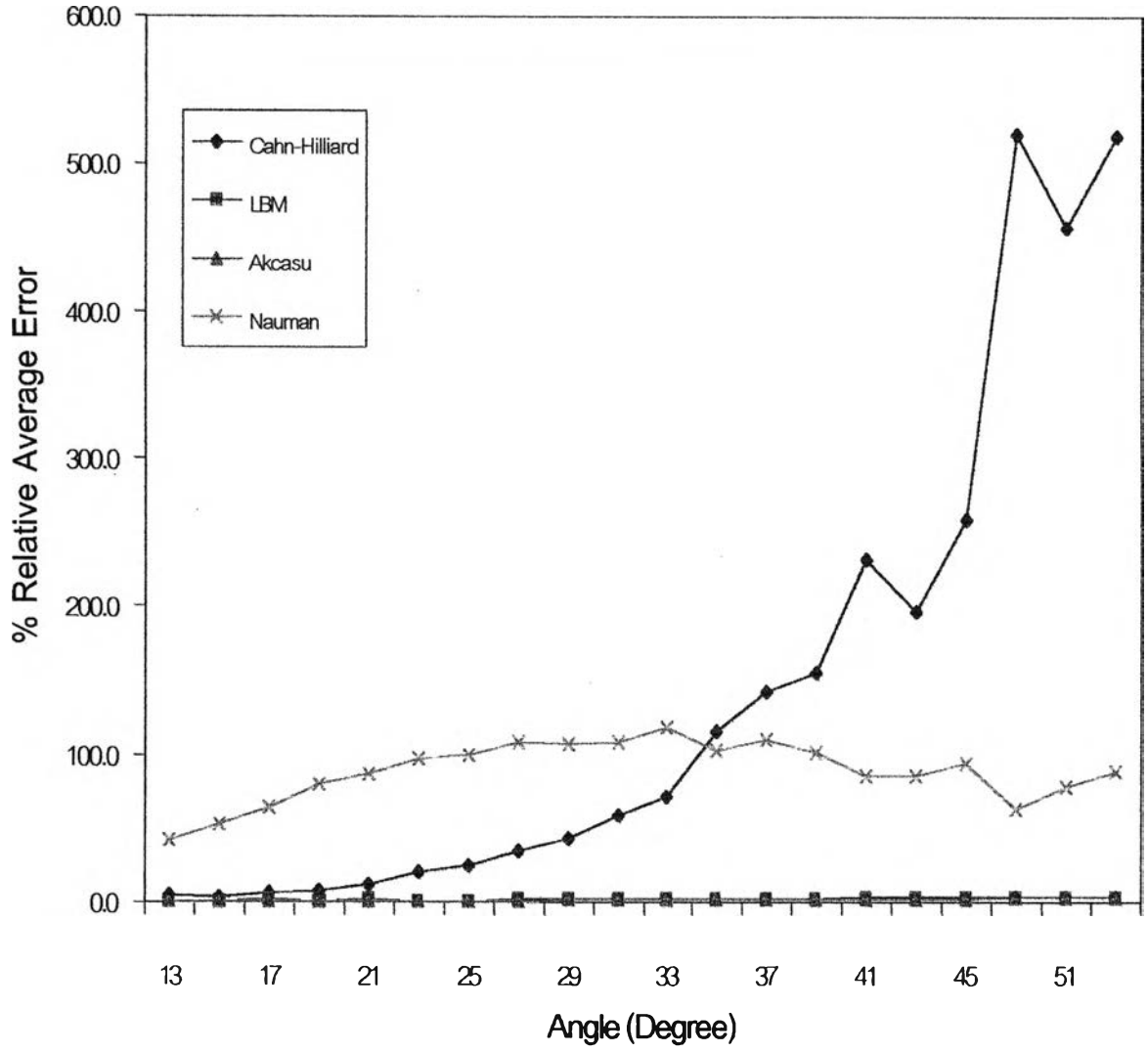

Fig.5.34 The percent relative average error of 50%w TMPC/PS blends (Prepared by solvent casting) at 237 °C of each theory.

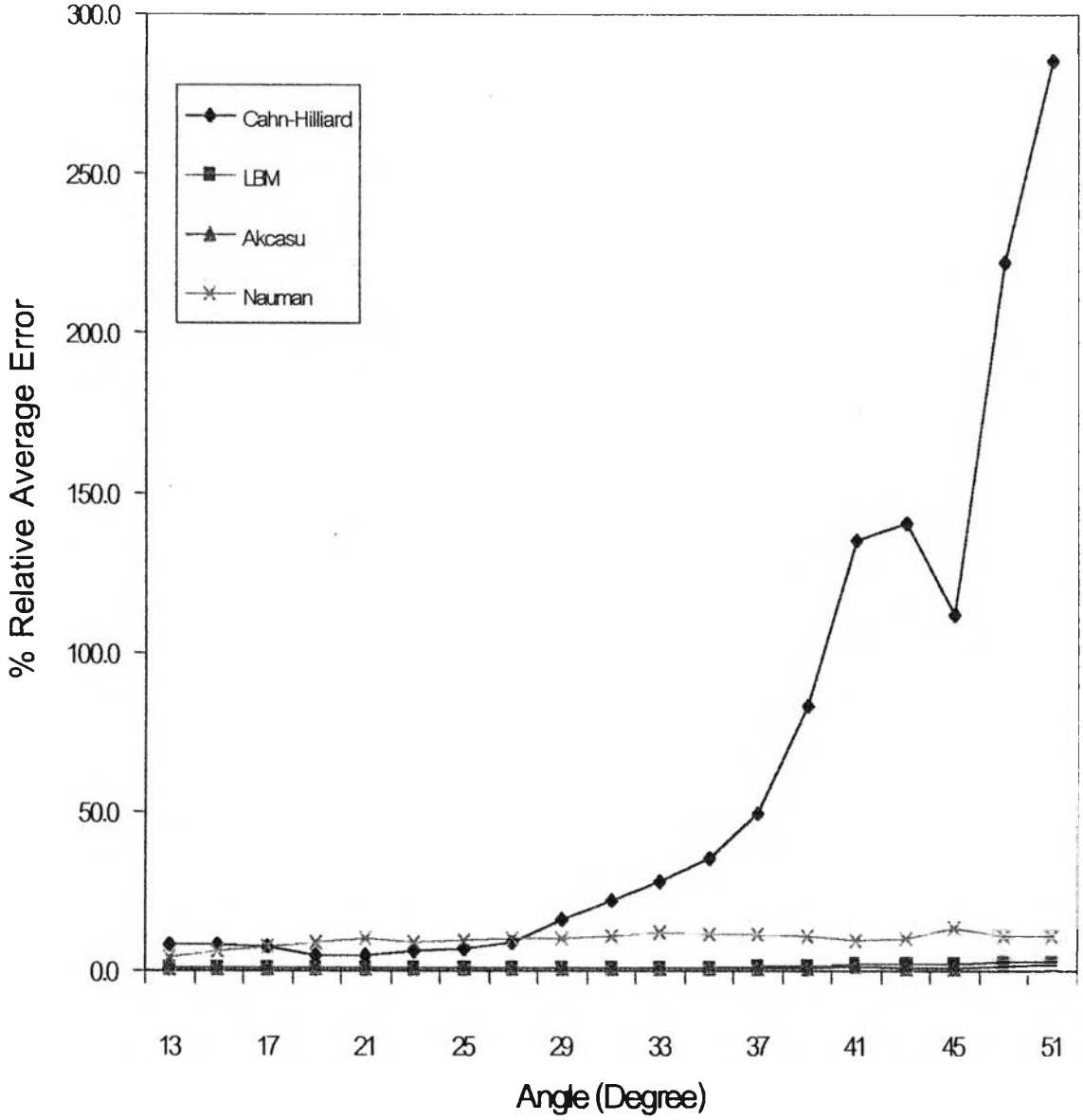

Fig.5.35 The percent relative average error of 50%w TMPC/PS blends (Prepared by solvent casting) at 239 °C of each theory.

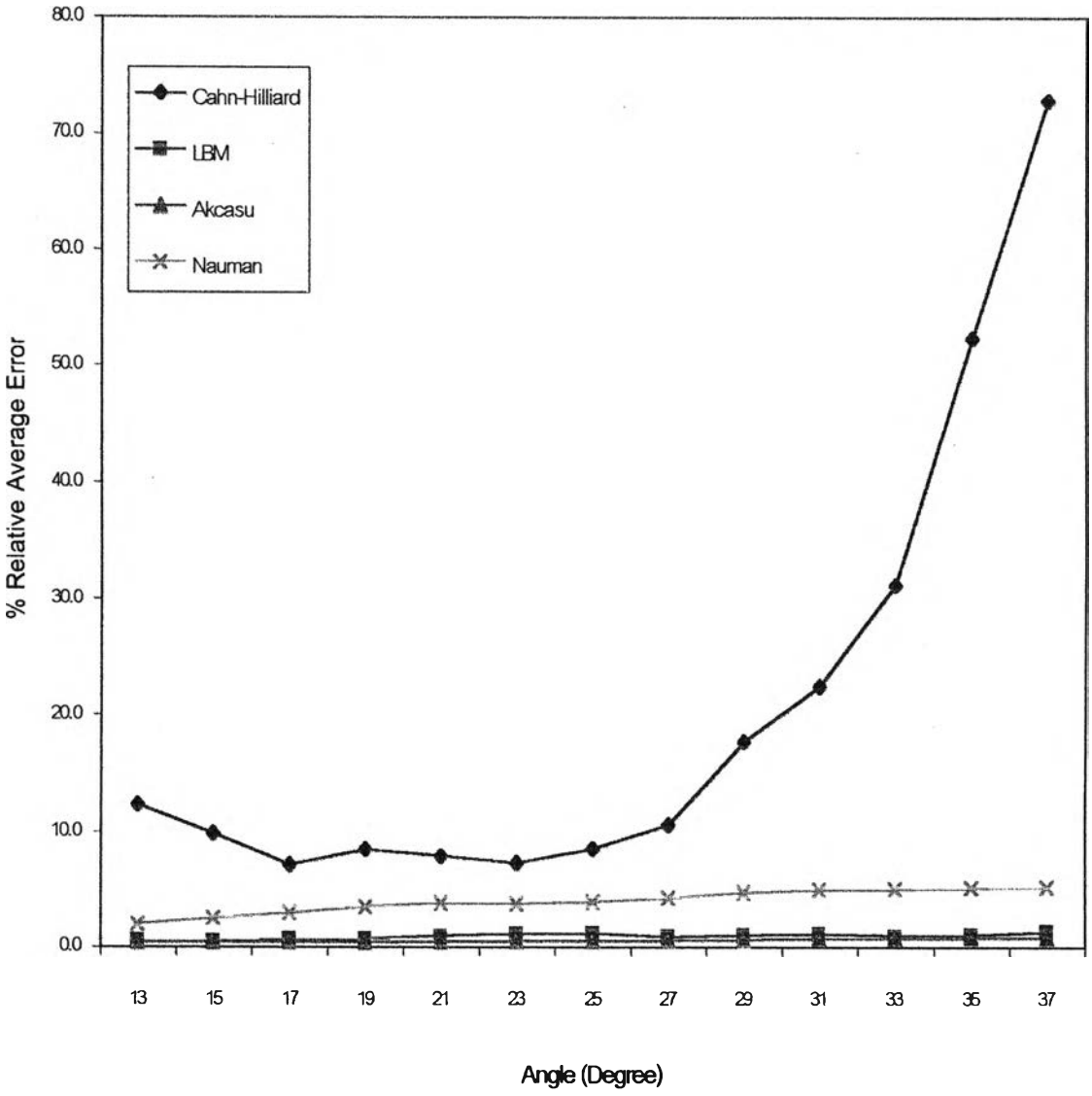

Fig.5.36 The percent relative average error of 50%w TMPC/PS blends (Prepared by solvent casting) at 242 °C of each theory.

In Fig.5.37, it shows the percent relative average error of 50%w TMPC/PS blends at 245°C. The percent relative average error from Langer, Bar-on and Miller's, and Akcasu's theories are small compared to the percent relative average error from Cahn-Hilliard's and Nauman's theories. So these theories can fit with experimental data better than the Cahn-Hilliard's and Nauman's theories. The percent relative average error of Cahn-Hilliard's theory increase with the increasing angle.

In Fig.5.38, shows the percent relative average error of 50%w TMPC/PS blends at 247°C. The percent relative average error from Langer, Bar-on and Miller's, and Akcasu's theories are small compared to the percent relative average error from Cahn-Hilliard's and Nauman's theories. So these theories can fit with experimental data better than the Cahn-Hilliard's and Nauman's theories. The percent relative average error of Cahn-Hilliard's theory increase with the increasing angle.

5.3.6.3 Comparison of each theory on 50%TMPC/PS blends (Prepared by Melt Mixed)

In Fig. 5.39-1, it shows the percent relative average error of 50%w TMPC/PS blends at 249 °C of Langer, Bar-on and Miller's, Nauman and Akcasu's theories. Fig.5.39-2 shows the percent relative average error of Cahn-Hilliard's theory. They appeared that the percent relative average error from Langer, Bar-on and Miller's, and Akcasu's theories are less than those from Canh-Hilliard's and Nauman's theories. The percent relative average error of Cahn-Hilliard's theory increase with increasing angles of the scattered intensity. It shows that Akcasu's and Langer, Bar-on and Miller's theories can fit experimental data better than other two theories.

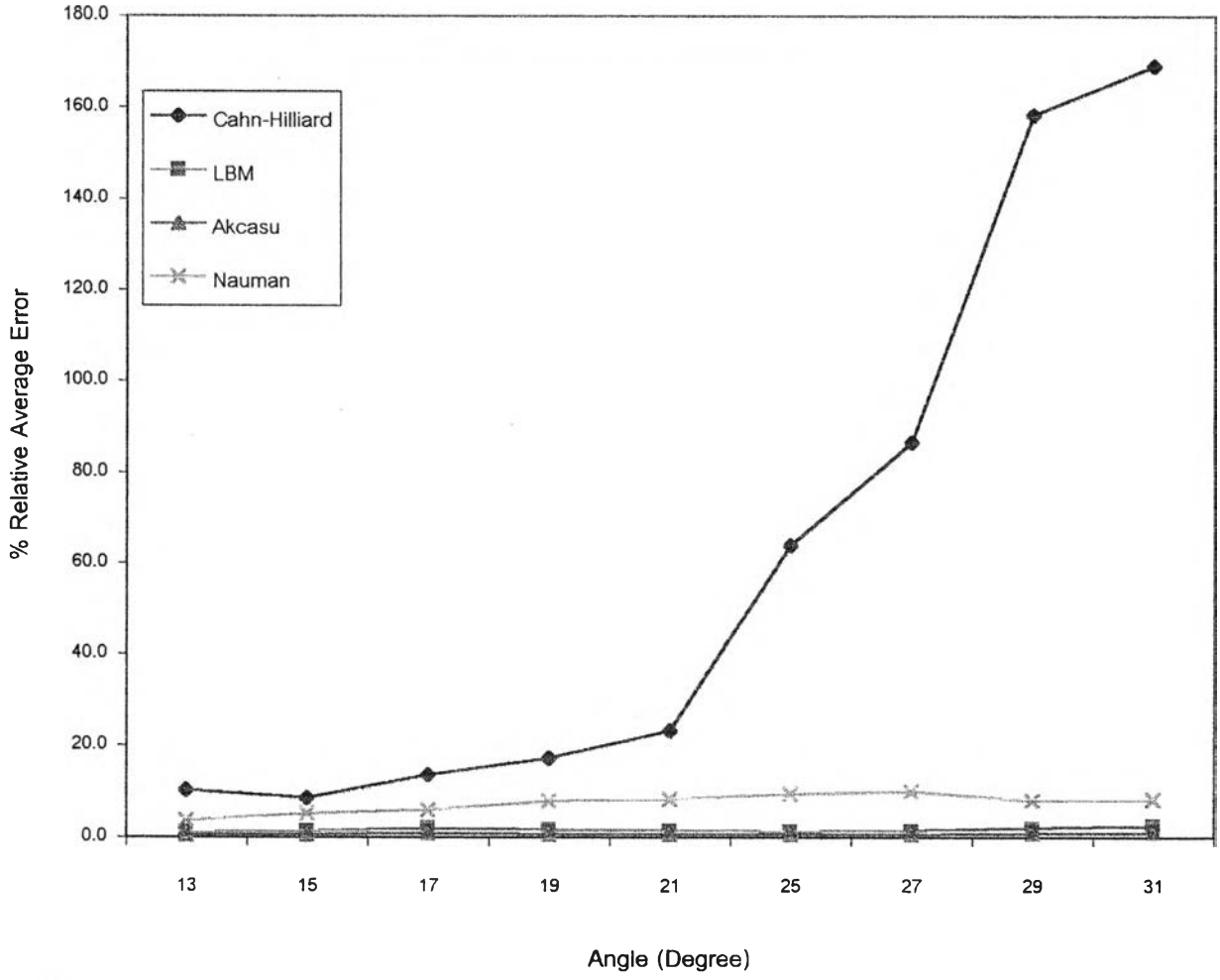

Fig.5.37 The percent relative average error of 50%w TMPC/PS blends (Prepared by solvent casting) at 245 °C of each theory.

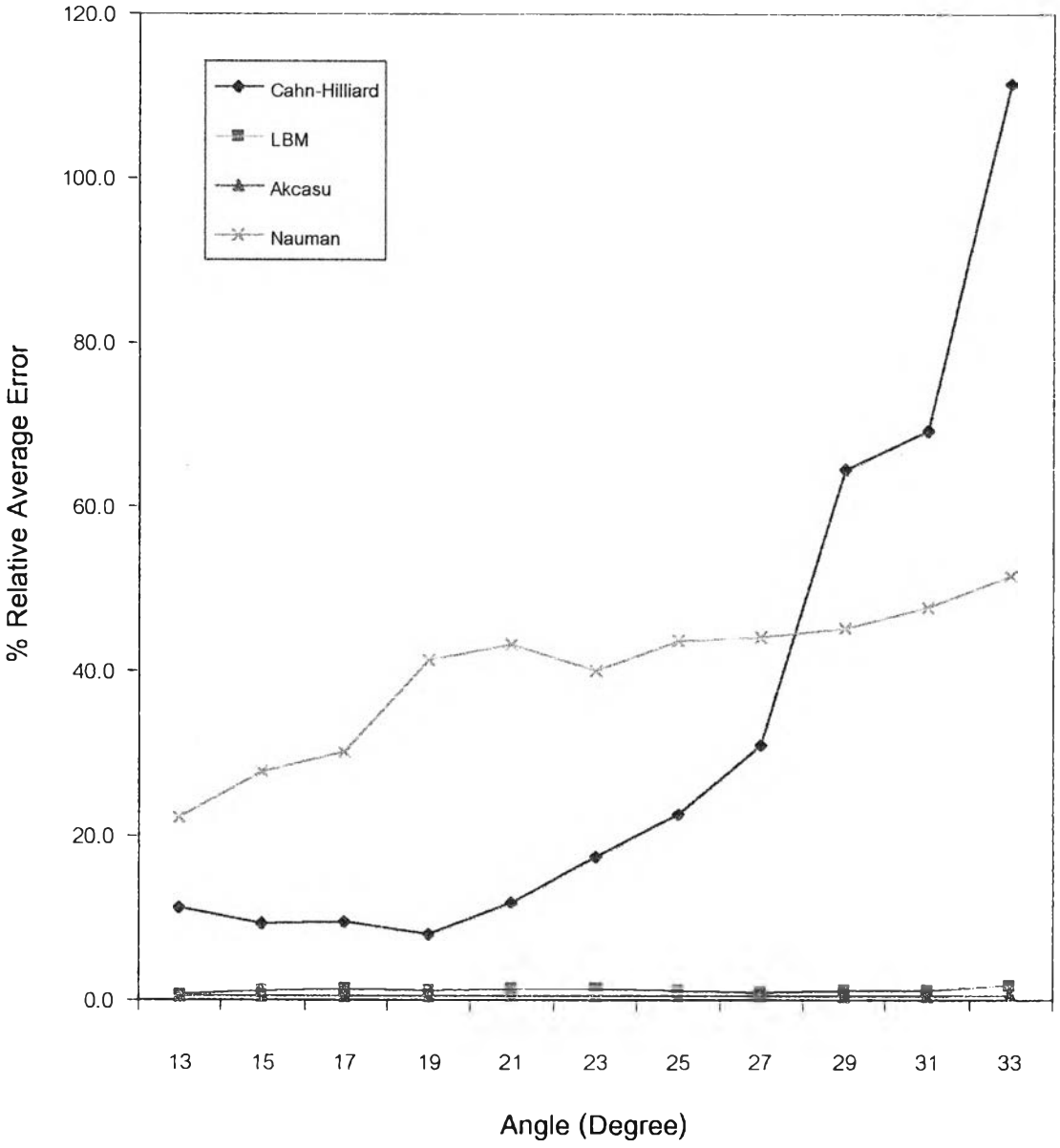

Fig.5.38 The percent relative average error of 50%w TMPC/PS blends (Prepared by solvent casting) at 247 °C of each theory.

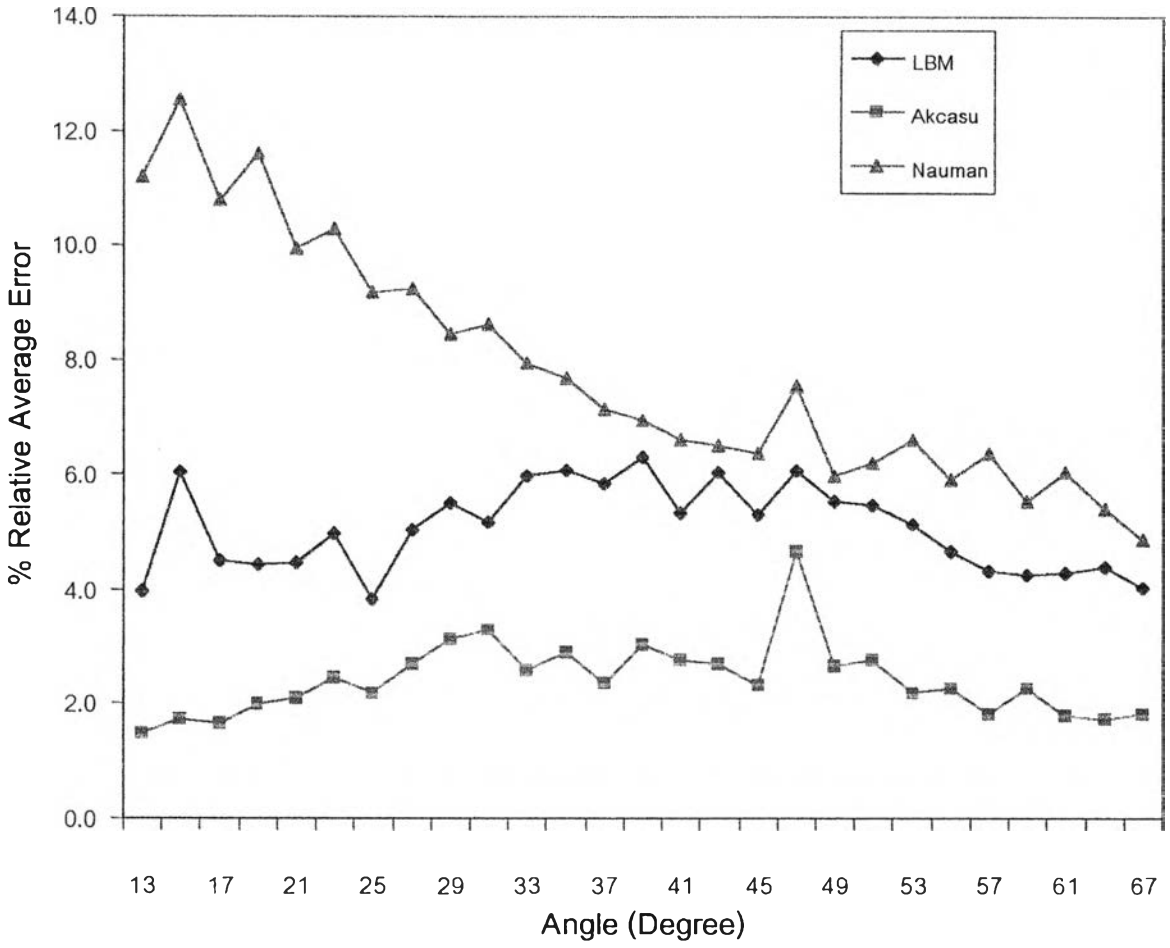

Fig.5.39-1 The percent relative average error of 50%w TMPC/PS blends (Prepared by melt mixed) at 249 °C of three theories.

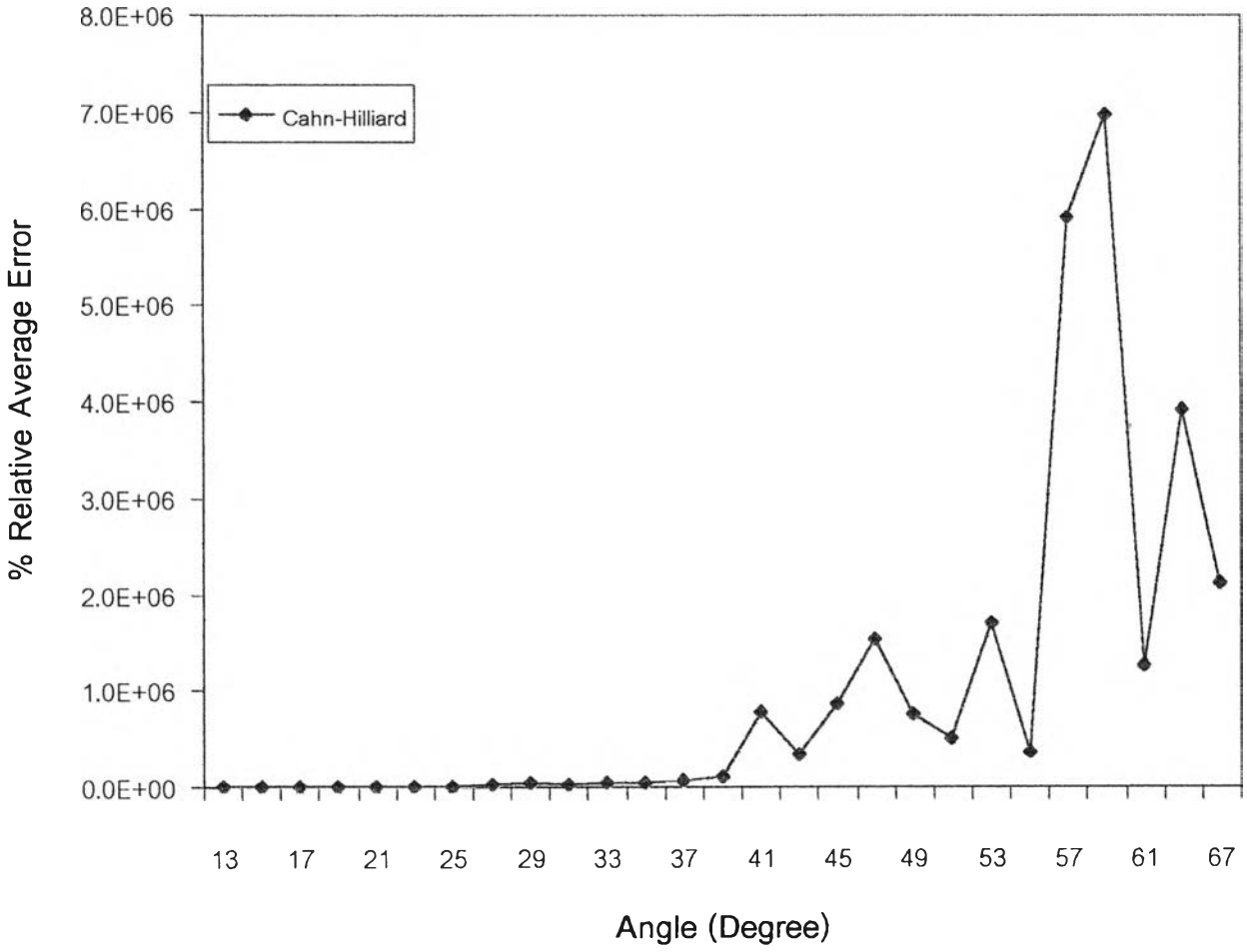

Fig.5.39-2 The percent relative average error of 50%w TMPC/PS blends (Prepared by melt mixed) at 249 °C of one theory.

In Fig. 5.40-1, it shows the percent relative average error of 50%w TMPC/PS blends at 250 °C of Langer, Bar-on and Miller's, Nauman and Akcasu's theories. Fig.5.40-2 shows the percent relative average error of Cahn-Hilliard's theory. They appeared that the percent relative average error from Langer, Bar-on and Miller's, and Akcasu's theories are less than those from Canh-Hilliard's and Nauman's theories. The percent relative average error of Cahn-Hilliard's theory increase with increasing angles of the scattered intensity. It shows that Akcasu's and Langer, Bar-on and Miller 's theories can fit experimental data better than other two theories.

In Fig. 5.41-1, it shows the percent relative average error of 50%w TMPC/PS blends at 251 °C of Langer, Bar-on and Miller's, Nauman and Akcasu's theories. Fig.5.41-2 shows the percent relative average error of Cahn-Hilliard's theory. The percent relative average error of Langer, Bar-on and Miller, and Akcasu' s theories are small compared to the percent relative average error from Cahn-Hilliard's and Nauman's theories. These two theories can fit with experimental data better than the Cahn-Hilliard's and Nauman's theories, and can be used to explain the phase separation data more widely.

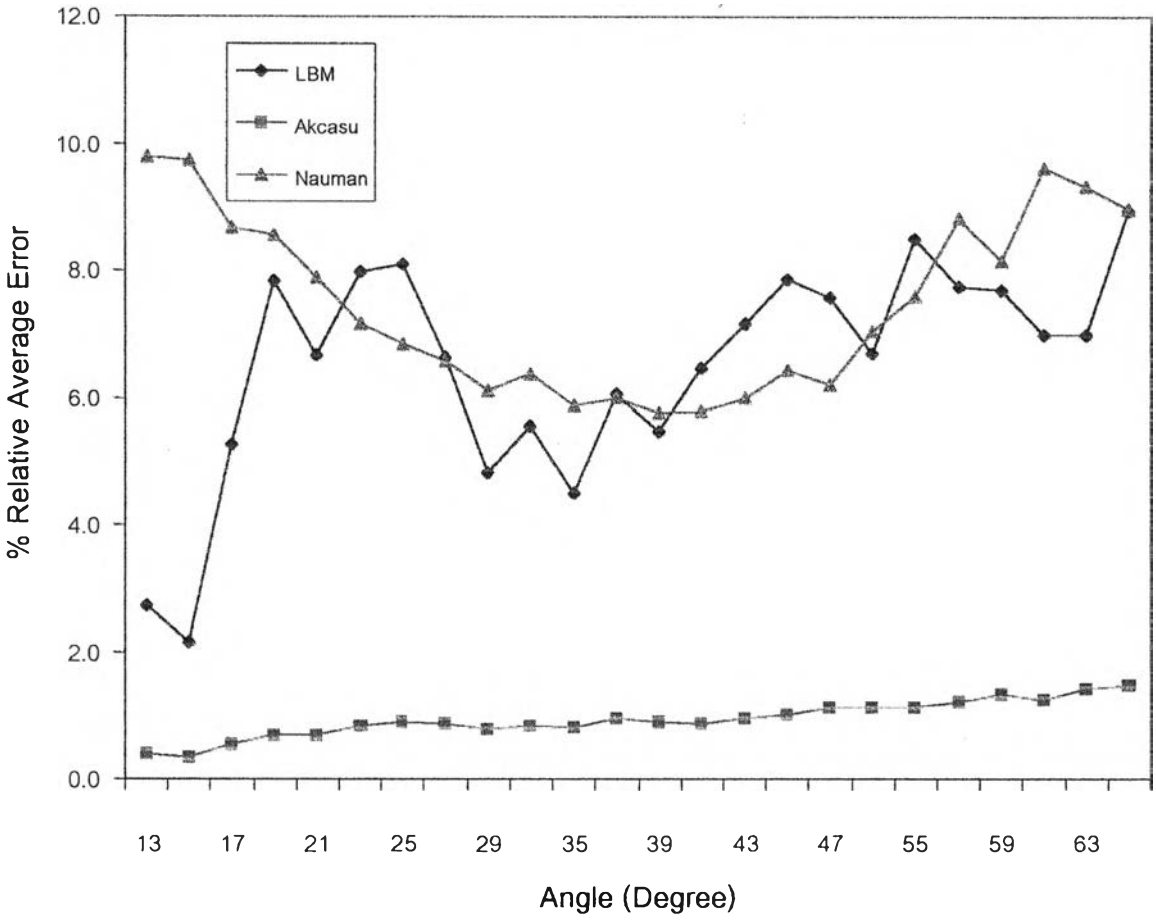

Fig.5.40-1 The percent relative average error of 50%w TMPC/PS blends (Prepared by melt mixed) at 250 °C of three theories.

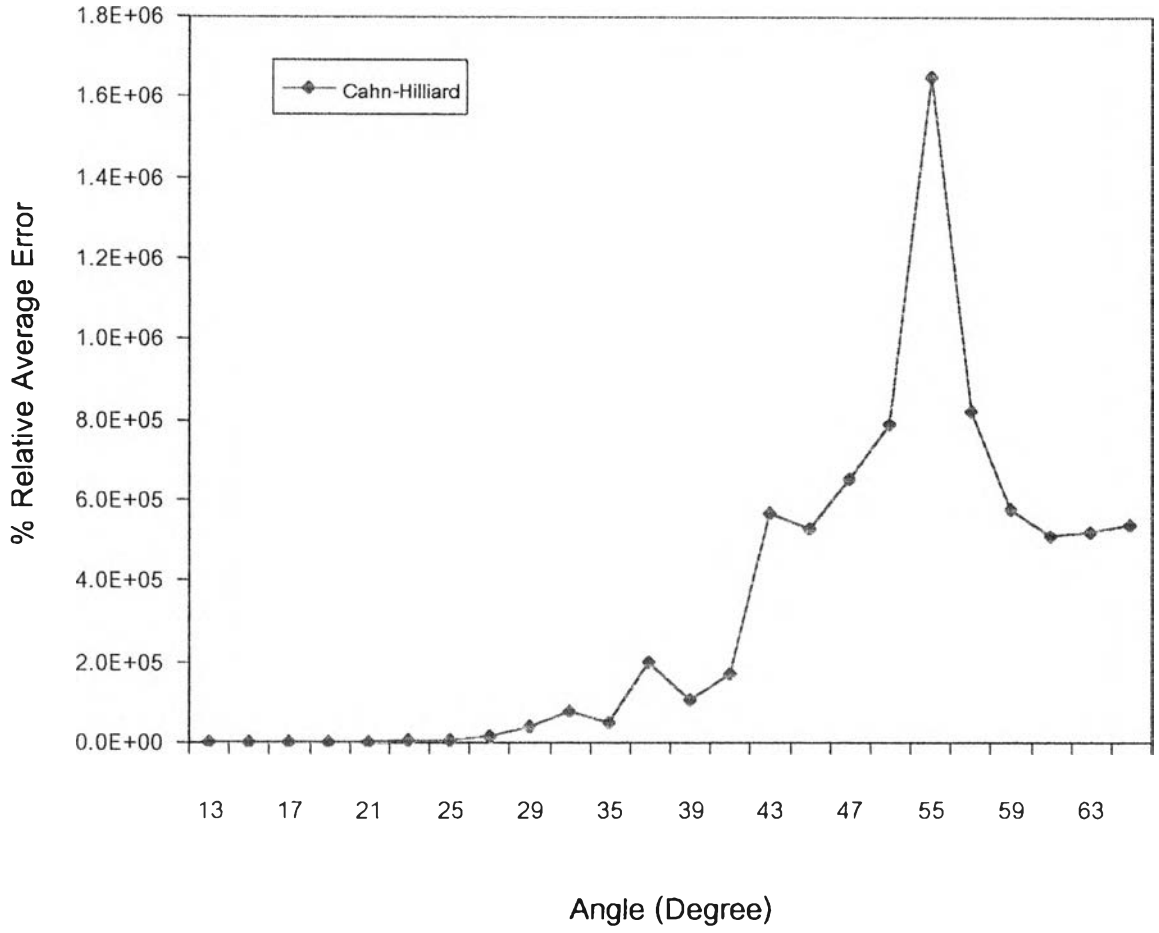

Fig.5.40-2 The percent relative average error of 50%w TMPC/PS blends (Prepared by melt mixed) at 250 °C of one theory.

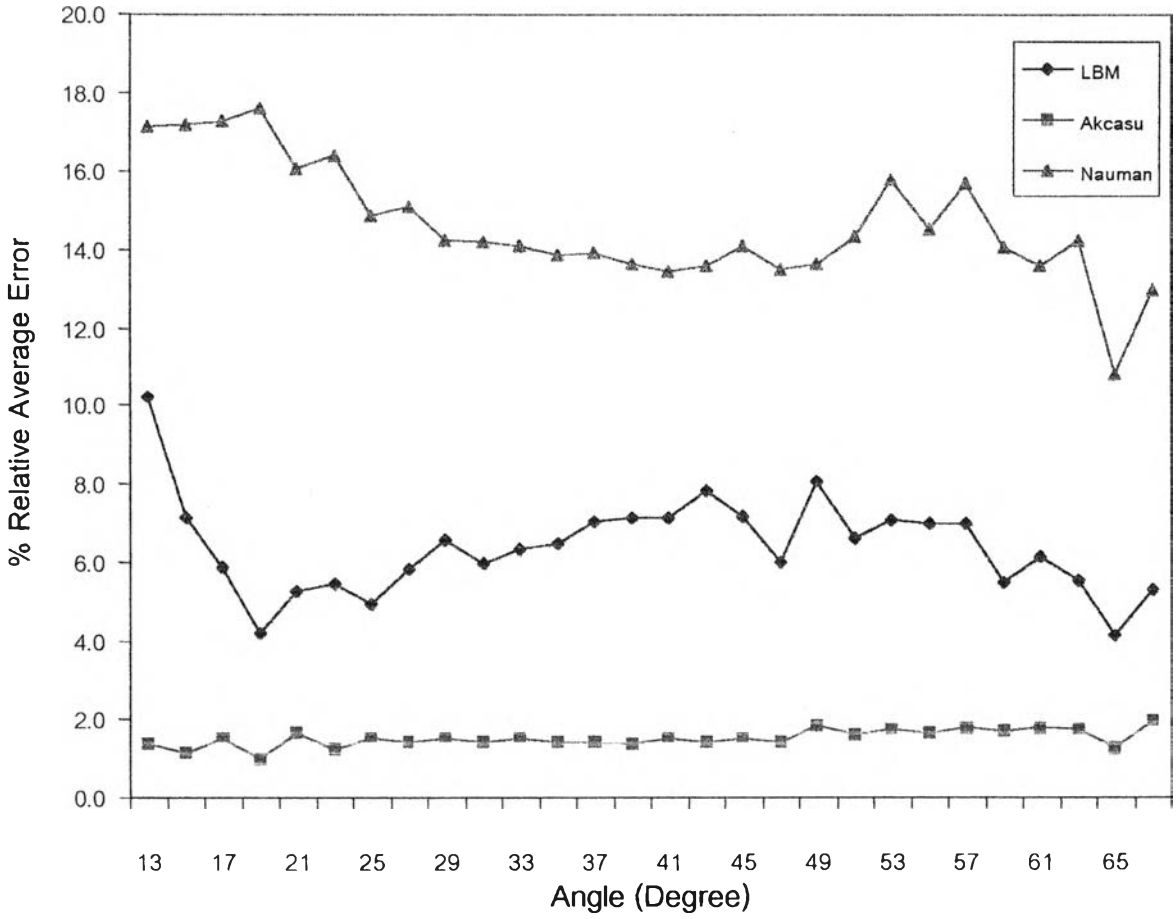

Fig.5.41-1 The percent relative average error of 50%w TMPC/PS blends (Prepared by melt mixed) at 251 °C of three theories.

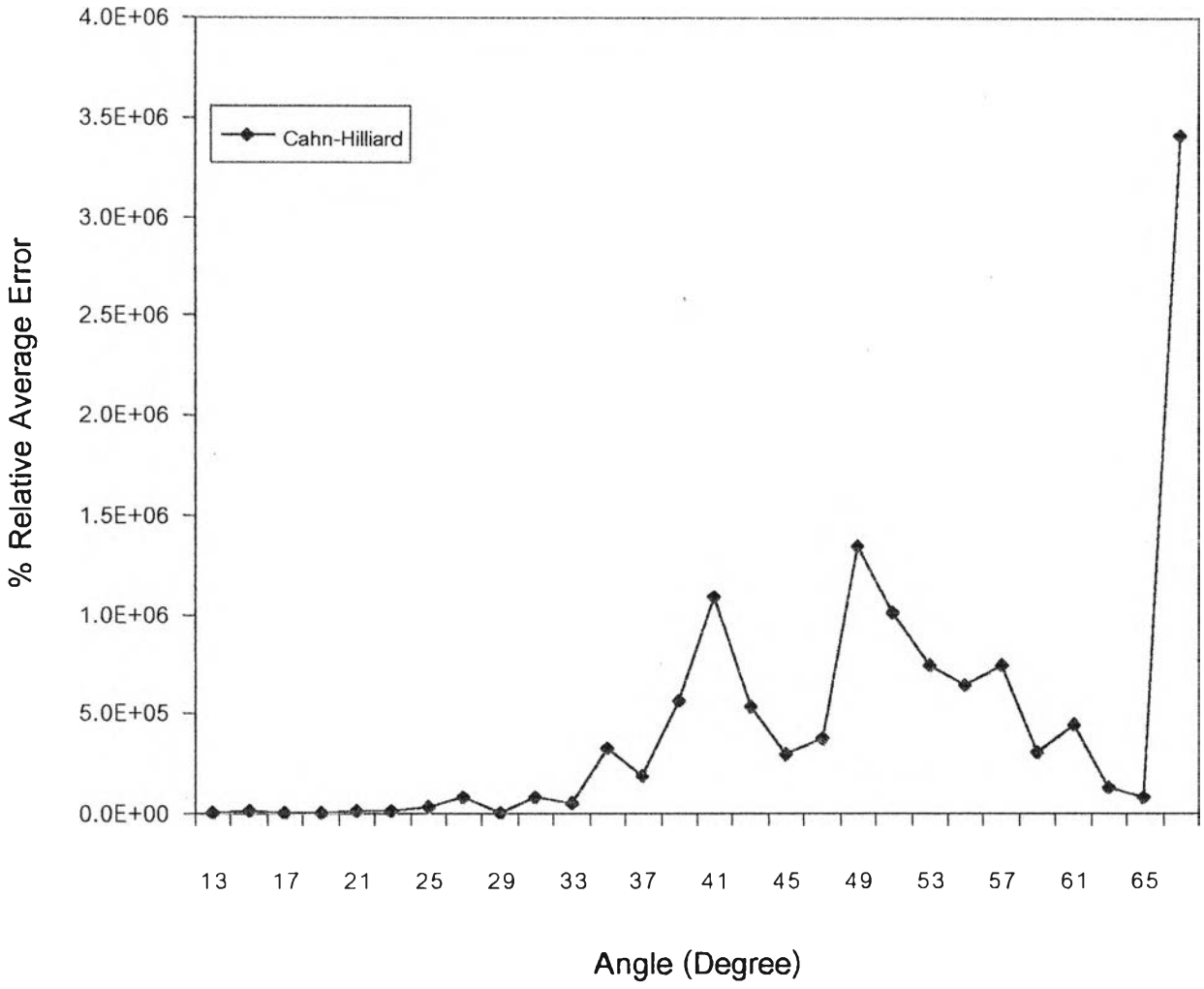

Fig.5.41-2 The percent relative average error of 50%w TMPC/PS blends (Prepared by melt mixed) at 251 °C of one theory.

In Fig. 5.42-1, it shows the percent relative average error of 50%w TMPC/PS blends at 252 °C of Langer, Bar-on and Miller's, Nauman and Akcasu's theories. Fig.5.42-2 shows the percent relative average error of Cahn-Hilliard's theory. They appeared that the percent relative average error of Langer, Bar-on and Miller's and Akcasu's theories are less than those from Cahn-Hilliard's and Nauman's theories. The percent relative average error of Nauman decreases with increasing angles.

In Fig. 5.43-1, it shows the percent relative average error of 50%w TMPC/PS blends at 253 °C of Langer, Bar-on and Miller's, Nauman and Akcasu's theories. Fig.5.43-2 shows the percent relative average error of Cahn-Hilliard's theory. They appeared that the percent relative average error of Langer, Bar-on and Miller's, and Akcasu's theories are less than those from Cahn-Hilliard's and Nauman's theories. These two theories can fit with experimental data better than the Cahn-Hilliard's and Nauman's theories, and can be used to explain the phase separation data more widely. The percent relative average error of Nauman decrease with increasing angles, while the percent relative average error of Cahn-Hilliard's increase.

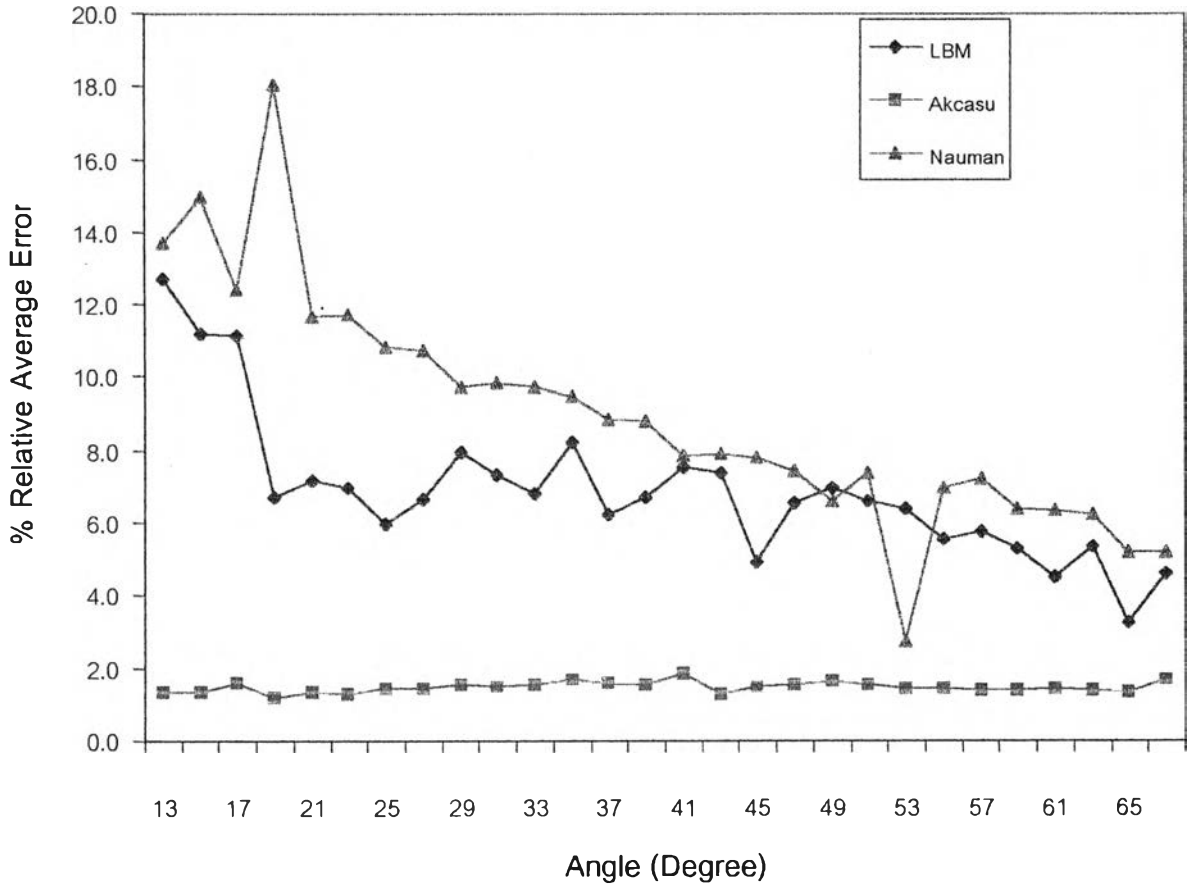

Fig.5.42-1 The percent relative average error of 50%w TMPC/PS blends (Prepared by melt mixed) at 252 °C of three theories.

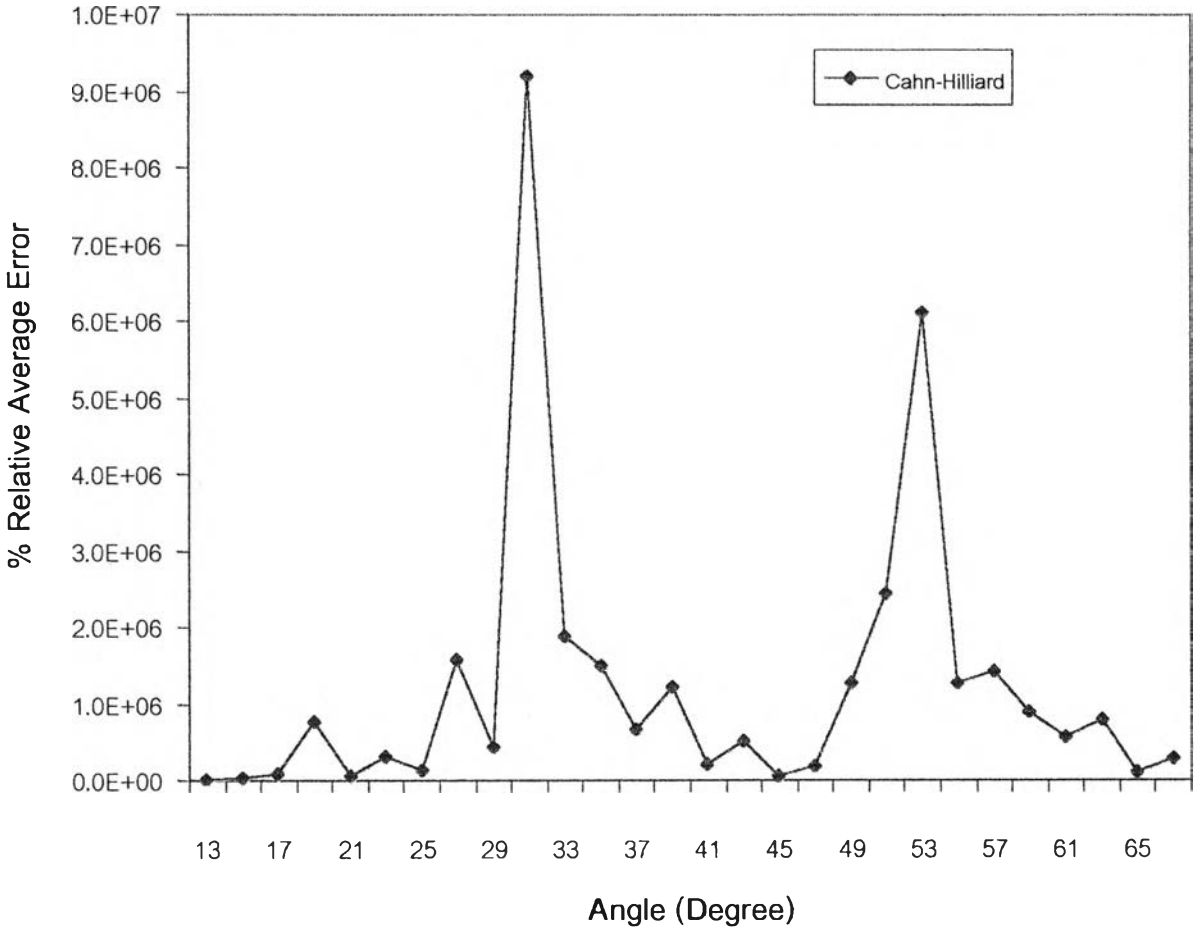

Fig.5.42-2 The percent relative average error of 50%w TMPC/PS blends (Prepared by melt mixed) at 252 °C of one theory.

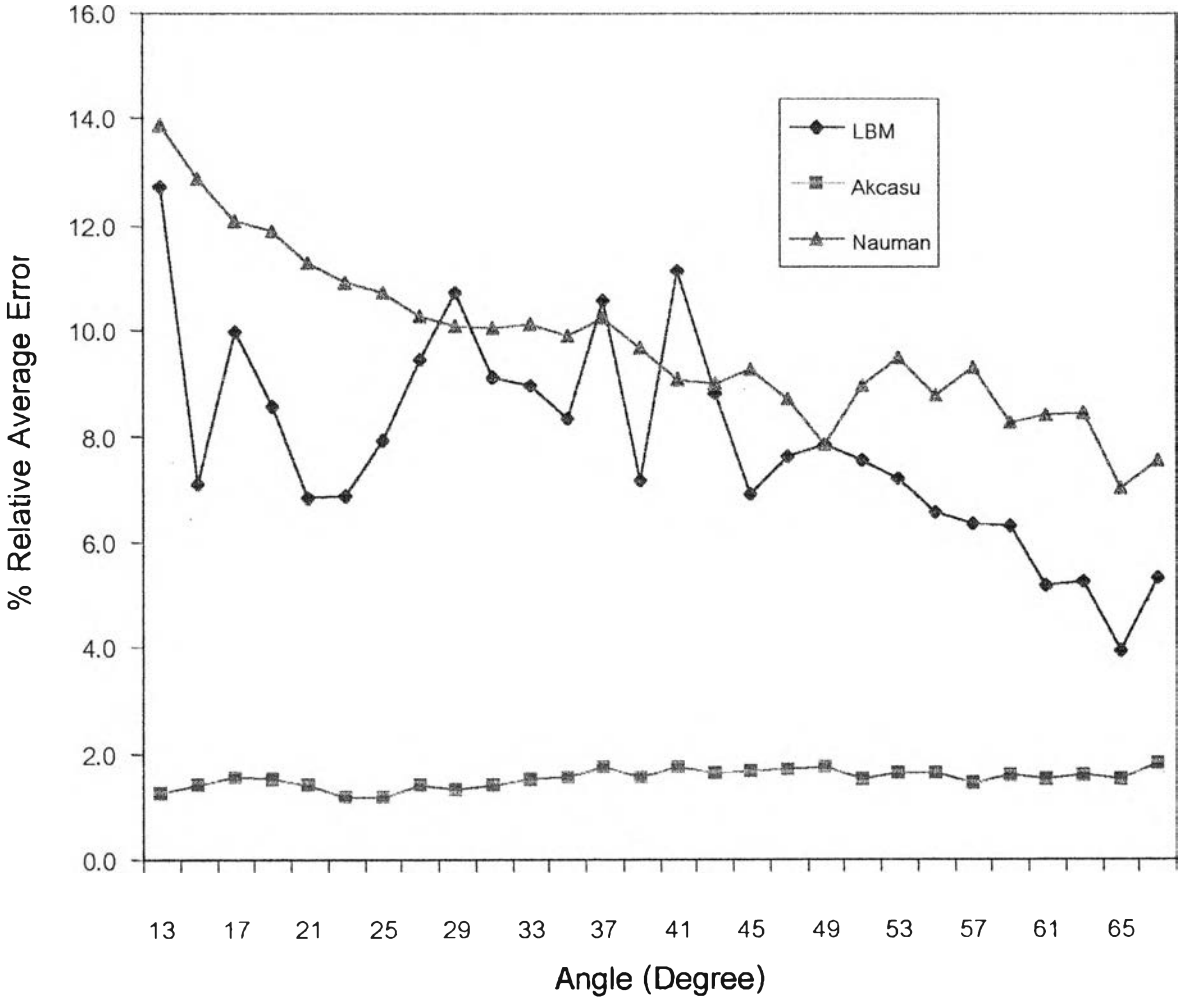

Fig.5.43-1 The percent relative average error of 50%w TMPC/PS blends (Prepared by melt mixed) at 253 °C of three theories.

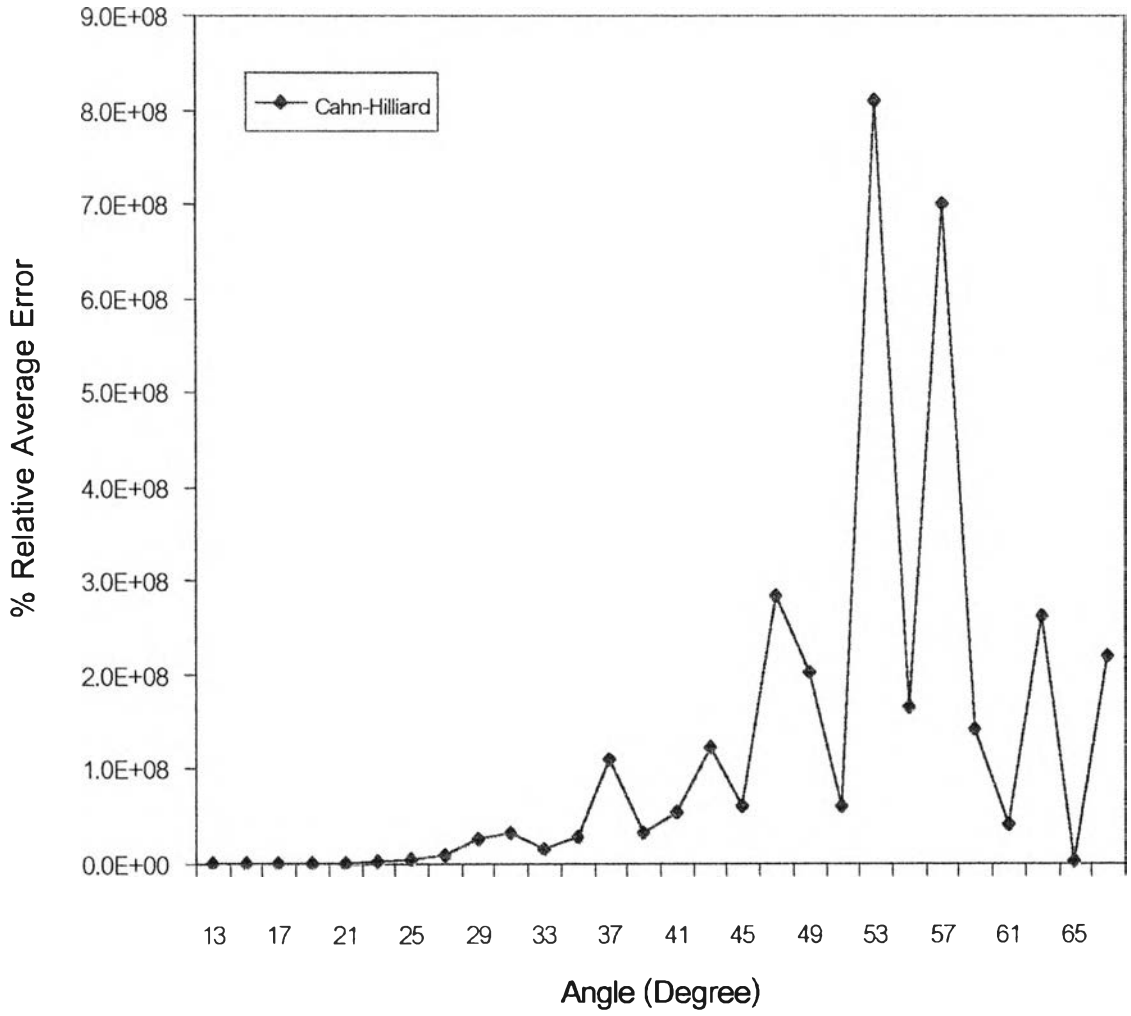

Fig.5.43-2 The percent relative average error of 50%w TMPC/PS blends (Prepared by melt mixed) at 253 °C of one theory.

5.3.6.4 Comparison of each theory on 70%w TMPC/PS blends

In Fig.5.44, it shows the percent relative average error of 70%w TMPC/PS blends at 293 °C. It appeared that the percent relative average error of each theory is small. The percent relative average error from Akcasu's and Langer, Bar-on and Miller 's theories are not different among each other.

In Fig. 5.45, it shows the percent relative average error of 70%w TMPC/PS blends at 295 °C. It appeared that the percent relative average error from Langer, Bar-on and Miller's, Akcasu's and Nauman's theories are less than those from Canh-Hilliard's theory. The percent relative average error of Canh-Hilliard decrease with increasing angles.

In Fig.5.46, it shows the percent relative average error of 70%w TMPC/PS blends at 297 °C. It appeared that the percent relative average error of Akcasu's theory gives less difference than Langer, Bar-on and Miller's, Nauman's and Cahn-Hilliard's theories. It shows Akcasu's theory can fit with experimental data better than other three theories.

In Fig.5.47, it shows the percent relative average error of 70%w TMPC/PS blends at 299 °C.It appeared that the percent relative average error of each theories is small, so these theories can fit with experimental data, and can be used to explain the experimental data for this system.

In Fig.5.48, it shows the percent relative average error of 70%w TMPC/PS blends at 301°C. It appeared that the percent relative average error of Langer, Bar-on and Miller's, and Akcasu's and Nauman's theories are small. The percent relative average error of Cahn-Hilliard's theory increase with the increasing angle.

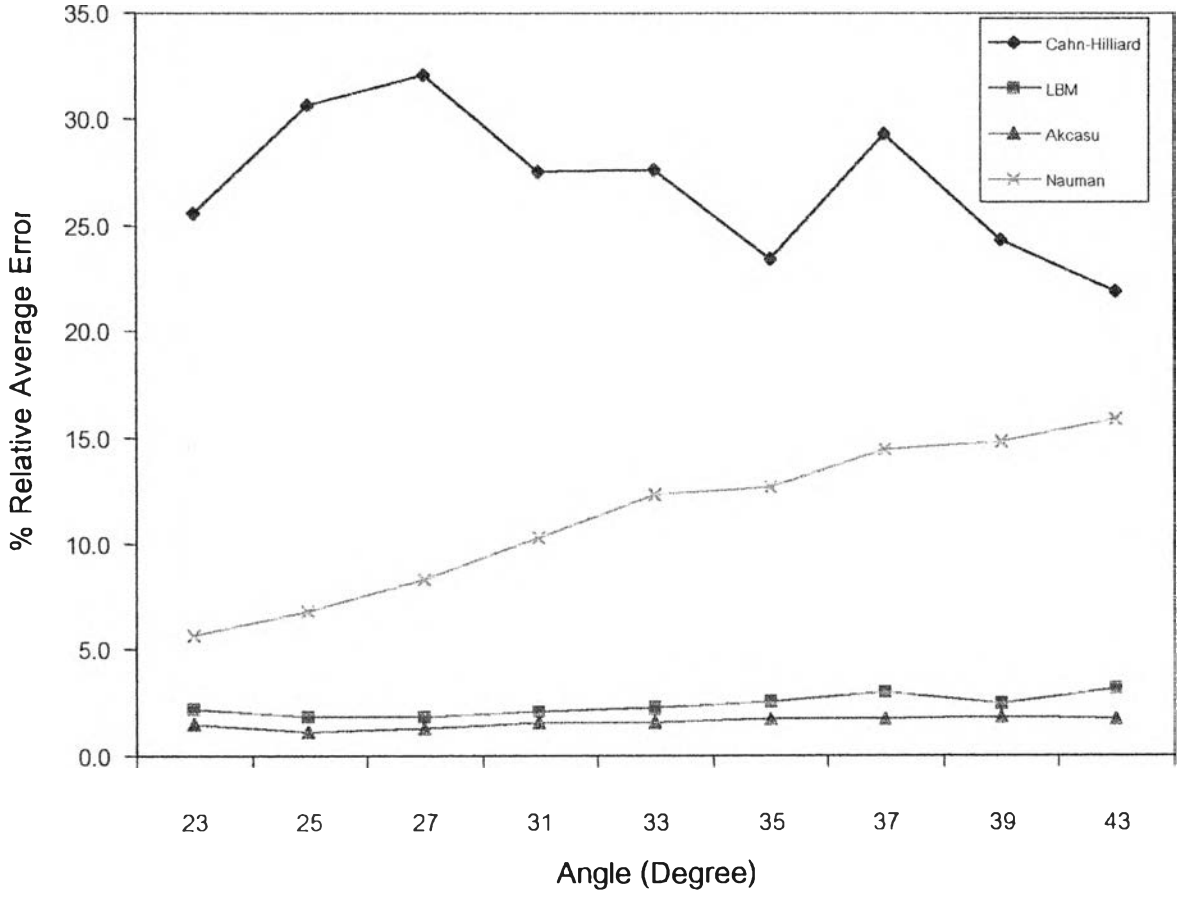

Fig.5.44 The percent relative average error of 70%w TMPC/PS blends at 293 °C of each theory.

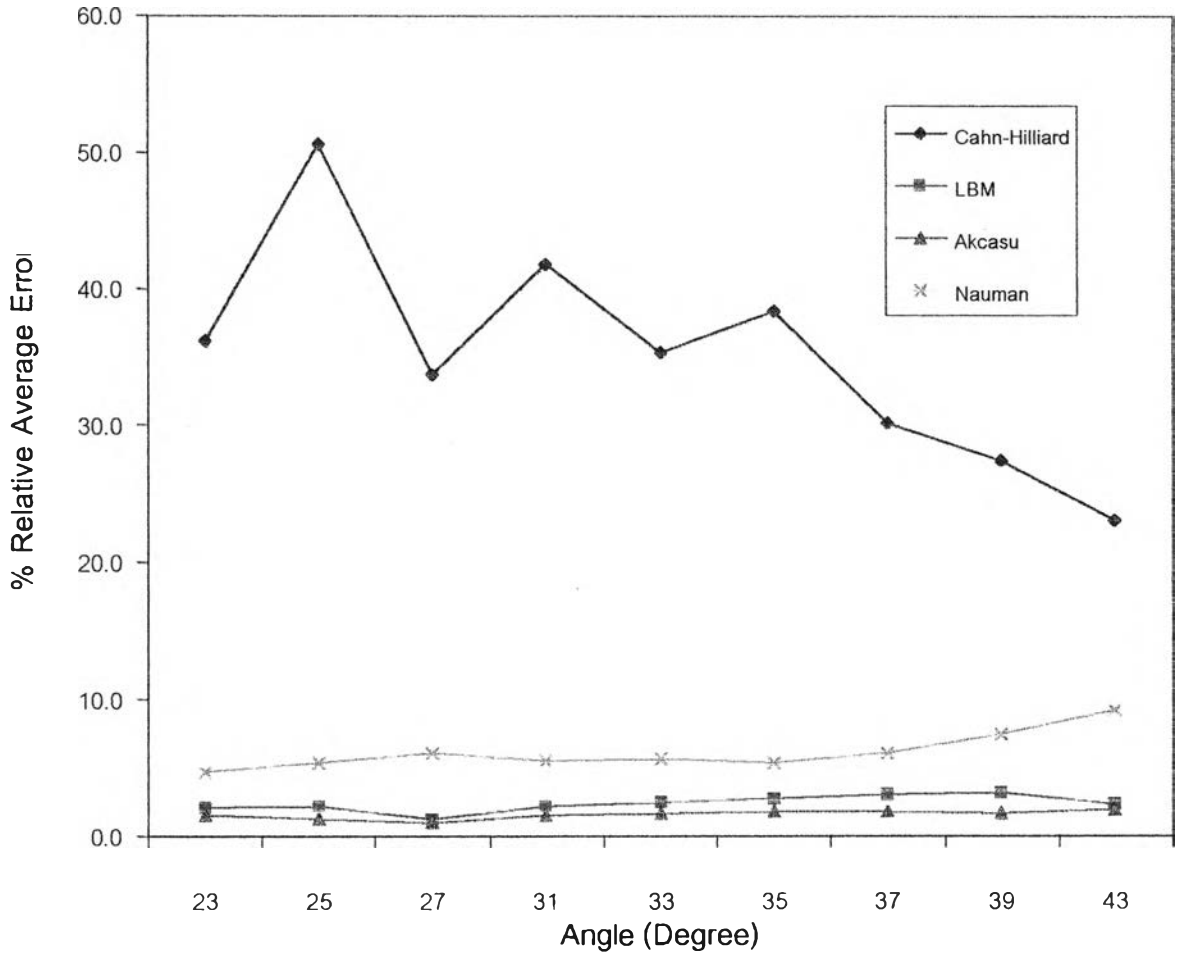

Fig.5.45 The percent relative average error of 70%w TMPC/PS blends at 295 °C of each theory.

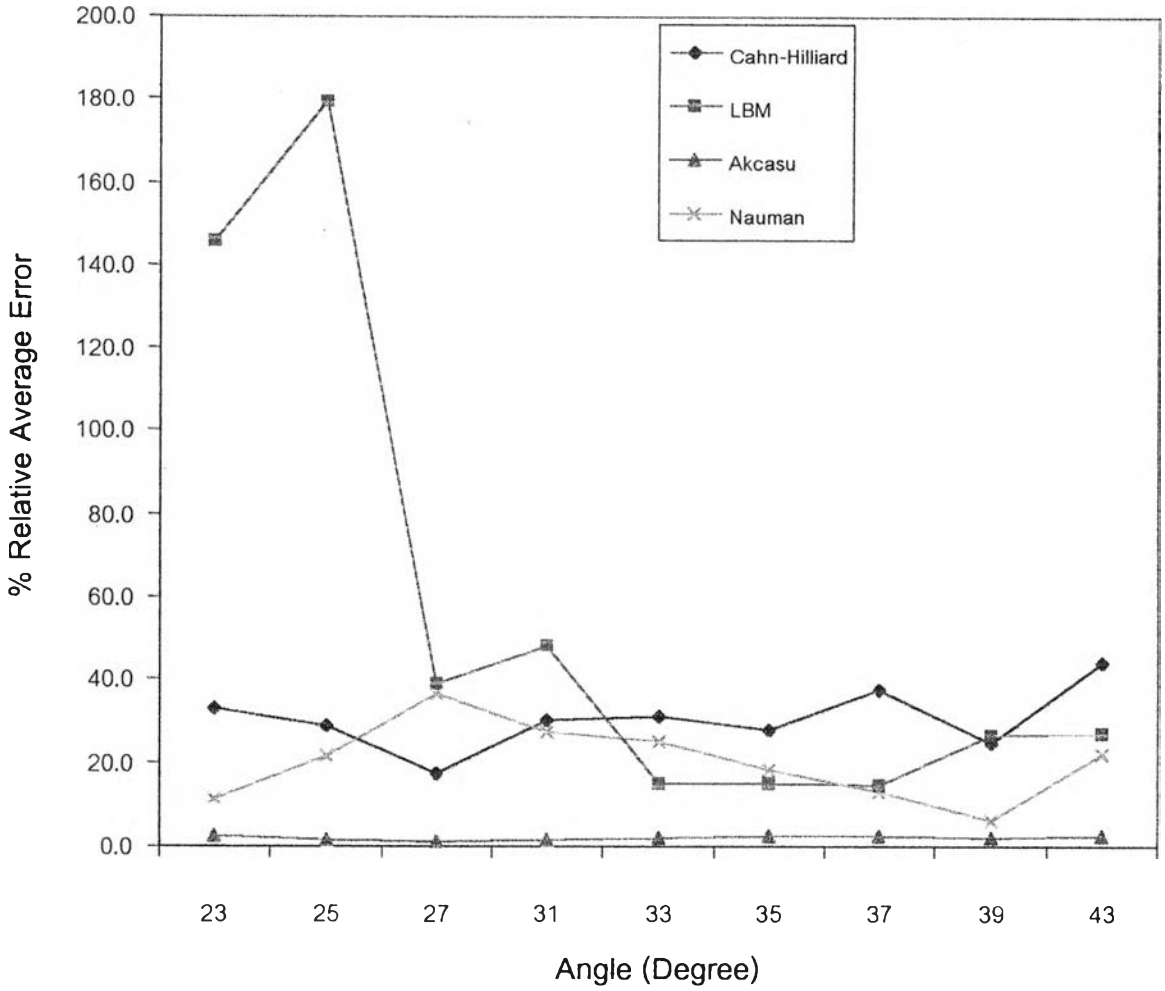

Fig.5.46 The percent relative average error of 70%w TMPC/PS blends at 297 °C of each theory.

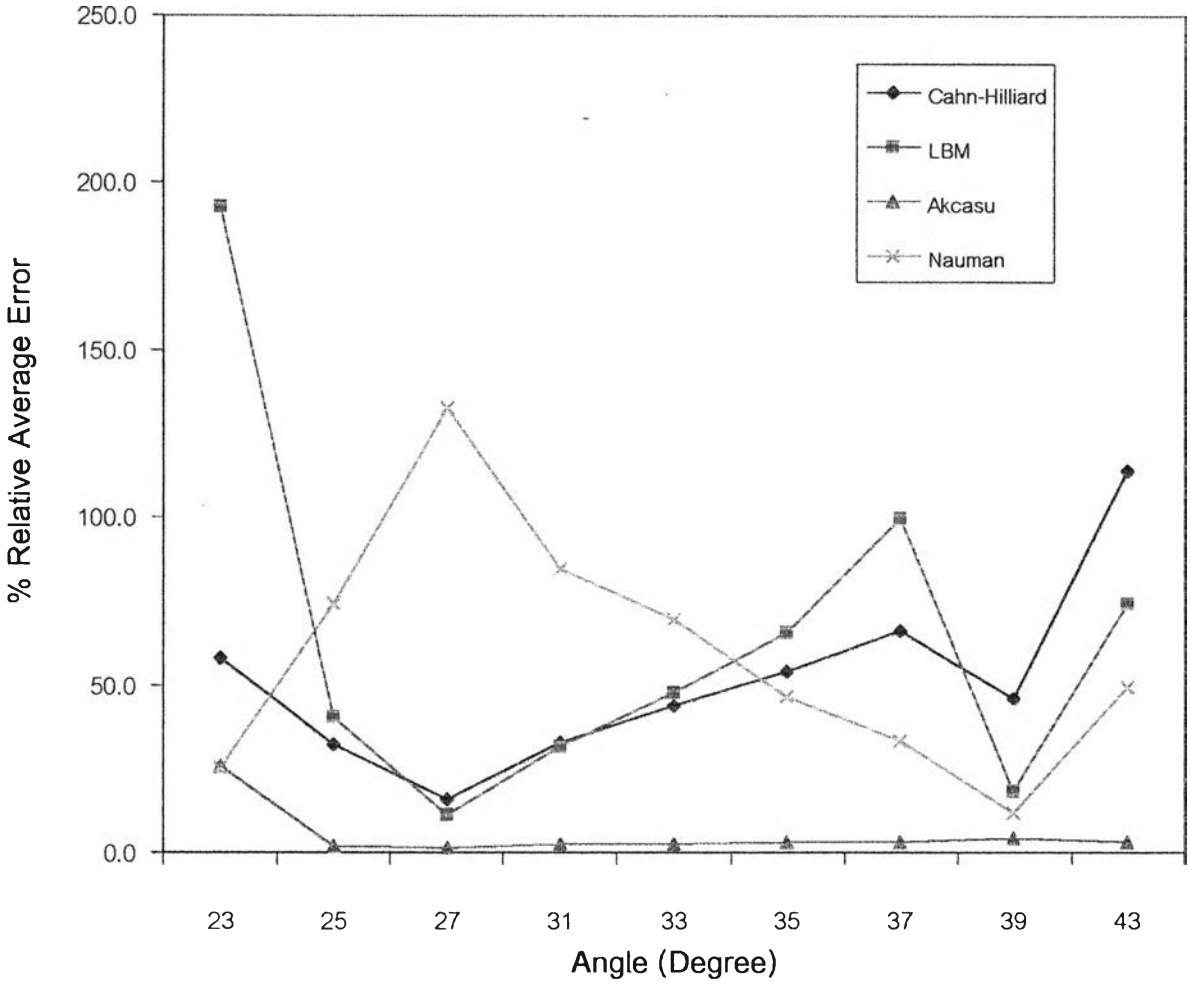

Fig.5.47 The percent relative average error of 70%w TMPC/PS blends at 299 °C of each theory.

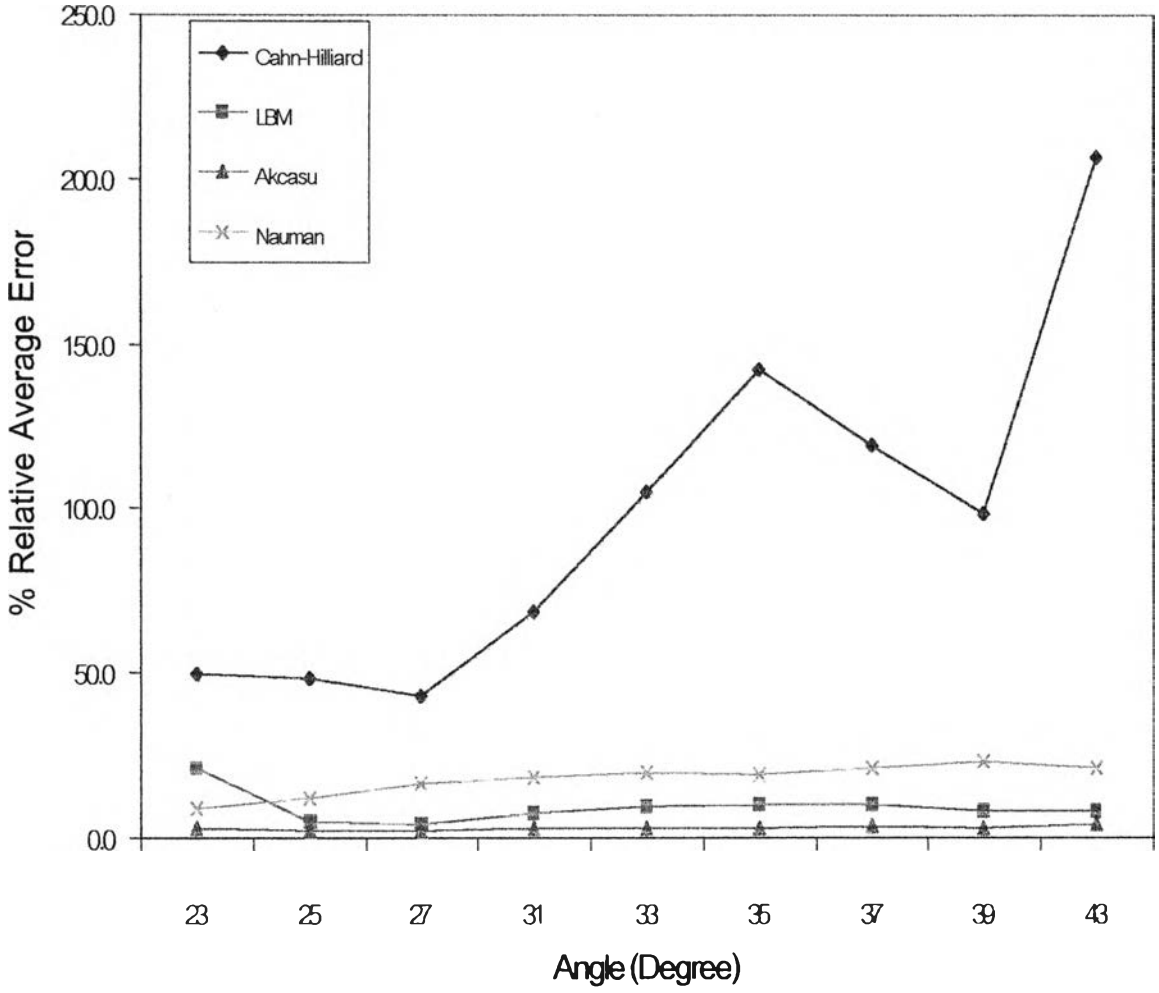

Fig.5.48 The percent relative average error of 70%w TMPC/PS blends at 301 °C of each theory.

5.4 Part II: Test of Experimental Results of SMA/PMMA Blends

5.4.1 Test of Experimental Results of each Theory on SMA/PMMA Blends

5.4.1.1 Test of Cahn-Hilliard's Theory

In Fig.5.49, it shows the percent relative average error of SMA/PMMA blends at the compositions of 20/80, 30/70, and 40/60. It appeared that for each composition, the percent relative average error do not change much with the angle of light scattered data.

5.4.1.2 Test of Langer, Bar-on and Miller's Theory

In Fig.5.50, it shows the percent relative average error of SMA/PMMA blends at the compositions of 20/80, 30/70, and 40/60. It appeared that for each composition, the percent relative average error do not change much with the angle of light scattered data.

5.4.1.3 Test of Akcasu's Theory

In Fig.5.51, it shows the percent relative average error of SMA/PMMA blends at the compositions of 20/80, 30/70, and 40/60. It appeared that for each composition, the percent relative average error do not change much with the angle of light scattered data.

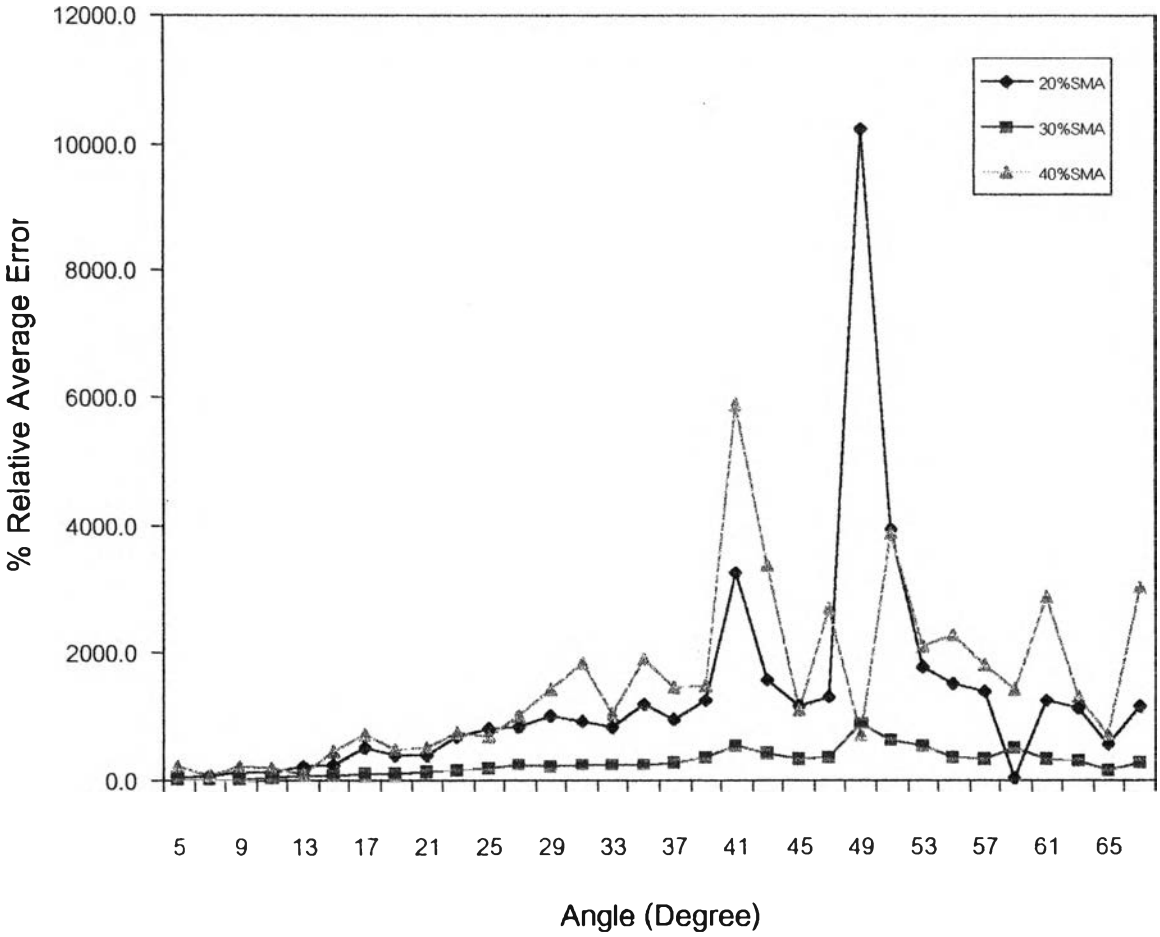

Fig.5.49 The percent relative average error of Cahn-Hilliard's theory from three compositions of SMA/PMMA blends.

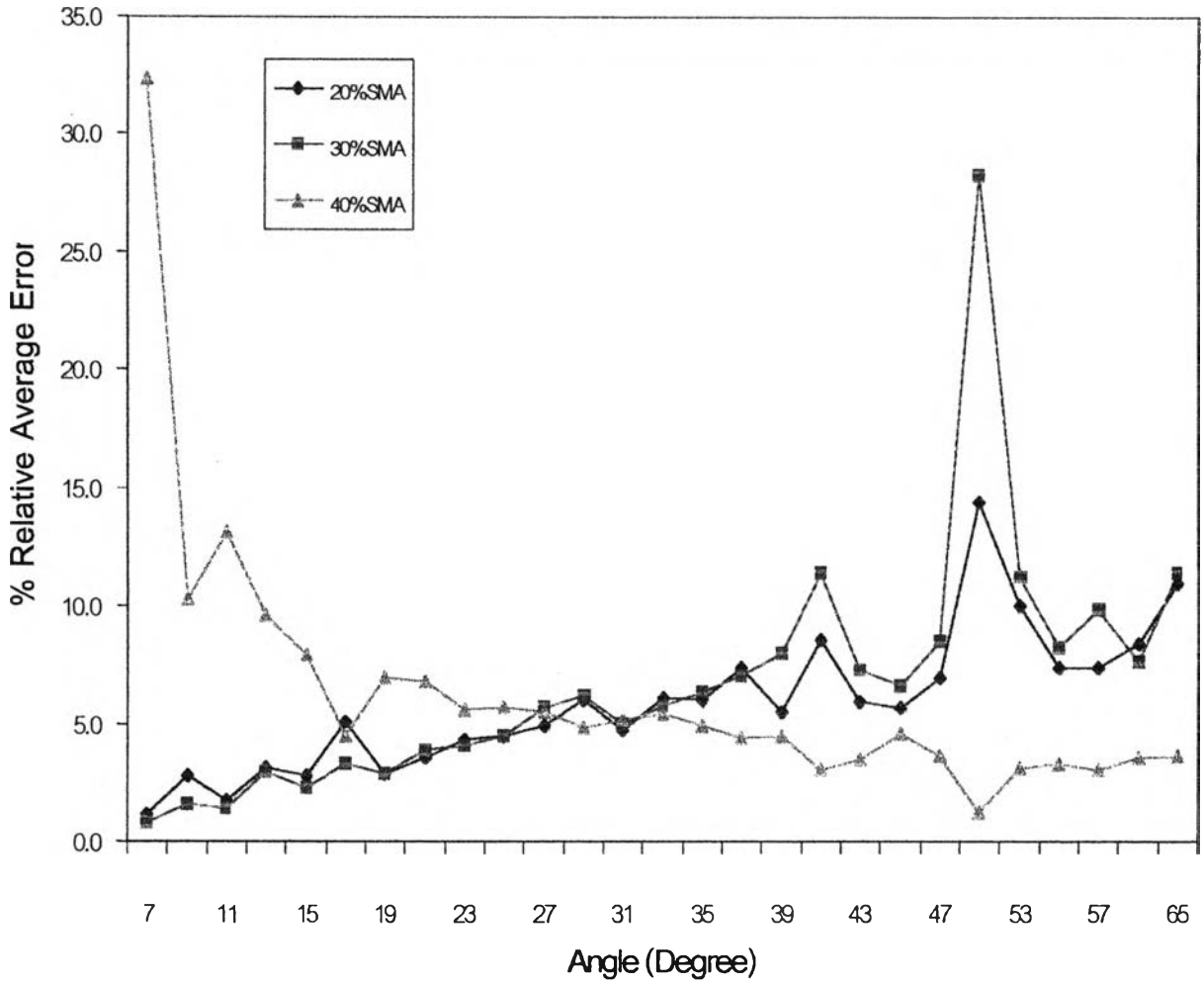

Fig.5.50 The percent relative average error of Langer, Bar-on and Miller's theory from three compositions of SMA/PMMA blends.

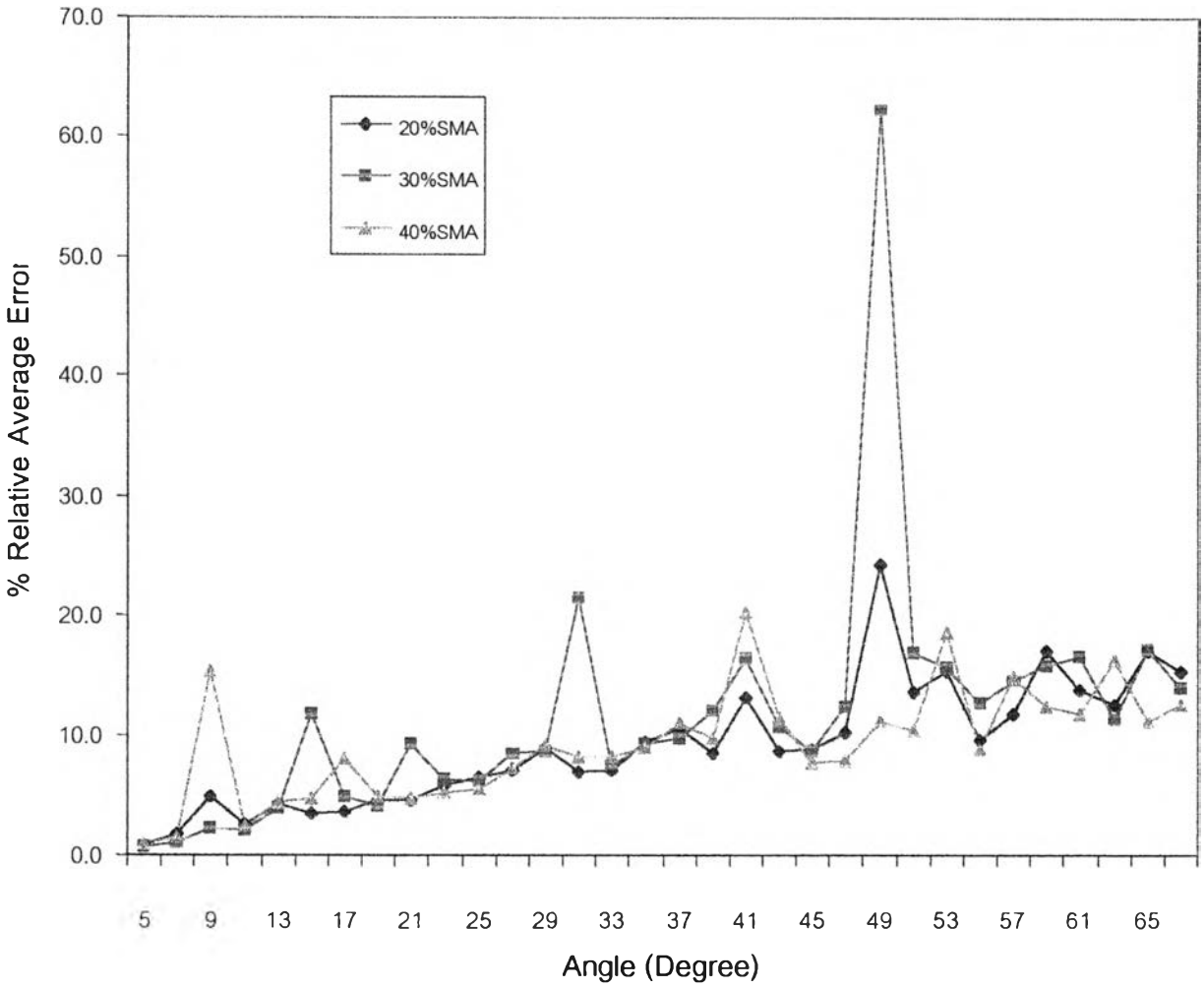

Fig.5.51 The percent relative average error of Akcasu's theory from three compositions of SMA/PMMA blends.

5.4.1.4 Test of Nauman's Theory

In Fig.5.52, it shows the percent relative average error of SMA/PMMA blends at the compositions of 20/80, 30/70, and 40/60. It appeared that for each composition, the percent relative average error do not change much with the angle of light scattered data.

5.4.2 Comparison of each Theory on SMA/PMMA Blends

5.4.2.1 Comparison of each Theory on 20% SMA/PMMA Blends

In Fig.5.53-1, it shows the percent relative average error of SMA/PMMA (20/80) blends of Langer, Bar-on and Miller's, Nauman's and Akcasu's theories. In Fig.5.53-2, it shows the percent relative average error of SMA/PMMA (20/80) blends of Cahn-Hilliard's theory. When the scattering angle increased, the percent relative average error of Cahn-Hilliard's theory increased. The percent relative average error from Langer, Bar-on and Miller's, Akcasu's and Nauman's theories are less than those of Cahn-Hilliard's theory. It shows that Akcasu's, Langer, Bar-on and Miller's and Nauman's theories can fit with the experimental data better than other theories.

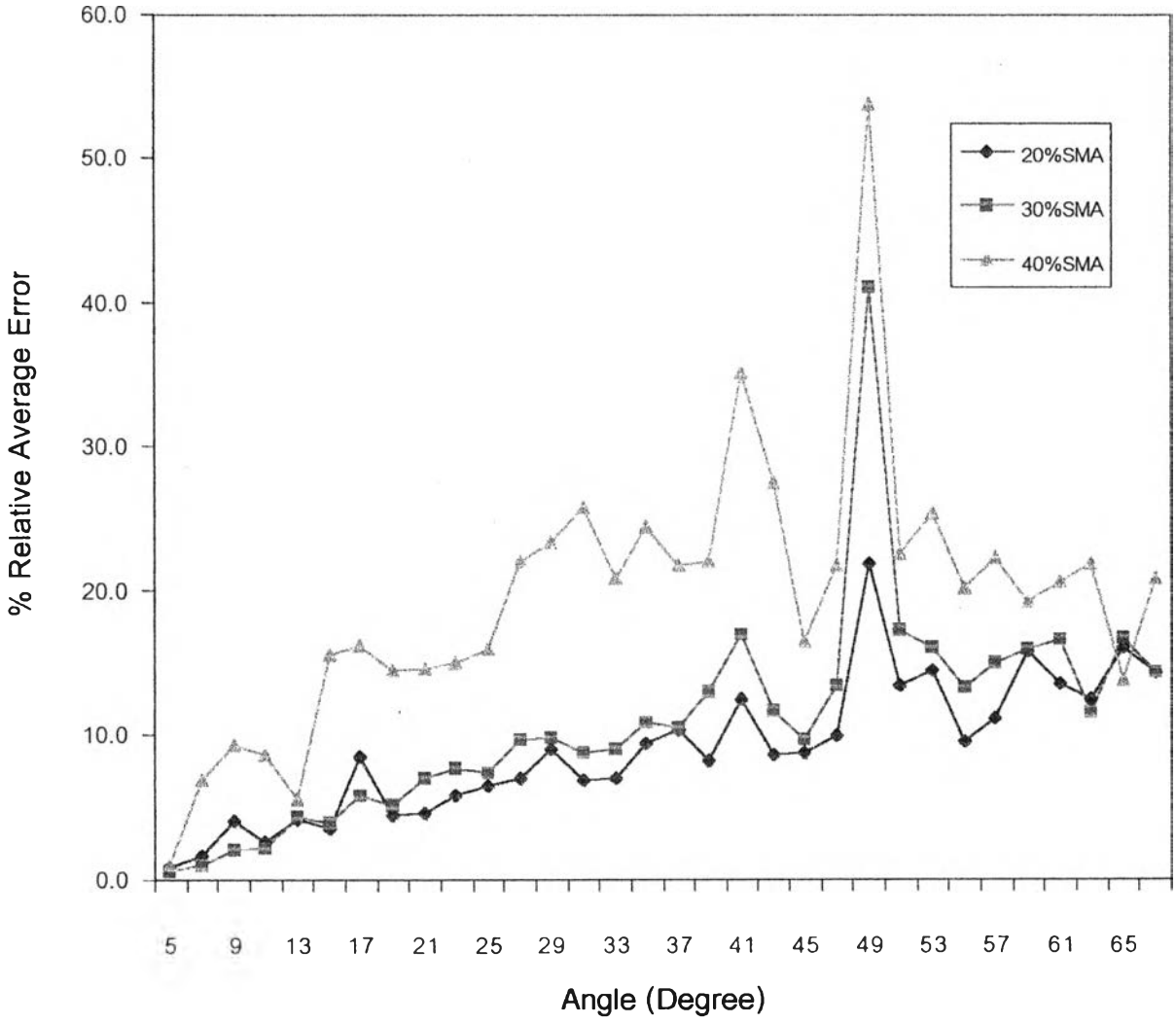

Fig.5.52 The percent relative average error of Nauman's theory from three compositions of SMA/PMMA blends.

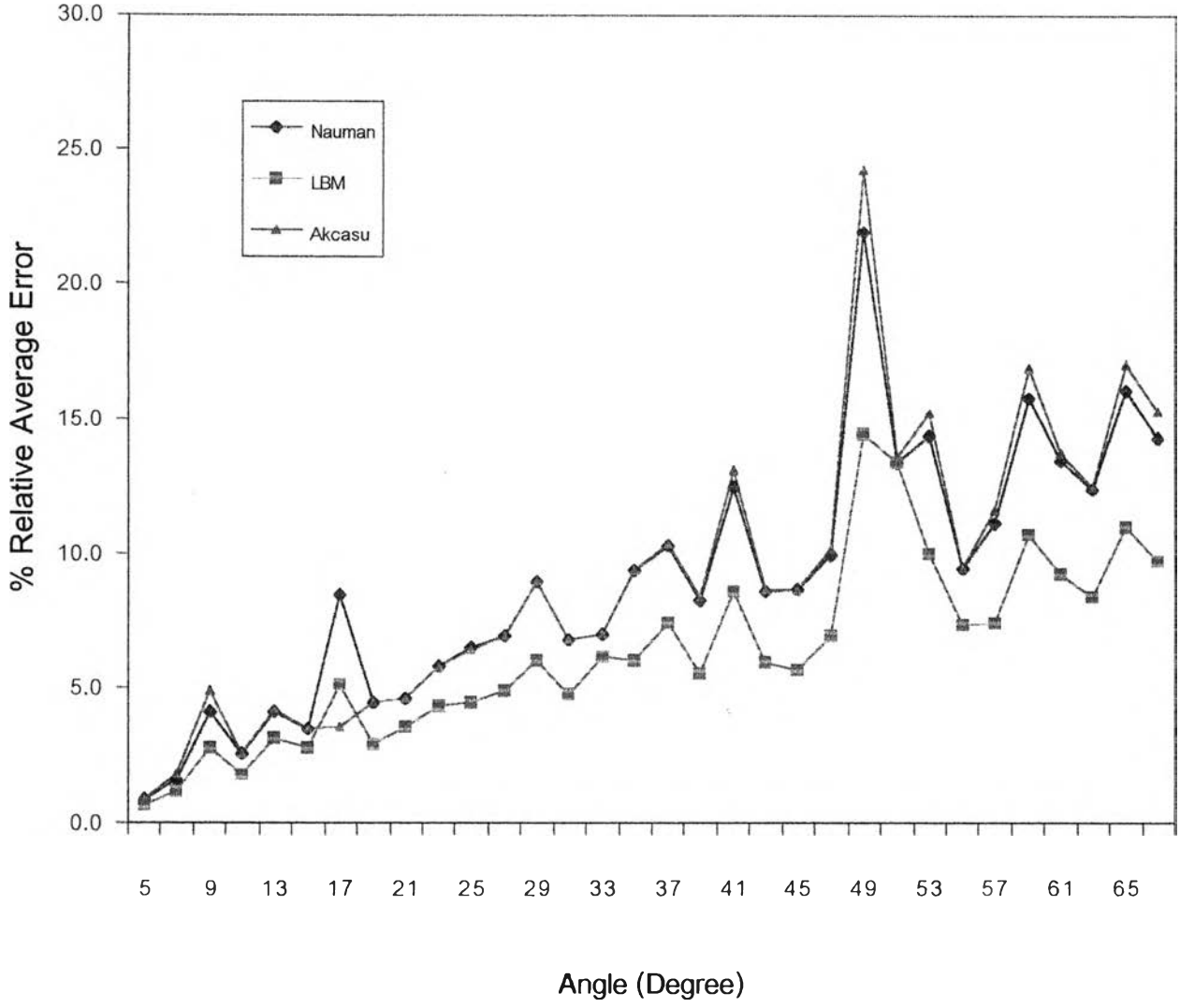

Fig.5.53-1 The percent relative average error of 20%w SMA/PMMA blends at 210 °C from three theories.

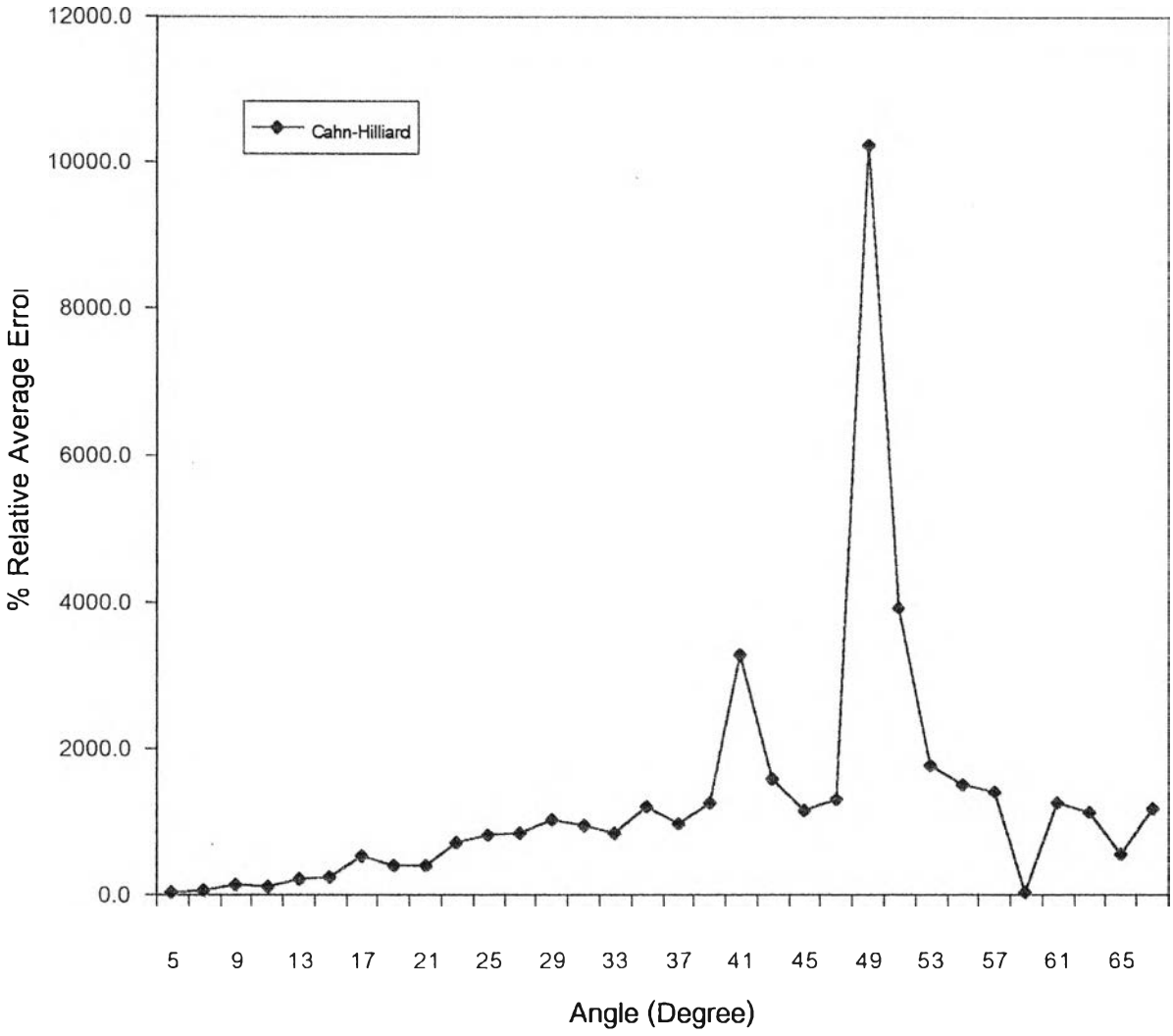

Fig.5.53-2 The percent relative average error of 20%w SMA/PMMA blends at 210 °C from one theory.

5.4.2.2 Comparison of each Theory on 30% SMA/PMMA Blends

In Fig.5.54-1, it shows the percent relative average error of SMA/PMMA (20/80) blends of Langer, Bar-on and Miller's, Nauman's and Akcasu's theories. In Fig.5.54-2, it shows the percent relative average error of SMA/PMMA (20/80) blends of Cahn-Hilliard's theory. When the scattering angle increased, the percent relative average error of Cahn-Hilliard's theory increased. The percent relative average error from Langer, Bar-on and Miller's, Akcasu's and Nauman's theories are less than those of Cahn-Hilliard's theory. It shows that Akcasu's, Langer, Bar-on and Miller's and Nauman's theories can fit with the experimental data better than other theories.

5.4.2.3 Comparison of each Theory on 40% SMA/PMMA Blends

In Fig.5.54-1, it shows the percent relative average error of SMA/PMMA (20/80) blends of Langer, Bar-on and Miller's, Nauman's and Akcasu's theories. In Fig.5.54-2, it shows the percent relative average error of SMA/PMMA (20/80) blends of Cahn-Hilliard's theory. When the scattering angle increased, the percent relative average error of Cahn-Hilliard's theory increased. The percent relative average error from Langer, Bar-on and Miller's and Akcasu's theories are less than those of Cahn-Hilliard's and Nauman's theories. It shows that Akcasu's and Langer, Bar-on and Miller's theories can fit with the experimental data better than other theories.

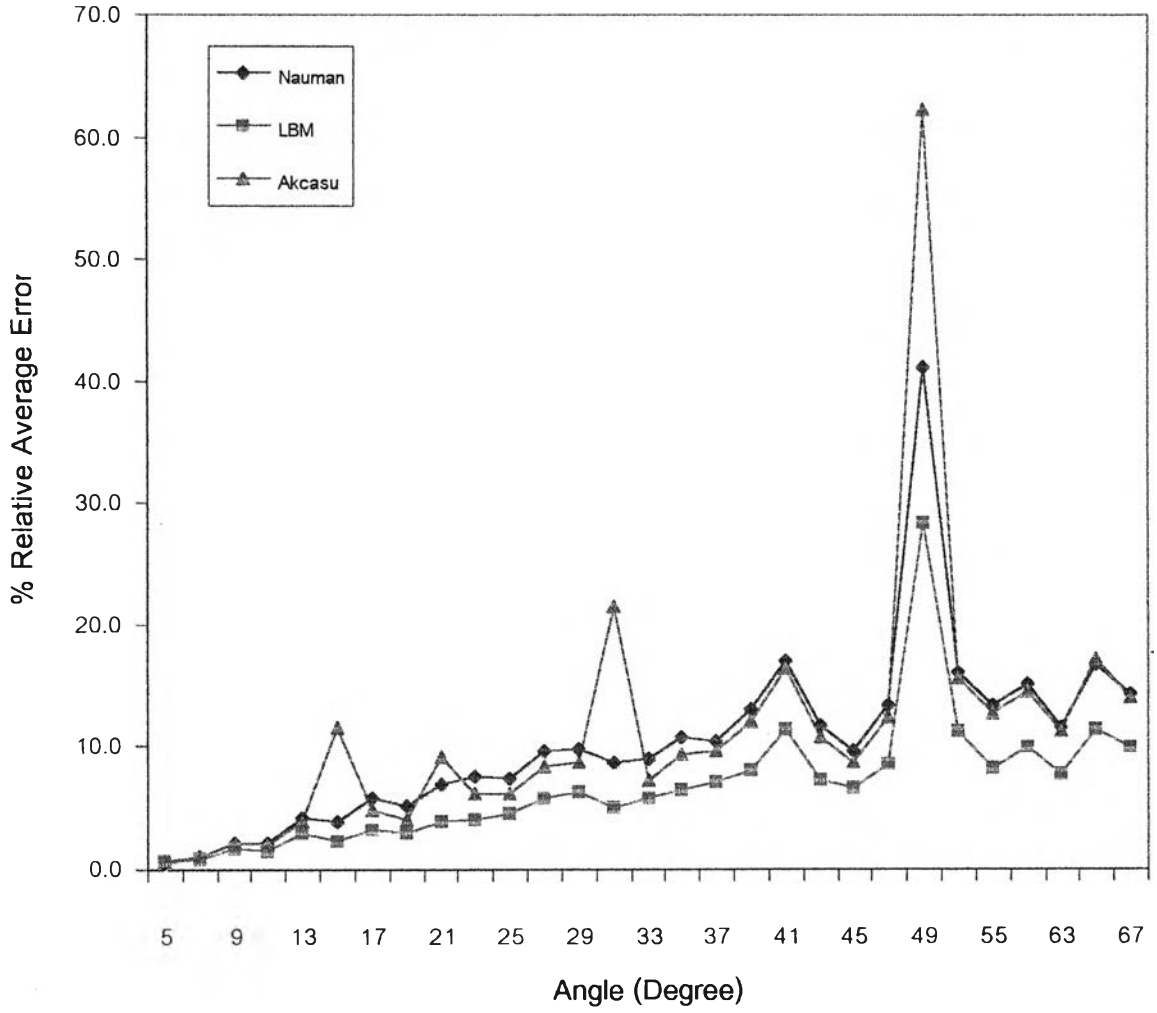

Fig.5.54-1 The percent relative average error of 30%w SMA/PMMA blends at 210 °C from three theories.

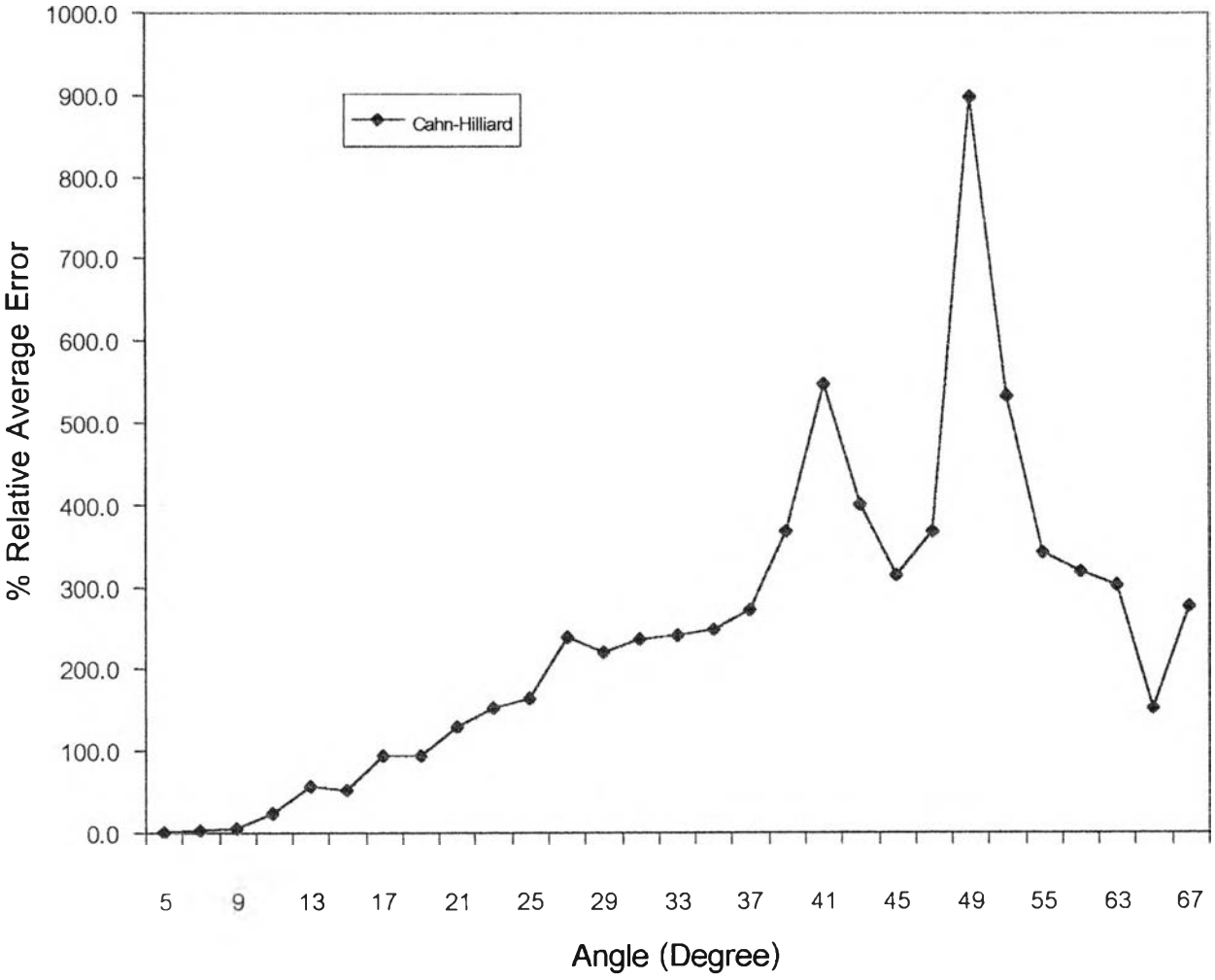

Fig.5.54-2 The percent relative average error of 30%w SMA/PMMA blends at 210 °C from one theory.

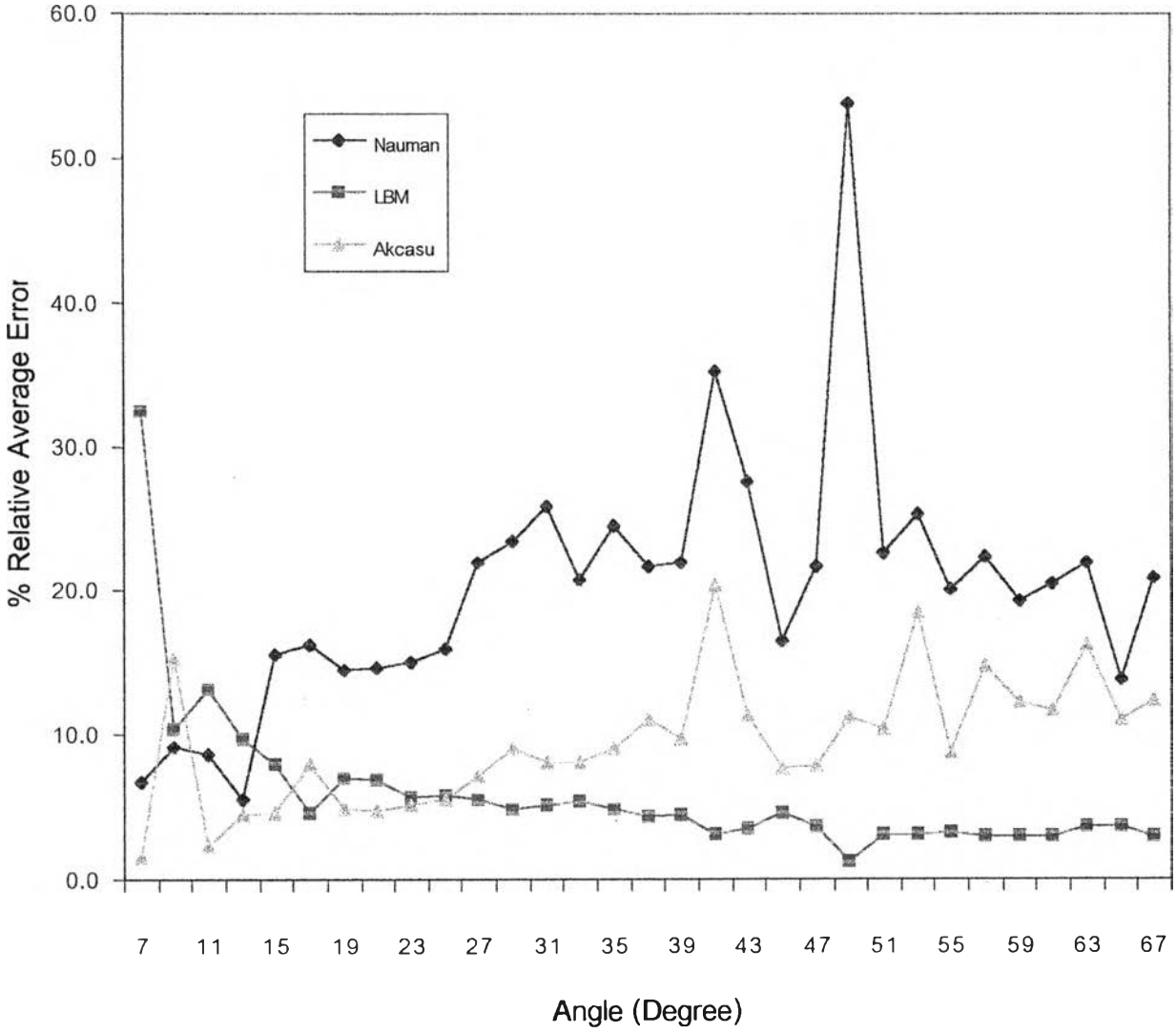

Fig.5.55-1 The percent relative average error of 40%w SMA/PMMA blends at 210 °C from three theories.

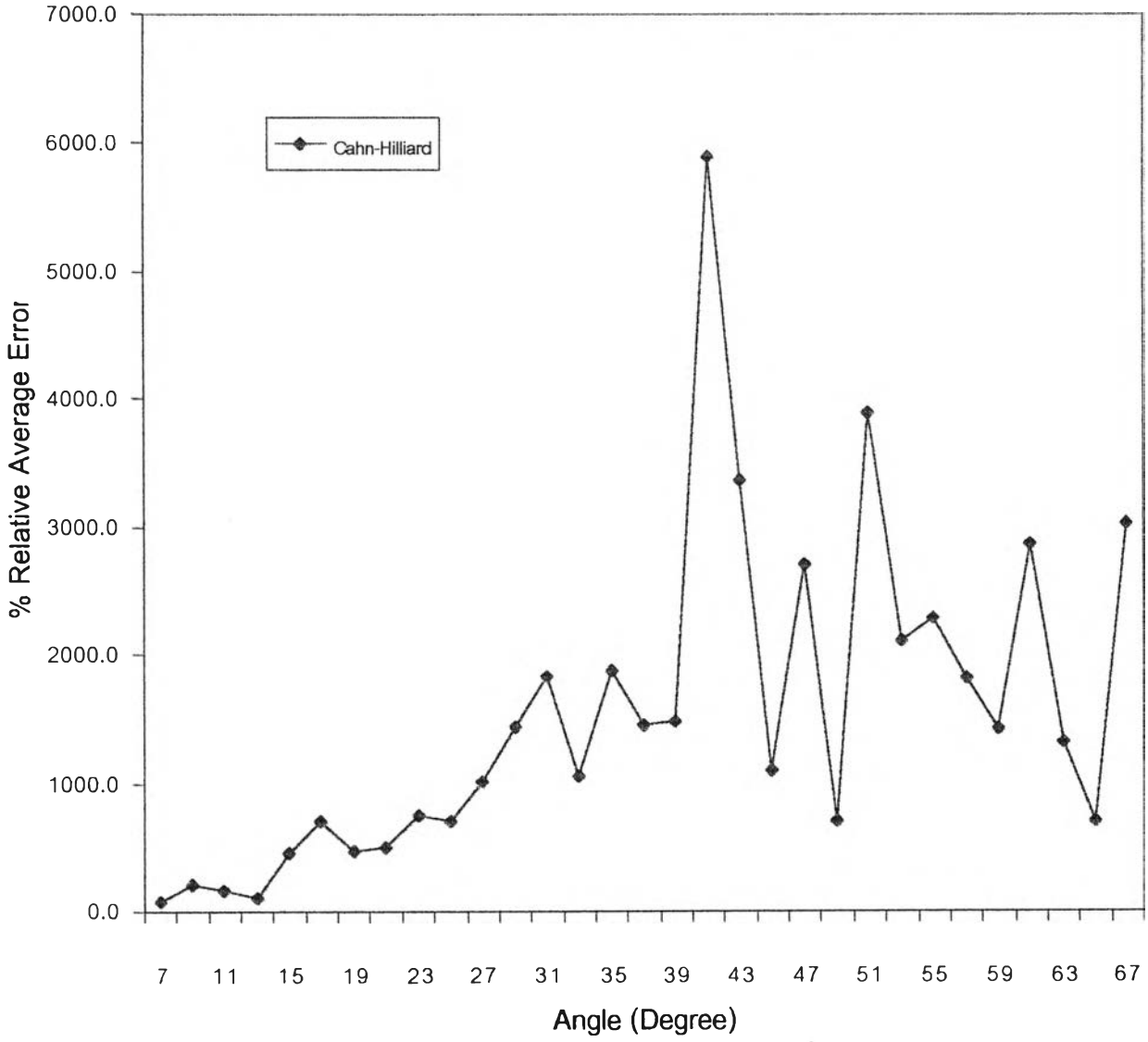

Fig.5.55-2 The percent relative average error of 40%w SMA/PMMA blends at 210 °C from one theory.

From Fig. (5.49) to Fig. (5.55), it shows that the percent relative average error values from Akcasu's theory are less than those from Langer, Bar-on and Miller's, Cahn-Hilliard's and Nauman's theories.

Considering all results on the percent relative average error, we can devide our results into two groups; 1) results from Akcasu's and Langer-Bar-on-Miller's theories and 2) results from Cahn-Hilliard's and Nauman's theories. The percent relative average error obtained from Akcasu and Langer, Bar-on and Miller are less than the ones from Cahn-Hilliard and Nauman. It therefore can be showed that Akcasu's and Langer-Bar-on-Miller's theories should be able to describe the spinodal decomposition process of polymer blends better than Cahn-Hilliard's and Nauman's theories.

Comparing between Akcasu's and Langer-Bar-on-Miller's theories, Akcasu's theory appears to fit experimental result better than Langer-Bar-on-Miller's theory as seen from smaller values of the percent relative average error. Considering Cahn-Hilliard and Nauman results, Cahn-Hilliard results shows larger values of error than those of Nauman. It is clear that Nauman's theory can fit with the experimental results better than theory of Cahn-Hilliard. According to this work, Akcasu's theory seems to be the best theory to fit with the selected experimental results, followed by Langer-Bar-on-Miller's, Nauman's and Cahn-Hilliard's theories.